

**Novel small molecules targeting Ag85C, mycolyl transferase of  
*Mycobacterium tuberculosis***

Dissertation  
zur Erlangung des Akademischen Grades  
*doctor rerum naturalium*  
(Dr. rer. nat.)  
im Fach Biologie  
eingereicht an der  
Mathematisch-Naturwissenschaftlichen Fakultät I  
Humboldt-Universität zu Berlin

von

Thulasi Warriar (M.Sc. Biological Sciences)  
geboren am 24.10.1983 in Trichur, Kerala, Indien

Präsident der Humboldt-Universität zu Berlin  
Prof. Dr. Dr. h.c. Christoph Marksches

Dekan der Mathematisch-Naturwissenschaftlichen Fakultät I  
Prof. Dr. Lutz-Helmut Schön

Gutachter/innen:

- 1) Prof. Dr. Stefan H. E. Kaufmann
- 2) Prof. Dr. Richard Lucius
- 3) Prof. Dr. Kai Matuschewski

Tag der mündlichen Prüfung:

15.03.2010

<b>ZUSAMMENFASSUNG .....</b>	<b>5</b>
<b>ABSTRACT .....</b>	<b>7</b>
<b>1 Introduction .....</b>	<b>9</b>
1.1 Phylogeny of <i>Mtb</i> .....	10
1.2 Pathogenesis of <i>Mtb</i> .....	11
1.3 Characteristics of <i>Mtb</i> .....	12
1.3.1 Cell Envelope.....	12
1.3.1.1 Structure.....	13
1.3.1.2 Mycolic acids .....	14
1.3.1.2.1 Antigen85 complex.....	17
1.3.1.3 Arabinogalactan Peptidoglycan (AGP).....	18
1.3.1.4 Extractible lipids .....	19
1.3.1.5 Immunological relevance of lipids.....	20
1.3.2 Persistence/Dormancy .....	21
1.4 Intervention.....	22
1.4.1 Drugs.....	22
1.4.1.1 Current regimen .....	23
1.4.1.2 New drug candidates.....	25
<b>2 Aim of the study.....</b>	<b>29</b>
<b>3 Results.....</b>	<b>31</b>
3.1 <i>In vitro</i> anti-mycobacterial activity .....	31
3.1.1 Qualitative assay of anti-mycobacterial activity.....	31
3.1.2 Quantitative assay of anti-mycobacterial activity.....	32
3.1.3 Activity against drug resistant strains.....	33
3.2 Growth of mycobacteria in macrophages .....	34
3.2.1 Toxicity.....	35
3.2.2 [ <sup>3</sup> H]-Uracil incorporation assay.....	35
3.2.3 Colony forming unit measurement .....	36
3.3 <i>In vivo</i> studies .....	37
3.4 <i>Mtb</i> lipid analysis .....	39
3.4.1 TDM and TMM .....	39
3.4.2 Free mycolic acids .....	41
3.4.3 Time course analysis of TDM, TMM and free mycolic acid biosynthesis .....	43

3.4.4	Cell wall linked mycolic acids.....	44
3.4.5	Total mycolic acids.....	46
3.5	Permeability of cell wall.....	47
3.6	Inhibition of <i>Mtb</i> deficient in Ag85C.....	48
3.6.1	<i>In vitro</i> anti-mycobacterial assay.....	48
3.6.2	TDM and TMM analysis.....	49
3.7	Gene expression analysis.....	50
3.7.1	MBT operon.....	52
3.7.2	MMPL transporter proteins.....	54
3.7.3	Lipid biosynthesis.....	55
<b>4</b>	<b>Discussion.....</b>	<b>56</b>
4.1	Activity of Ag85C antagonists.....	56
4.1.1	Effect of Ag85C inhibition on <i>in vitro</i> <i>Mtb</i> culture.....	57
4.1.1.1	Activity against MDR <i>Mtb</i> .....	59
4.1.2	Activity in <i>ex vivo</i> infection model.....	59
4.1.3	<i>In vivo</i> studies.....	60
4.2	Mechanisms of action.....	62
4.2.1	Lipid analysis.....	62
4.2.1.1	TDM and TMM.....	63
4.2.1.2	Free mycolic acids.....	63
4.2.1.3	Cell wall linked mAGP and total mycolic acids.....	64
4.2.2	Permeability.....	65
4.2.3	Specificity.....	65
4.2.4	Gene expression analysis.....	66
<b>5</b>	<b>Conclusions and Outlook.....</b>	<b>70</b>
<b>6</b>	<b>Materials and methods.....</b>	<b>72</b>
6.1	Methods.....	72
6.1.1	Alamar blue assay.....	72
6.1.2	[ <sup>3</sup> H]-Uracil Incorporation Assay.....	72
6.1.3	MTT toxicity assay.....	72
6.1.4	[ <sup>3</sup> H]-Uracil Incorporation Assay during macrophage infection ..	73
6.1.5	Colony forming unit (CFU) assay.....	73
6.1.6	<i>In vivo</i> experiments.....	74
6.1.7	TDM and TMM synthesis assay.....	74

6.1.8	Detection and analysis of free mycolic acids .....	75
6.1.9	Time course analysis of TMM, TDM and free mycolic acids.....	76
6.1.10	mAGP synthesis assay .....	76
6.1.11	Mycolic acid synthesis assay .....	77
6.1.12	Data analysis for lipid synthesis assays .....	77
6.1.13	Purification of TDM, TMM and GMM.....	77
6.1.14	Permeability of <i>Mtb</i> cell wall .....	77
6.1.15	Gene expression analysis .....	78
6.1.16	cDNA synthesis and quantitative PCR.....	79
6.1.17	Mycobactin synthesis assay .....	80
6.2	Materials .....	81
6.2.1	<i>Mtb</i> strains .....	81
6.2.2	Mice .....	81
6.2.3	Buffers and media.....	81
6.2.4	Reagents.....	82
6.2.5	Instruments/Softwares .....	83
6.2.6	RT-PCR Primers.....	84
<b>References</b>	.....	<b>86</b>
Anhang.....		102
Chemical structures of compounds.....		102
Abbreviations.....		102
Publications .....		105
Acknowledgements .....		105
Erklärung .....		107

## ZUSAMMENFASSUNG

*Mycobacterium tuberculosis* (*Mtb*), der Erreger der Tuberkulose (TB) ist eines der erfolgreichsten Pathogene mit dem ein Drittel der Weltbevölkerung infiziert ist und das in Infizierten zumeist lebenslang persistiert. Es ist die Hauptursache für die Sterblichkeit HIV-koinfizierter Individuen. Zusammen mit dem Auftreten multi- und extensiv medikamentenresistenter (MDR und XDR) Stämme hat dies zu einem Anstieg der Todeszahlen insbesondere in Entwicklungsländern geführt. Es besteht dringender Bedarf, existierende Behandlungsstrategien zu verbessern. *Mtb* ist ein intrazellulärer Erreger, der tausende Jahre mit seinem menschlichen Wirt evolvierte. *Mtb* nimmt innerhalb des Wirtes einen oft als „Persistenz“ bezeichneten metabolischen Zustand an, der es widerstandsfähiger gegen Medikamente der Standardtherapie macht. Initiativen zur Medikamenten- und Impfstoffentwicklung fokussieren ihre Interventionsstrategien daher vermehrt auf alternative Leitmoleküle und Stoffwechselwege.

Ziel dieser Studie war, das Ag85C-Protein von *Mtb*, eine Mycolyltransferase, als neues Angriffsziel für medikamentöse Behandlungsstrategien, zu überprüfen. Ag85C gehört zu einer Familie von drei Proteinen, Ag85A, B und C, die hohe Sequenzhomologien und einen nahezu identischen katalytischen Bereich miteinander teilen. Sie sind an der komplexen Biogenese der Zellhülle in Mykobakterien beteiligt und möglicherweise redundant in ihrer Funktion. Diese Studie verwendet eine Reihe von Molekülen, Ag85C-1-4, die möglicherweise die katalytische Aktivität von Ag85C inhibieren. Die Fähigkeit dieser Moleküle an Ag85C zu binden wurde durch Nuklearmagnetresonanz (NMR) festgestellt. Ag85C-1 dient als Ausgangsstruktur; die Analoga Ag85C-2-4 wurden über Struktur-Aktivitäts-Beziehungen abgeleitet.

Die antimykobakterielle Aktivität dieser Moleküle wurde mit qualitativen und quantitativen Standardanalysen untersucht. Alle Verbindungen inhibierten das Wachstum von *Mtb* in Flüssigkulturen *in vitro*, aber nur das wirksamste Analog Ag85C-3 inhibierte auch das Wachstum intrazellulärer Bakterien in einem zellbasierten Makrophageninfektionssystem. Die Aktivität von Ag85C-3 wurde zusätzlich im Maus-*Mtb*-Aerosolinfektionsmodell getestet. Die Zugabe von Ag85C-3 führte an frühen Zeitpunkten zu einer schwachen Reduktion der mykobakteriellen Belastung in den Lungen der Mäuse. Kleine Moleküle, die die Funktion von Ag85C stören, können demnach das Wachstum von *Mtb* sowohl direkt als auch innerhalb von Makrophagen und Lungengranulomen inhibieren.

Um die Wirkmechanismen der Toxizität von Ag85C-3 auf *Mtb* zu entschlüsseln wurde eine detaillierte Untersuchung durchgeführt. Ag85C funktioniert hauptsächlich als Transferase von

Mykolsäuren zu seinem terminalen Substrat und führt so zum finalen Zusammenbau der lipidreichen Zellhülle von Mykobakterien. Analysen der Reaktionskomponenten, Trehalosemonomykolat (TMM, Substrat), Trehalosedimykolat (TDM, Produkt) und Mykolsäure gebundenes mit Arabinogalaktanpeptidoglykan (mAGP, Produkt) von *Mtb* zeigten nach Ag85C-3 Behandlung eine deutliche Hemmung dieses Syntheseschrittes. Zusätzlich zeigte die Analyse einer *Mtb* Mutante, dem Ag85C fehlt, dass diese Modulation der Glykolipide nicht spezifisch für Ag85C ist, sondern auch durch eine Blockade von Ag85A und B verursacht werden kann. Darüber hinaus führte die Perturbation der Lipidzusammensetzung durch Ag85C-3 zur einer schwachen Zunahme der Permeabilität der *Mtb*-Zellhülle. Folglich ist die unkontrollierte Diffusion die wahrscheinlichste Ursache für den Ag85C-3 induzierten *Mtb* Tod.

Eine umfassende Analyse der durch Ag85C-3 regulierten Signalwege wurde mittels genomweiter Studie der Genexpressionsmuster durchgeführt. Interessanterweise führte die Zugabe von Ag85C-3 zur Hochregulation von Gengruppen, die an die Biosynthese von Siderophoren und Lipidtransport beteiligt sind. Die Biosynthese von Siderophoren und damit eingehend der Eisenhomöostase sind kritisch für das Überleben jedes Organismus und ihre Modifikation könnte einen alternativen Mechanismus darstellen, durch den Ag85C-3 den Tod verursacht. Die Überprüfungen weiterer wichtiger regulierter Gene sollte die Generierung eines eindeutigen Profils dieser Klasse von Inhibitoren ermöglichen.

Zusammenfassend, ist die Inhibition von Ag85C durch Ag85C-3 eine vielversprechende Interventionsstrategie für die zukünftige TB-Medikamentenforschung. Erste Ergebnisse zeigen, dass Ag85C-3 ebenfalls *Mtb* MDR-Stämme inhibiert und unterstreichen das Potential von Ag85C-3 in der Bekämpfung von Breitbandresistenzen. Weitere Optimierung der Ag85C-3-Struktur zur Verbesserung der Aktivität und Löslichkeit sollten hierfür folgen. Diese Studie untermauert die zielorientierte Identifikation chemischer Inhibitoren als berechtigte und wertvolle Vorgehensweise in der Medikamentenentwicklung.

**ABSTRACT**

*Mycobacterium tuberculosis* (*Mtb*), the causative agent of tuberculosis (TB) is one of the most successful pathogens infecting about one-third of the world's population and mostly persists in the host for life. It is the main cause of mortality in HIV coinfecting individuals. This combined with emergence of multiple and extensively drug resistant strains (MDR and XDR) has led to an escalation in number of cases worldwide. Therefore there is an urgent need to improve existing intervention strategies. *Mtb* is an obligate intracellular pathogen which has co-evolved with its human host for thousands of years. It has thus devised means to convert the adversity of the immune response to its own advantage enabling its survival inside macrophages. *Mtb* adapts an alternate metabolic state often referred to as 'persistence' within the host which makes it refractory to current first line drugs. Persistent and drug-resistant *Mtb* emphasize the need for alternate molecules and pathways as targets for novel drug discovery and vaccine development initiatives.

This study aimed to evaluate the *Mtb* Ag85C protein, a mycolyl transferase, as a novel target for drug mediated intervention strategies. Ag85C belongs to a family of three cognate proteins, Ag85A, B and C, which share high sequence homology and an almost identical catalytic site. They are involved in the final steps of the complex cell envelope biogenesis in mycobacteria and are assumed to be partially redundant in function. Nevertheless, the essentiality of their catalytic activity makes them relevant targets for drug development. A panel of chemical molecules, Ag85C-1-4, which bind to Ag85C as detected by Nuclear Magnetic Resonance (NMR) were utilized as inhibitors of Ag85C in this study. Ag85C-1 was the starting structure while the analogues Ag85C-2-4 were derived through structure activity relation (SAR) studies.

Anti-mycobacterial activity of the molecules was examined with standard qualitative and quantitative assays both in liquid medium cultures and in a cell-based macrophage infection system. All the compounds inhibited growth of *Mtb in vitro* but only the most potent analogue Ag85C-3 had an effect on intracellular bacteria. The activity of Ag85C-3 was also tested in the well studied mouse aerosol infection model of TB. A mild reduction of *Mtb* survival in lungs was observed at early time points after dosage with Ag85C-3. Targeting Ag85C by small molecules can thus inhibit growth of *Mtb* both directly as well as within macrophages and in lung granulomas. Importantly, Ag85C-3 can inhibit *in vitro* survival of a MDR strain of *Mtb* making it a relevant molecule in the current search for novel classes of anti-mycobacterial compounds.

Unravelling the mechanisms by which Ag85C-3 induces toxicity in *Mtb* is essential to further modify its structure and improve its efficacy. For this, a detailed functional characterization of its effect on *Mtb* was performed. Ag85C primarily functions as transferase of mycolic acids to its terminal substrates leading to the final assembly of the lipid rich cell envelope of mycobacteria. Analysis of the reaction components, trehalose monomycolate (TMM, substrate), trehalose dimycolate (TDM, product) and mycolic acid linked arabinogalactan-peptidoglycan (mAGP) upon Ag85C-3 treatment of *Mtb* clearly demonstrated a block at this step. TDM amounts were reduced with a concomitant increase in TMM while mAGP remained unaffected. There was also an unexpected accumulation of free mycolic acids. This modulation of glycolipids was not specific to Ag85C and could be through blockade of Ag85A and B also as indicated by growth inhibition of an *Mtb* mutant strain lacking Ag85C. Moreover perturbations of the lipid composition by Ag85C-3 led to mild increase in permeability of *Mtb* cell envelope which might be the major cause of death through uncontrolled diffusion.

A more comprehensive analysis of signaling pathways regulated by Ag85C-3 was performed through whole genome level study of *Mtb* gene expression patterns upon treatment. Interestingly gene clusters involved in siderophore biosynthesis and lipid transport were markedly up-regulated with Ag85C-3 treatment. These could either be indirect effects of Ag85 inhibition or be totally independent effects of Ag85C-3. Siderophore biosynthesis and iron homeostasis is crucial for survival of any organism and modification of this could be an alternate mechanism by which Ag85C-3 induces death. Further validation of other relevant regulated genes could enable generation of a unique signature profile for this class of inhibitors.

Thus the target, Ag85C and the inhibitor, Ag85C-3 are promising candidates for future TB drug research aimed at combating broad spectrum resistance development. Further optimization of Ag85C-3 structure for improving activity and solubility is necessary for this process. This study also reinforces target based identification of chemical inhibitors as a valid and valuable approach in drug development.



## 1 Introduction

Tuberculosis (TB) has resurged as one of the deadliest infectious diseases causing up to 2 million deaths annually (WHO, 2009). *Mtb*, the etiologic agent, is only second to HIV in number of deaths caused by any infectious agent and is the biggest killer amongst bacterial pathogens. *Mtb* was discovered in 1882 by Robert Koch (Koch, 1882). It commonly attacks the lung but also affects the central nervous system, lymph nodes, bones and skin. Development of Bacille-Calmette-Guerin (BCG) vaccine in 1920s by Albert Calmette and Camille Guerin was the first milestone in intervention against TB (Dockrell, et al., 2008). This vaccine entered clinics in 1921 and has been administered more than 4 billion times worldwide. In spite of its variable efficacy against pulmonary TB (Kaufmann, 2000). Nevertheless, chemotherapy has been identified as the only means of treating TB.

The seminal discovery of streptomycin (SM) by Selman Waksman and Albert Schatz ushered in the golden era of TB drug discovery (Schatz, et al., 1944). This was followed by identification of anti-tubercular activity of para-aminosalicylic acid (PAS) and nicotinamides like isoniazid (INH) and pyrazinamide (PZA) (Bernstein, et al., 1952; Lehmann, 1946; Malone, et al., 1952). In the 1950s and 60s a number of anti-TB drugs like D-cycloserine, viomycin, capreomycin, rifamycin and its derivative rifampin (RIF) were obtained from soil isolates (Bartz, et al., 1951; Kurosawa, 1952; Maggi, et al., 1966). Current TB therapy was mostly designed based on combination of these agents with the broad range quinolones being the only later addition (Tsunekawa, et al., 1987). Though this regimen along with BCG vaccination led to a decline in TB cases initially, the emergence of drug resistant *Mtb* strains and HIV co-infection has drastically escalated number of TB infected individuals in recent years. This forced WHO to declare it a 'Global Emergency' in 1993 (WHO, 1993).

More than half a century after streptomycin discovery, TB continues to plague millions, especially, in the developing world. Recent WHO report estimates about 9.27 million incident cases of TB in 2007 with most of the cases occurring in Asia (55%) and Africa (31%) (WHO, 2009). Of these an estimated 1.37 million (15%) were HIV positive and 80% of these cases were reported in Africa indicative of the dangerous liaison between HIV and TB. Additionally there were 0.5 million cases of MDR TB and 55 countries reported XDR TB. MDR is defined as those strains resistant to at least INH and RIF, 2 of the 4 frontline drugs, INH, RIF, PZA and EMB, while XDR are those MDR strains with additional resistance to any fluoroquinolone and one of the three injectable second-line anti-TB drugs (capreomycin, kanamycin and amikacin). Rapid spread of the virtually untreatable XDR TB threatens to jeopardise existing therapeutic regimens calling for new intervention strategies (Raviglione and Smith, 2007). To

develop these, the scientific community has revisited the complex biology of *Mtb*, with support from global policymakers and public and private funding organizations (Kaufmann and Parida, 2007). Current understanding of this biology with an update on intervention strategies is detailed in this section.

### 1.1 Phylogeny of *Mtb*

*Mtb* belongs to phylum *Actinobacteria*, comprising gram positive bacteria with high G+C content and one of the largest taxonomic units within the domain *Bacteria*. Within this, the genera *Corynebacterium*, *Mycobacterium* and *Nocardia* form a monophyletic taxon called CMN group characterized by an unusual waxy cell envelope mainly composed of unique long chain fatty acids called mycolic acids (Ventura, et al., 2007). The genus *Mycobacterium* comprises 85 different species indicating its high diversity. Majority of these are non-pathogenic environmental bacteria related to soil growing *Streptomyces* or *Actinomyces* but a few like *Mtb* and *M. leprae* belonging to the slow growing sub-lineage are highly successful pathogens. *Mtb* belongs to the *M. tuberculosis* complex consisting of *Mtb*, *M. africanum*, *M. canettii*, *M. bovis* and *M. microti* which share more than 99% identity at the nucleotide level (Brosch, et al., 2002).

Whole genome sequencing of *Mtb* and *M. leprae* has given immense boost to understanding of evolutionary relationships between members of *Mtb* complex (Cole, et al., 1998; Cole, et al., 2001). Analyses looking into gene deletion events have shown that *Mtb* and *M. canettii* are the most ancestral with lowest number of gene deletions while *M. bovis* has evolved more recently. The presence or absence of an *Mtb* specific deletion (TbD1) also divides *Mtb* strains into ancestral and "modern" strains, the latter comprising representatives of major epidemics like the Beijing, Haarlem, and African *Mtb* clusters (Brosch, et al., 2002). Though initial studies indicated very low sequence diversity amongst *Mtb* strains, recent analysis suggests that at the whole genome level there is substantial genetic variation which has led to identification of large sequence polymorphisms (LSPs) and single nucleotide polymorphisms (SNPs). Analyses of these by different investigators have given rise to classification of *Mtb* isolates into four distinct lineages (Gagneux and Small, 2007). The high congruency amongst these studies is indicative of the well known clonal nature of *Mtb* population structure. These studies also revealed that *Mtb* isolates displayed a clear phylogeographic distribution meaning distinct lineages were associated with specific geographical regions.

Though these studies are a big leap forward, more data is needed; especially sequence data of isolates from high TB burden areas like east and South-east Asia, Indian subcontinent and Africa to completely define the phylogeny of *Mtb*. This information has huge implications in

development of better and more reliable diagnostic tools, drugs, vaccines and biomarkers since strain variation can be a deciding factor in their success.

## 1.2 Pathogenesis of *Mtb*

Chronic infections represent some of the most advanced forms of crosstalk between host and pathogen, TB being a classical example. *Mtb*, the causative agent, is transmitted via aerosol and is taken up by alveolar macrophages once it reaches the lung (Fig.1) (Kaufmann, 2001). Macrophages play the contradictory roles of being the first line of defense against *Mtb* as well as its primary niche. *Mtb* efficiently counters the extensive anti-microbial artillery of macrophages and establishes itself in the phagosome by blocking its fusion with acidic lysosome. Meanwhile, activation of macrophages and dendritic cells induces an elaborate immune response initiated by secretion of cytokines like Interleukin-12 (IL-12) and Tumour necrosis factor- $\alpha$  (TNF- $\alpha$ ) and chemokines like (C-C) Ligand 5 (CCL5) and Macrophage inflammatory protein-1 $\alpha$  (MIP-1 $\alpha$ ) finally leading to organized cellular structures called granulomas, hallmark of chronic infections (Flynn and Chan, 2001). These are organized collections of differentiated macrophages mainly but other cells like T cells, some B cells, neutrophils, dendritic cells and fibroblasts are also found in *Mtb* granulomas (Ulrichs and Kaufmann, 2006). Though *Mtb* is primarily found inside macrophages adaptive response facilitated by T cells is also crucial for the completion and maintenance of these structures wherein *Mtb* is walled off from host tissue (Russell, 2007).

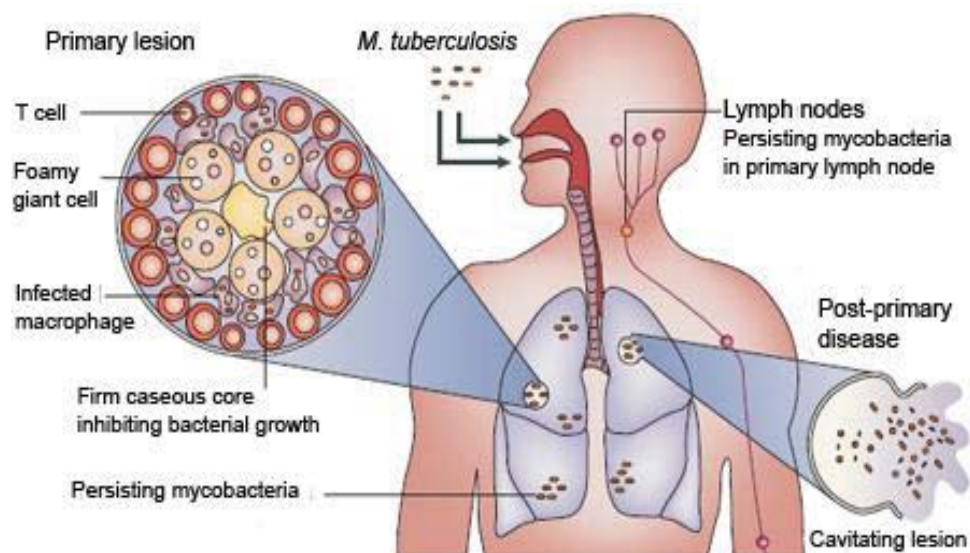


**Figure 1: Pathogenesis of *Mtb*.**

Adapted from Stewart, G.R. *et al.* (2003).

*Mtb* infection can have multiple outcomes including an early clearance which does not leave any imprint or immediate progress to active disease also called primary disease or a sub-clinical asymptomatic infection called latent TB which can reactivate at a later time point. The

last is the most likely scenario with about two billion individuals, almost a third of the world's population, harbouring dormant *Mtb* with a 10% risk of reactivation while 90% of individuals remain protected (Cosma, et al., 2003; Kaufmann and McMichael, 2005). In these individuals, *Mtb* is never completely eliminated and likely switches to an alternate metabolic state which is considered almost dormant or non-replicating (Connolly, et al., 2007). These dormant bacteria which are refractive to current anti-TB drugs are also found to co-exist with actively dividing bacteria in diseased individuals leading to prolonged therapy. This results in frequent patient non-compliance and thus emergence of resistance. Reactivation leading to post-primary disease is mostly a consequence of immune suppression either due to a disease like AIDS or diabetes or even therapies like anti-TNF antibody treatment (Barry, et al., 2009). Persistence, reactivation and drug resistance in the context of the pathogen as well as the host are the primary areas of research in TB.

### **1.3 Characteristics of *Mtb***

*Mtb* is aerobic, prototrophic bacterium shaped as irregular rod 0.3-0.5 $\mu$ m in diameter and of variable length (Fig. 2 i) (Cook, et al., 2009). When cultured on artificial media it forms characteristic ruffled colonies reflecting the unique composition of its lipid rich cell wall (Middlebrook, 1947). *Mtb* is a very slow growing organism with an average replication time of 22-24 hours and has only about 10% metabolic activity of fast growing *E. coli*. Additionally, slow growing pathogenic species tend to switch to a state of dormancy or persistence when exposed to extreme stress environments in the host. Its enormous success as pathogen can be attributed to its ability to evade host defense mechanisms and adapt to adverse environments with relative ease unmatched by other pathogenic bacteria. Two of its characteristic features, cell envelope and persistence, which are relevant to this study are described here.

#### **1.3.1 Cell Envelope**

The complex cell wall of *Mtb* is distinct in its chemical nature from that of both gram positive and gram negative bacteria thus making it amenable only to acid fast staining procedures (Brennan and Nikaido, 1995). Acid fastness is a physical property by which mycobacteria resist decolorization by mild acid or ethanol after staining with Ziehl-Neelsen dye making it visible as bright red rods against blue background. The cell wall lipids make up about 40% of dry weight of bacterial cells and are made mostly of unusual lipids like mycolic acids and mycocerosic acids linked to polysaccharides and/or proteins (Daffe, 2008). Mycobacteria possess unique biosynthetic modules devoted to their production which due to their singularity and essentiality are attractive targets for existent and future intervention strategies (Cole, et al., 1998). For example INH and ethambutol (EMB) two prominent front line drugs target

mycolic acid and arabinogalactan synthesis, respectively (Dover, et al., 2008). The cell envelope also gains special importance being at the interface between pathogen and host mediating their interactions and promoting the pathogen's survival.

### 1.3.1.1 Structure

Though it has been known that mycobacterial envelope consists of the innermost plasma membrane, an intermittent layer of peptidoglycan like gram positive bacteria and an outer membrane like gram negative bacteria, clear evidence of its layout has been elusive. Recent developments in cryo-electron microscopy techniques have overcome this, capturing the whole cell envelope of *M. bovis* and *M. smegmatis* in its native form (Hoffmann, et al., 2008; Zuber, et al., 2008). These studies indicate the presence of a zone similar to periplasmic space in gram positive bacteria and a semi-dense layer made up of peptidoglycan. Beyond this is the outer membrane mostly made up of mycobacteria specific lipids (Fig. 2 b). Contrary to popular belief, it is a symmetric bilayer of 7-8nm thickness which is only slightly thicker than that of plasma membrane though the carbon chain length of mycolic acids is almost 5 times that of phosphatidylcholine/serine. Hence this suggests an intercalated zipper like arrangement of hydrophobic mycolic (with the meromycolic chain folded upon itself) and other fatty acid tails with exposure of hydrophilic sugar/protein head groups to external environment. Glucans, made of repeating sugar molecules and other lipid moieties like lipoarbinomannan and phenolic glycolipids are also found decorating this outer membrane.

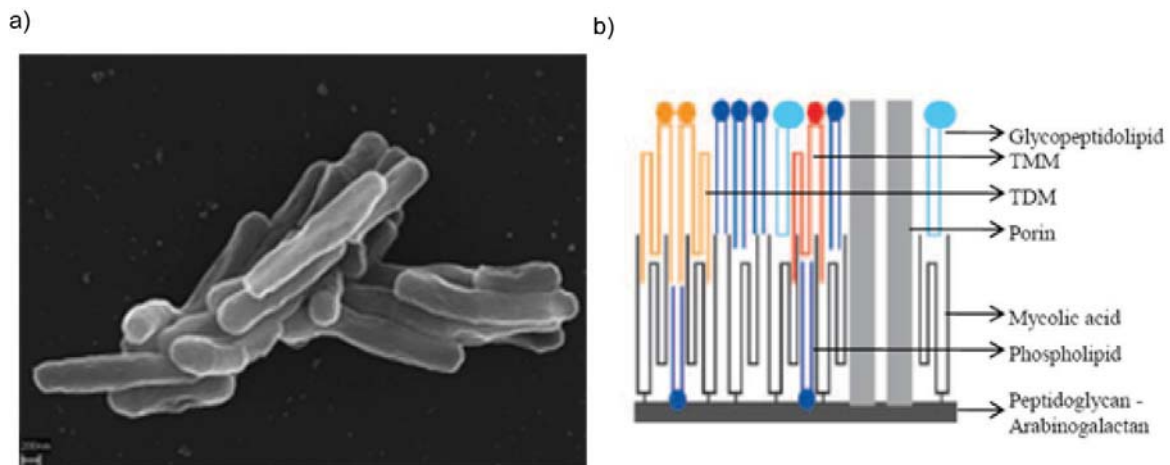


**Figure 2:** *Mycobacterium tuberculosis*.

(a) Scanning electron microscopy image of *Mtb* H37Rv showing the rod shaped cells (b) Schematic of outer-membrane of *Mtb* adapted from Zuber, B. *et al.* (2008).

This closely interlinked arrangement drastically reduces the permeability of the cell wall and also makes it highly resistant to antibiotics and host derived stress. In fact, the permeability of mycobacterial cell wall is found to be 10 to 100 times less than that of notoriously impermeable *Pseudomonas aeruginosa* (Jarlier and Nikaido, 1994). This scenario makes the role

played by transporter proteins, like porins, embedded in the cell envelope, in uptake of nutrients and other essential hydrophilic molecules crucial for bacterial survival. A clear understanding of the mechanisms underlying transport across the envelope is still lacking and is an active area of research.

Thus mycolic acids and peptidoglycan-arabinogalactan provide the structural framework to which extractible lipids are attached. The following sections describe the biosynthetic pathways associated with these and their relevance to host pathogen interaction as well as intervention strategies.

### 1.3.1.2 Mycolic acids

Mycolic acids, the major building blocks of mycobacterial cell envelope, are long  $\alpha$ -chain branched,  $\beta$ -hydroxylated fatty acids which upon pyrolysis are cleaved into a meroaldehyde main chain also called meromycolic chain and a meroacid or shorter  $\alpha$  branch (Asselineau and Lederer, 1950; Marrakchi, et al., 2008). They consist of 60 to 90 carbon atoms depending on mycobacterial species and various chemical functions like cyclopropane rings and oxygenated groups. *Mtb* mycolic acids are of three main types:  $\alpha$ , methoxy and keto, where  $\alpha$  is the most apolar with 74 to 80 carbon atoms and generally two double bonds or two cis cyclopropyl groups located in the meromycolic chain (Fig.3) (Daffe, et al., 1983). The other two subtypes contain supplementary oxygen functions namely methoxy and keto groups located in the distal part of the meromycolic chain and have 84 to 88 carbon atoms, 4 to 6 carbon atoms longer than the  $\alpha$  mycolates.

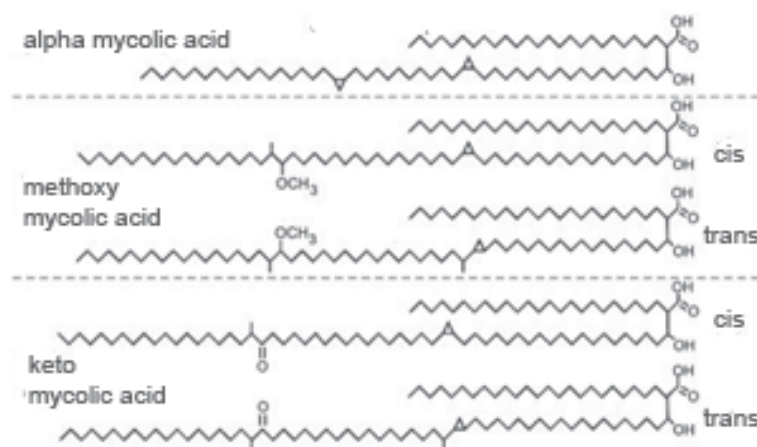


**Figure 3: Types of mycolic acids in *M. tuberculosis*.**

Adapted from Takayama, K. *et al.* (2005).

A diverse panel of up to 24 known enzymes are involved in the three basic steps of synthesis and elongation of  $\alpha$ -alkyl branch and meromycolic chains, their modification and condensation to final product. Initial steps in synthesis involve fatty acid synthase (FAS) systems which use malonyl- coenzyme A as the basic building block (Fig. 4). These are generated by acyl-

CoA carboxylases (ACCases) from acetyl-CoA and *Mtb* carries an unusually high number of these enzymes in its genome. FAS are of two main types: FAS-I, the multifunctional polypeptide (type I) and the FAS-II system which is made of a series of discrete soluble enzymes (Bloch and Vance, 1977; Fernandes and Kolattukudy, 1996; Odriozola, et al., 1977). FAS-I aids in *de novo* synthesis of long chain acyl-CoA from acetyl-CoA using malonyl-CoA producing both C<sub>16-18</sub> and C<sub>24-26</sub> chains. The shorter C<sub>16-18</sub> are substrates for elongation by FAS-II to give rise to meromycolic chain precursors while the longer chain C<sub>24-26</sub> give rise to the  $\alpha$  branch precursors. Additionally these fatty acids also contribute to the conventional phospholipids of plasma membrane.

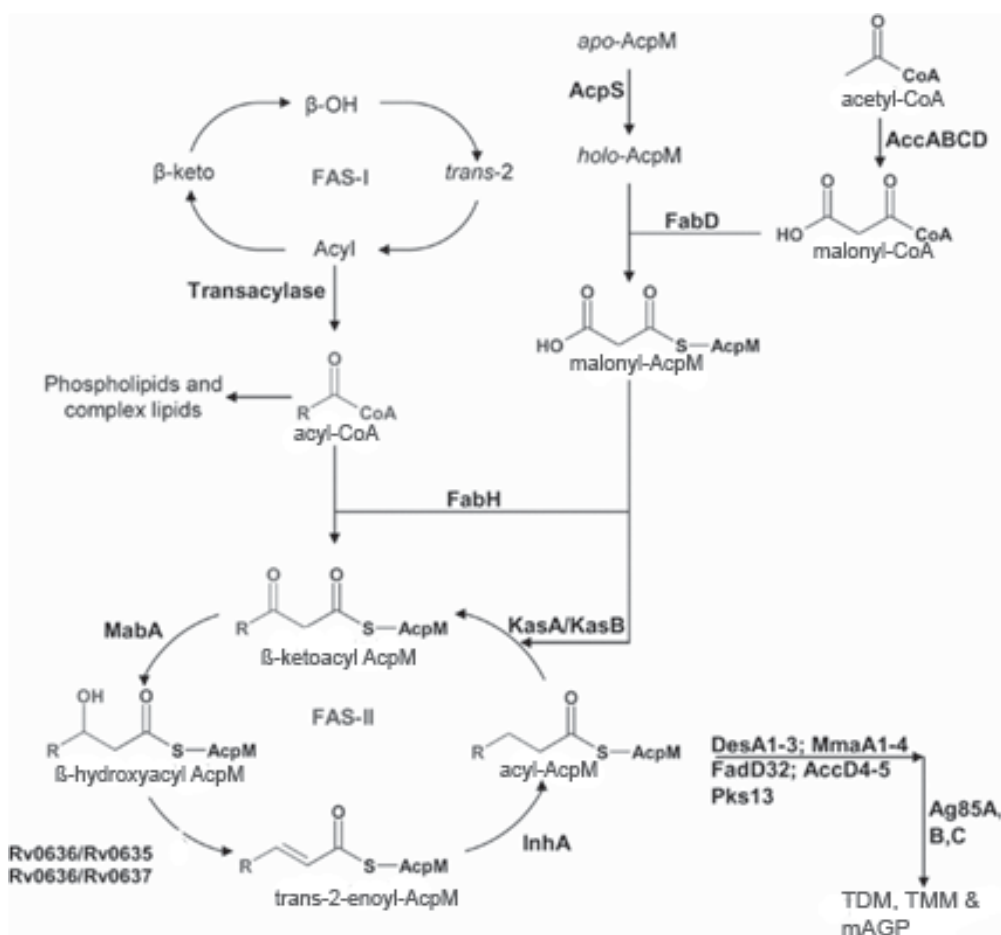


**Figure 4: Biosynthesis of mycolic acids.**

Schematic representation of steps in mycolic acid biosynthesis involving FAS-I and FAS-II systems. Adapted from Bhowruth, V. et al. (2008).

Mycobacterial FAS-II is incapable of *de novo* fatty acid synthesis unlike other bacterial FAS-II and depends on Acyl-carrier-protein M (AcpM) to transfer intermediates between the discrete monofunctional enzymes (Fig.4) (Bhowruth, et al., 2008). Elongation is initiated by condensation of acyl-CoA product of FAS-I with malonyl-ACP by  $\beta$ -ketoacyl-ACP-synthase III (MtFabH). Four enzymes catalyze each step of the elongation: NADPH dependent MabA reduces  $\beta$ -ketoacyl-ACP into  $\beta$ -hydroxyacyl ACP and subsequently dehydrated to an enoyl-

ACP by dehydratase (Marrakchi, et al., 2002). Next NADPH dependent InhA reduces the enoyl chain to produce acyl-ACP. Final elongation step is performed by the condensing enzymes KasA/KasB which uses malonyl CoA to increase chain length by two carbon atoms, giving rise to  $\beta$ -ketoacyl-ACP which feeds into the cycle. This process is probably terminated when the acyl-CoA-ACP attains the chain length required for meromycolic precursors. The observation that FAS-II is the target of the frontline antitubercular drug, INH, proves its importance in the physiology of *Mtb* (Marrakchi, et al., 2000).

Modifications of the meromycolic chain lead to the chemical diversity of mycolic acid species. *Mtb* harbours cyclopropyl rings (in  $\alpha$  mycolates) and keto or methoxy groups in combination with cyclopropyl rings and loss of these groups can lead to drastic changes in virulence and pathogenicity underlying their importance (Glickman, et al., 2000). Eight putative S-adenosylmethionine (SAM) dependent methyltransferases could introduce these modifications. CmaA1, CmaA2, PcaA (UmaA2) and MmaA2 have been studied with mutant analysis and shown to be important for cyclopropane ring formation in distal and proximal positions of meromycolic chain (Glickman, et al., 2001; Glickman, et al., 2000). Hma (MmaA4), on the other hand, is responsible for introducing keto and methoxy groups at proximal position in addition to introducing a methyl group. Condensation of modified meromycolic and alkyl branch precursors is the final step performed by polyketide synthase 13 (Pks13) belonging to type I Pks enzyme as the probable condensase (Portevin, et al., 2004). Prior to condensation meromycolic precursor need to be activated to an acyl-AMP derivative by fadD32 while the alkyl precursor gets carboxylated by AccD4 to yield an alkyl-malonyl intermediate. These are then condensed by Pks13 to give a keto ester which is then reduced to form mature mycolic acids.

The final processing steps where mature mycolic acids get transferred outside the plasma membrane to cell envelope components is not fully understood. Putative mycolyltransferases I and II (unknown identity) have been postulated in transfer of mycolic acid from Pks13 to trehalose phosphate to give rise to trehalose monomycolate (TMM) which is transported across plasma membrane by an ABC transporter (Takayama, et al., 2005). In the periplasmic space Antigen85 (Ag85) proteins play the critical role of transferring mycolic acids from TMM to peptidoglycan- arabinogalactan and another molecule of TMM to form mAGP and trehalose dimycolate (TDM) respectively. TDM, found on the outer layer of the envelope, has been associated with the typical cording phenotype of mycobacteria, earning it the name 'cord factor' (Glickman, 2008). Recent studies indicate that quality of mycolic acids meaning their chemical modifications rather than quantity drives this cord like structure formation. TDM is



also a high virulence lipid capable of inducing granulomas in a mouse aerosol model of *Mtb* infection (Perez, et al., 2000). Thus the two mycolic acid carrying molecules are important for the structural integrity (mAGP) as well as pathogenicity (TDM) of *Mtb*.

### 1.3.1.2.1 Antigen85 complex

Ag85 A, B and C are the three members of the Ag85 complex which share 68-79% identity at sequence level in *Mtb*. They are some of the most abundant proteins in the culture filtrate of *Mtb*. This also explains their high immunogenicity which is of interest in vaccine and TB biomarker development. Ag85 A, B and C are located in distinct regions of genome and are independently transcribed. Ag85B has a molecular mass of 30KDa while Ag85 A and C have the mass of 32KDa each and exist as monomers. They are secreted in the ratio of Ag85 B: A: C of 3:2:1 into the culture filtrate (Harth, et al., 1996). Initial studies focussed on their fibronectin binding property (fbp) and hence were named fbp A, B and C2 (Abou-Zeid, et al., 1988). But presence of these proteins in non-pathogenic *M. smegmatis* and elegant in vitro studies showed a more fundamental role in biogenesis of complex cell wall of mycobacteria (Belisle, et al., 1997).

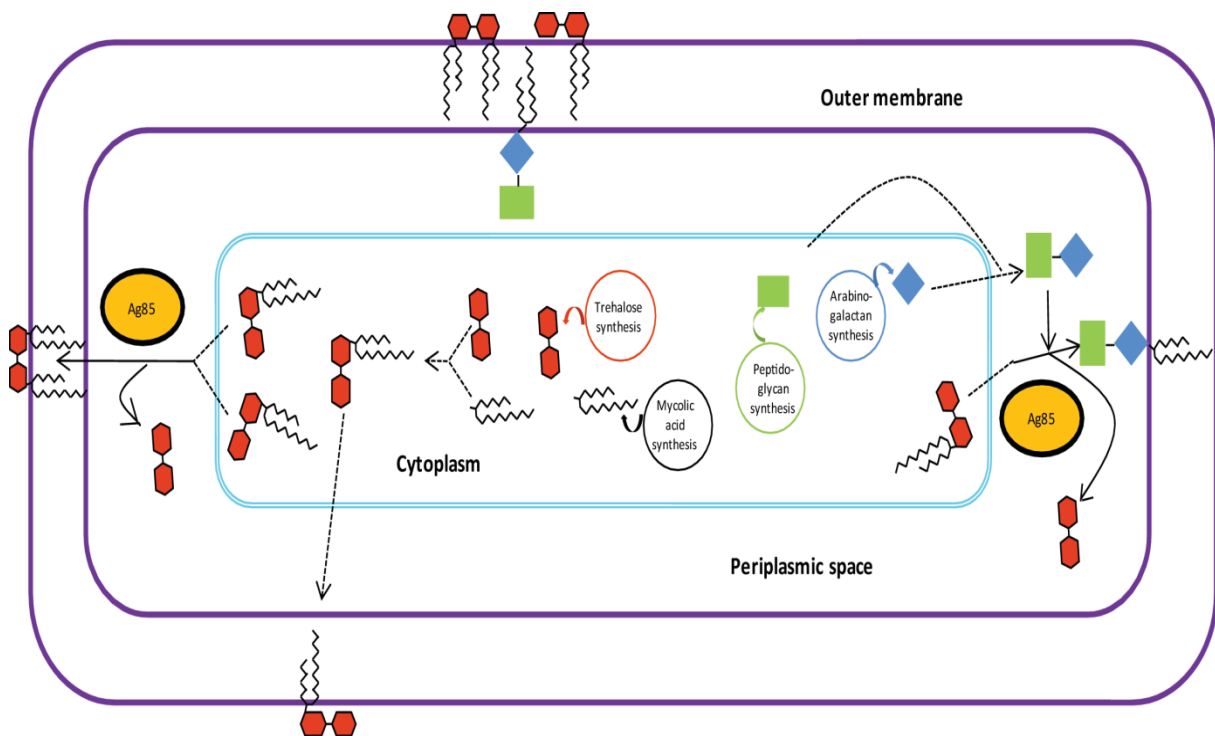


**Figure 5: Ag85 complex and cell wall biogenesis.**

Schematic representation of the function of Ag85 proteins.

Their location in the periplasmic space is ideal for their function as mycolyl transferases involved in the final transfer of mature mycolic acids from its substrate, TMM to give rise to TDM and m-AGP (Fig. 5). Structure studies implicate a highly conserved carboxyl esterase sequence in this activity (Anderson, et al., 2001; Ronning, et al., 2000; Ronning, et al., 2004).

Mutant and anti-sense knockdown studies have indicated that these proteins might have partially redundant functions in cell wall synthesis and hence survival (Armitage, et al., 2000; Harth, et al., 2002; Jackson, et al., 1999; Puech, et al., 2002). Nevertheless, absence of similar proteins in the genome suggests that they cannot be bypassed and hence have been targeted via chemical inhibitors extensively with some degree of success (Gobec, et al., 2007; Rose, et al., 2002; Wang, et al., 2004). In this study, we investigate the effects of a panel of chemical molecules which bind to Ag85C on the growth and physiology of *Mtb*.

### 1.3.1.3 Arabinogalactan Peptidoglycan (AGP)

Peptidoglycan (PG), a polymer of sugars and amino acids, is found in all bacteria outside the plasma membrane. It serves a structural role providing structural strength as well as counteracts osmotic pressure of cytoplasm. PG of mycobacteria is made of linear glycan chains consisting of alternating N-acetyl- $\beta$ -D-glucosamine (GlcNAc) and modified muramic acid (Mur) with a peptide side chain that is cross linked with parallel glycan strands (Crick and Brennan, 2008). It forms a rigid layer providing shape and strength to the envelope. The major cell wall polysaccharide of mycobacteria, branched- chain arabinogalactan (AG) is linked to peptidoglycan. It is mostly made of arabinose and galactose residues in the furanose configuration and lacks repeating units. About two-thirds of the non-reducing ends of terminal hexaarabinofuranosides carry mycolic acids giving rise to mAGP. Polyprenylphosphate (Pol-P), a lipid carrier of activated sugars, plays a pivotal role in the synthesis of this cell wall core. Mycobacteria use at least three forms of Pol-P where *Mtb* predominantly uses a decaprenyl phosphate (Dec-P).

Though PG biosynthesis pathway is not well characterized in *Mtb*, the arrangement of genes is very similar to that in other bacteria; hence the biochemistry is assumed to be almost the same. Initial steps in synthesis involve the enzymes MurA and MurB which generate UDP-MurNAc from UDP-GlcNAc. Then pentapeptide chain is linked to it by subsequent reactions catalyzed by orthologs of MurC, MurD, MurE and MurF of *E. coli*. This UDP-MurNAc-pentapeptide is then transferred to Dec-P to form Lipid-I. GlcNAc is then added to it to form Lipid-II which is then translocated across the membrane to add to the peptidoglycan chain. Penicillin binding proteins (PBPs) catalyze the formation of peptide crosslinks leading to mature PG. Mycobacterial peptidoglycan has a variety of alterations to the murapeptides including the presence of MurNGlyc and GlyNAc when most other bacteria have only MurNAc. Amidation at the carboxylic functions of the peptide side chains have also been reported. These modifications occur at the level of Lipid-II.

AG synthesis also uses Dec-P and is initiated with the synthesis of the linker unit, Dec-P-GlcNAc-Rha. Gal $f$  residues are then added to the linker unit from UDP-Gal $f$  followed by Ara $f$  residues which are added to the linker unit-galactan polymer from a decaprenyl-phosphoryl-Ara $f$  (DPA). Synthesis of the arabinan and galactan moieties seems to comprise concomitant events involving arabinosyl transferases and galactosyl transferases respectively. EmbABC are prominent glycosyl transferases which are postulated as cellular targets of another front-line antituberculosis drug, EMB, again underlining the importance of AG for bacterial survival. Mature AG is linked to PG by as yet unidentified ligase and could most probably occur at the level of Lipid-II. PG and AG synthesis pathways provide numerous novel targets for future drug discovery, in fact, a recently characterized lead molecule, benzathiazinone, targets DPA isomerases (Makarov, et al., 2009).

#### 1.3.1.4 Extractible lipids

Lipids located in the outer most layer of the envelope also function as the first points of contact between *Mtb* and the host. The most prominent extractible lipids are lipomannans (LM) and mannosylated lipoarabinomannan (ManLAM), phenolic glycolipids (PGL), pthiocerol dimycocerosates (PDIM) and sulfolipids (SLs) in addition to TDM which was discussed in previous section. LMs and MANLAMs are structurally similar lipoglycans generated by related biosynthetic pathways which use phosphatidyl-myo-inositol mannosides (PIM) as the starting point (Gilleron, et al., 2008). The exact localization of these phospholipids is not yet resolved with studies suggesting both an outer membrane anchoring which would expose them to host receptors as well as a more hidden localization within periplasmic space.

PGLs and PDIMs share a common lipid core which is synthesised by the polyketide synthase family of enzymes and they are mostly clustered on a 73kbp region called DIM-PGL locus (Guilhot, et al., 2008). PGLs are species specific and are significantly produced by *M. leprae*, a few strains of *Mtb*, *M.kansasii*, many strains of *M.bovis* and a few other slow-growing mycobacteria. PGLs and PDIMs are found in the outermost layers of the cell envelope and could be important for the permeability barrier of the *Mtb* envelope. However, most *Mtb* clinical isolates do not produce PGL while PDIM is found in all suggesting that PDIM might be playing a structural role (Daffe and Laneelle, 1988). Additionally, a DIM-less strain is more permeable to the hydrophobic probe, chenodeoxycholate (Camacho, et al., 2001).

SLs, also found in the outer membrane of cell envelope associated with mycolic acids initially attracted interest as virulence factors (Bertozzi and Schelle, 2008). They have a trehalose base with long acyl groups but the sulphate ester functionally distinguishes it from other *Mtb* lipids. There are about five types of SLs with SL-1 being the most abundant and a whole operon

found to be regulated by the *phoP/R* two component system has been dedicated to their synthesis (Gonzalo Asensio, et al., 2006; Lee, et al., 2008). In spite of much speculation no clear evidence has yet been unearthed linking sulfolipids and virulence *in vivo*.

### 1.3.1.5 Immunological relevance of lipids

As described in Section 1.2, the extensive host response mounted against *Mtb* fails to clear the infection completely and the complex mycobacterial lipids play an important role in this phenomenon. Cells of the innate immune system like macrophages and dendritic cells get activated when exposed to specific components of pathogens called pathogen associated molecular patterns (PAMPs) which could be of protein, sugar or lipid origin and are recognised by specific receptors in these cells. It is well known that ManLAM, LM and PIM are prominent PAMPs of *Mtb* recognized by various host cell receptors activating signalling cascades initiating host-pathogen cross-talk (Gilleron, et al., 2008). ManLAMs have been postulated to bind to the C-type lectin dendritic cell-specific intercellular adhesion molecule 3 grabbing nonintegrin (DC-SIGN) on dendritic cells and mannose receptor on macrophages leading to suppression of the pro-inflammatory cytokines (Geijtenbeek, et al., 2003). On the other hand, LMs and PIMS are Toll-like receptor-2 (TLR-2) agonists which induce inflammation. ManLAM can also induce phago-lysosome arrest in macrophages similar to live *Mtb* and PIMs and LMs also stimulate non-conventional T cells (Kang, et al., 2005).

TDM, another exposed lipid, is also important for inducing macrophages to secrete inflammatory cytokines like TNF- $\alpha$  and IL-12 as demonstrated by up regulation of expression of these genes in mouse lungs after TDM administration (Guidry, et al., 2007; Perez, et al., 2000; Welsh, et al., 2008). Removal of TDM from *Mtb* surface also reduces secretion of these cytokines and chemokines from macrophages (Indrigo, et al., 2002). TDM also blocks phago-lysosome fusion in macrophages similar to other virulence lipids (Axelrod, et al., 2008; Indrigo, et al., 2003).

PGLs and PDIM have been closely linked with virulence. DIM-less mutants show reduced multiplication in mouse lungs especially in the initial phases of infection and also appeared to induce higher amounts of pro-inflammatory cytokines from macrophages accompanied by a defective phago-lysosomal block (Camacho, et al., 1999; Cox, et al., 1999). PGLs on the other hand have been associated with the hypervirulence phenotype associated with a clinical isolate (HN878) of the Beijing family genotype (Reed, et al., 2004). Strains belonging to this genotype are believed to have originated in China, have been linked to major outbreaks of TB and are now found distributed worldwide (van Soolingen, et al., 1995). All Beijing strains

have been found to harbour structural variants of DIM and eventually PGLs suggesting a close link between virulence and lipid moieties (Constant, et al., 2002).

### 1.3.2 Persistence/Dormancy

Drug persistent *Mtb* refers to those that survive in the host in spite of extensive antibiotic treatment (Sacchetti, et al., 2008). This could either be because of reduced access of these drugs to *Mtb* enclosed in granulomas or the adaptation of bacteria to a non-replicating state. Persistent *Mtb*, thus, acquires phenotypic tolerance to antibiotics due to their distinct metabolic status leading to prolonged treatment, frequent non-compliance and thus drug resistance. This complex phenotype continues to confound mycobacteriologists but development of new intervention methods necessitates its better understanding (Stewart, et al., 2003).

A variety of simplified *in vitro* models; Wayne model of hypoxia, nutrient starvation, nitrosative stress model, acid stress model and macrophage infection, have been employed with whole gene expression analysis as starting points towards understanding *Mtb* biology under various stress conditions (Betts, et al., 2002; Schnappinger, et al., 2003; Voskuil, et al., 2003; Wayne and Hayes, 1996). The low level of replication or activity in this alternative state might explain resistance to current antibiotics which target pathways used in actively replicating bacilli. Even then, a minimal level of metabolism involving ATP synthesis, NAD- NADH shuttling and cell wall remodeling should be operative which can be attractive targets for therapy. The *dosR* regulon and recently the enduring hypoxic response (EHR) cluster are a few of the candidate regulatory networks which seem to be important for this process (Park, et al., 2003; Rustad, et al., 2008). An accumulation of tri-acyl glycerides and subsequent switch to fatty acid catabolism involving isocitrate lyase has also been postulated (McKinney, et al., 2000). An inclusive analysis of datasets generated by different model systems rather than exclusive studies would aid in throwing light on essential pathways active in persistent *Mtb* and thus bring up more relevant candidates.

Additionally, the absence of a reliable mouse model mimicking persistence has made *in vivo* validation of these studies even more difficult (Kaufmann, 2003). This has led to recent exploration of new animal models like non-human primates to better reconstruct human TB scenario but results are forthcoming (Barry, et al., 2009). What is now very well appreciated is the fact that human TB lesions display a wide range of phenotypes and *Mtb* could be exposed to varying environments depending on its location. Thus there is heterogeneity in *Mtb* subpopulations and design of new therapies need to take this in to account. Another important aspect of persistent infection is the host response, mainly the immune response which effectively contains *Mtb* but stops short of eliminating it. The mechanisms with respect to types of T cells

etc involved in persistent infection are still not completely understood and are relevant to vaccine development (Dorhoi and Kaufmann, 2009; Kaufmann, 2007). A better understanding and consideration of these phenomena, persistence and reactivation, in context of both *Mtb* and host is needed in the design and development of intervention methods.

#### 1.4 Intervention

Classically, two intervention strategies exist for infectious diseases: 1) Chemotherapy which aims at curing diseased individuals using chemical molecules which preferentially eliminate the pathogen and 2) Vaccination which aims at preventing infection in healthy individuals by priming their protective immune response. In the case of TB, both have existed since last century but recent escalation in cases has prompted research aimed at improving them.

BCG, an attenuated version of *M. bovis* is a neonatal vaccine which protects efficiently against childhood tuberculosis but is virtually ineffective against adult pulmonary tuberculosis. Presently, multipronged approaches with modification of current BCG combined with boost vaccines are being evaluated to deal with this issue (Kaufmann, 2005; Reece and Kaufmann, 2008). Chemotherapy which is more relevant to this study is described in detail below. Current strategies for TB control focuses on those with active disease thus eliminating chances of transmission but in order to achieve the ambitious goal of eradicating TB by 2050 the scientific community needs to come up with innovative ideas to tackle latency and drug resistance (Barry, et al., 2009; WHO, 2009).

##### 1.4.1 Drugs

Current treatment regimen against TB has not seen many changes since its inception more than 40 years ago. It is prolonged, taking up to 6-9 months, which has led to extensive patient non-compliance and thus emergence of drug resistance (Nathan, et al., 2008). Hence new drugs and/or regimens need to be urgently introduced to shorten treatment and in fact mathematical modelling predicts that if a 2 month regimen were introduced in 2012, it would prevent 20% of new cases and 25% of deaths in South-east Asia alone by 2020-30 (Salomon, et al., 2006).

One of the main reasons for this lengthy regimen is the ability of *Mtb* to shift to a non-replicating/persistent state in the host making it resistant to the current suite of anti-tuberculars (Sacchetti, et al., 2008). INH, EMB and RIF which are all part of the first line of therapy can kill or inhibit only actively multiplying bacteria. PZA, on the other hand, acts on less active bacteria in an acidic and hypoxic environment, the most likely situation inside macrophages and granuloma (Dover, et al., 2008). Thus, drugs targeting non-replicating/dormant bacteria are a main requirement to achieve the challenging goal of a short 2 month therapy.

Nevertheless, new molecules which target pathways distinct from that of current drugs are essential to tackle the existing problem of rampant drug resistance. Another major hurdle is the high prevalence of TB amongst HIV patients, calling for TB drugs which would not be antagonistic to current anti retro-virals.

#### 1.4.1.1 Current regimen

To improve or modify the present state of TB chemotherapy it is important to first understand the efficiency, mechanisms of action and resistance patterns of current drugs. Existing chemotherapeutic regimen consists of an initial 2 month phase with INH, RIF, PZA and EMB followed by a 4 month phase with INH and RIF (Mitchison, 2004). Second line drugs include aminoglycosides, polypeptides, fluoroquinolones, thioamides, cycloserine and p-aminosalicylic acid.

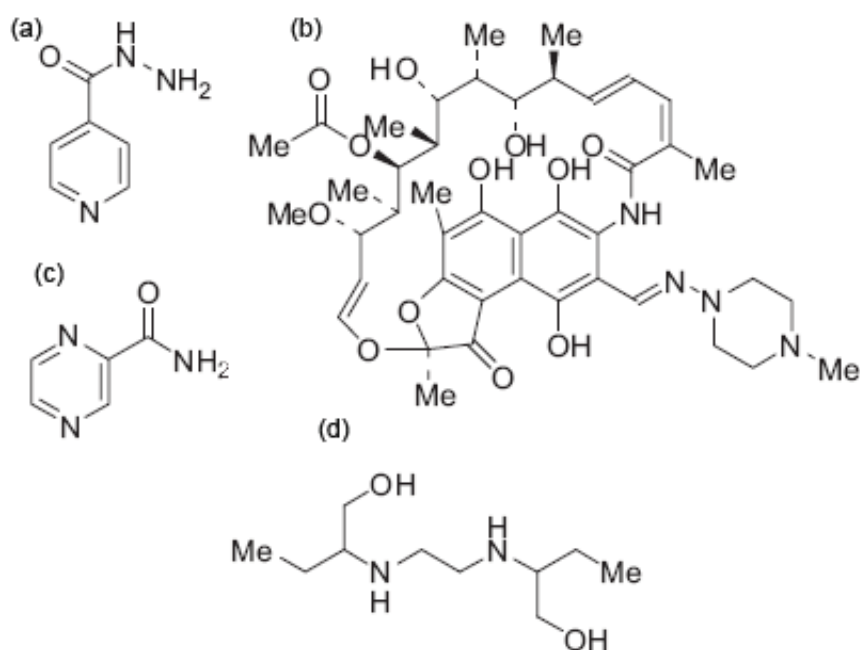


**Figure 6:** Current panel of drugs.

a) Isoniazid b) Rifampin c) Pyrazinamide d) Ethambutol

INH and EMB, as mentioned before, interfere with cell wall biosynthesis though at different points (Fig. 6 a & d). INH, belonging to the nicotinamide family, is still the most potent mycobactericidal drug with an MIC close to 0.2 $\mu$ g/ml (Bernstein, et al., 1952). INH is a pro-drug requiring activation by the catalase-peroxidase KatG leading to an INH-NAD adduct which binds to members of FAS II cycle (Zhang, et al., 1992). The exact target of INH is still a contentious issue with evidence suggesting involvement of InhA, the enoyl-ACP reductase and KasA, the  $\beta$ -Ketoacyl synthase (Banerjee, et al., 1994; Mdluli, et al., 1998). Regardless of this, INH blocks mycolic acid synthesis at level of meromycolic chain elongation leading to

accumulation of C<sub>24</sub>/C<sub>26</sub> fatty acids, drastic changes in cell wall envelope followed by cell lysis. Mutations in KatG, InhA and KasA have been implicated in INH resistance.

Ethionamide (ETH) is a second line drug whose mode of action is very similar to that of INH though a lack of cross-resistance suggests some uniqueness. Being a structural analogue of INH, ETH is also a pro drug though its activation route seems to be the distinctive characteristic. Two independent studies show that EthA, a FAD containing monooxygenase, and its repressor EthR play an important role in its activation and binding to InhA thus affecting mycolic acid synthesis (Baulard, et al., 2000; DeBarber, et al., 2000).

EMB belonging to the family of diamine analogues is another front line drug which interferes with cell wall synthesis as shown by the almost immediate destabilisation of cell envelope (Thomas, et al., 1961). Detailed radiolabel studies indicated that arabinogalactan synthesis was impaired at the level of arabinosyl transferases which was confirmed with resistance studies with mutants showing the EmbBAC arabinosyl transferase operon to be the target of EMB (Takayama and Kilburn, 1989; Telenti, et al., 1997).

PZA is another nicotinamide based anti-TB drug which needs activation by the *Mtb* protein PncA, a pyrazinamidase/nicotinamidase (Fig. 6 c) (Konno, et al., 1967). PZA is unique in that its high bactericidal activity is observed only *in vivo* while *in vitro* activity requires acidic pH and or hypoxia. This suggests activity against semi-dormant bacteria located inside cells and in anoxic or hypoxic lesions in the lung. There has been no clear resolution of its mechanism of action since resistant mutants mostly carry mutations in the activating PncA gene. Some studies suggest that it inhibits activity of the fatty acid synthase (Fas I) while others point to a dysregulation of plasma membrane potential (Zhang, et al., 2003; Zimhony, et al., 2000). Whatever might be the case it is generally accepted that PZA is one of the main factors responsible for shortening TB treatment from 9-12 months to 6-9 months.

RIF, a broad spectrum antibiotic and the other prominent mycobactericidal molecule, inhibits RNA synthesis by binding to the  $\beta$  subunit of the prokaryotic DNA-dependent RNA polymerase (Fig. 6 b) (Wehrli, 1983). This specific binding also prevents any toxic side effect on host cells since eukaryotic RNA polymerases are inhibited only at concentrations about 10<sup>4</sup> fold above MIC. The RIF-RNA polymerase complex is extremely stable though there are no covalent bonds formed between the two. Instead, hydrogen bonds and  $\Pi$ - $\Pi$  bond interactions involving aromatic residues in the protein are hypothesized to be responsible, hence mutations in the RpoB gene coding for the RNA polymerase mostly confer resistance to this drug. The main drawback of RIF is its inductive effect on cytochrome P450 enzymes leading to rapid



metabolism of certain AIDS drugs reducing efficiency of anti-retroviral (ARV) treatment in HIV co-infected individuals (Kwara, et al., 2005).

Second line anti-TB drugs are mostly less effective than the main front line drugs but are invaluable against drug resistant strains due to their distinct modes of action. Aminoglycosides like streptomycin, kanamycin and amikacin belong to this group and target 30S subunit of ribosomes inhibiting protein synthesis. Cyclic peptides like capreomycin and viomycin also target the ribosome machinery by binding to the interface between the subunits. Fluoroquinolones, on the other hand, act on DNA gyrases (Topoisomerase II) which maintain DNA supercoils necessary for DNA replication. Resistance to fluoroquinolones is attributed to stepwise mutations in the quinolone resistance determining region of *Mtb* GyrA and GyrB genes which encode topoisomerases (van den Boogaard, et al., 2009). The mechanism by which *p*-aminosalicylic acid inhibits *Mtb* growth is not well understood though thymidylate kinase and mycobactin synthesis pathways have been implicated.

#### **1.4.1.2 New drug candidates**

The current TB regimen is lengthy and involves multiple medications. Normal therapy requires 6-9 months whereas treatment of drug-resistant TB takes 18-24 months or even longer (Connolly, et al., 2007). Second-line drugs are also much more toxic and considerably more expensive than the standard first-line anti-TB regimen. Furthermore, current first-line treatment regimens are not compatible with certain common antiretroviral therapies used to treat HIV/AIDS (TBAlliance, 2009). Therefore, new drugs are needed that will be effective in treating children, and latent TB infection and will be compatible with antiretroviral therapy. A robust and sustainable pipeline of TB drug candidates and discovery programs has been initiated and some of the leading candidates in clinical trials are described below (TBAlliance, 2009).

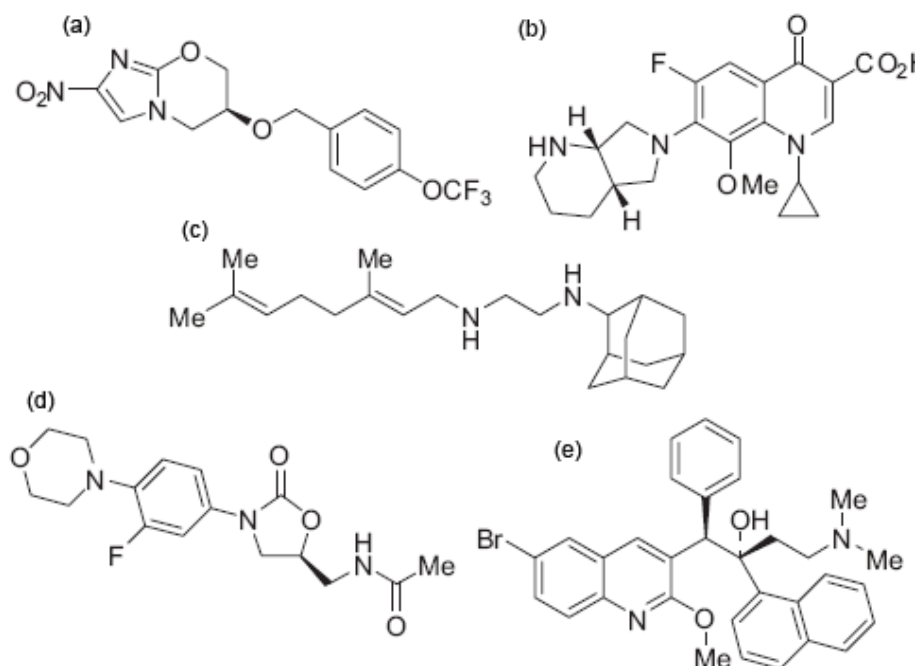


**Figure 7: New drug candidates.**

a) Moxifloxacin b) Linezolid c) SQ109 d) PA-824 e) TMC207

Cell wall synthesis inhibitors: Cell envelope continues to be the most attractive target for future TB drug development due to its proven essentiality for *Mtb* survival. Bicyclic nitroimidazoles like PA-284 and OPC-67683 are promising drug candidates now in clinical trials and are active not only against replicating bacteria but also those which are non-replicating due to hypoxia addressing the key issue of eradicating the so-called ‘dormant *Mtb*’ (Fig. 7 d) (Matsumoto, et al., 2006; Stover, et al., 2000). These pro-drugs are activated by the deazaflavin cofactor F420 and the non-essential F420 dependent glucose-6-phosphate dehydrogenase, Fgd1 and deazaflavin (F420) dependent nitroreductase, Ddn and mutations in these genes render *Mtb* highly resistant to PA-824 (Manjunatha, et al., 2006). Though both PA-824 and OPC-67683 affect the amount of mycolic acids specifically of oxygenated mycolic acids, in the case of PA-824, this cannot explain their activity against non-replicating bacteria since cell wall remodelling barely occurs in this metabolic state. Recent *in vitro* studies have shown a novel mechanism leading to formation of reactive nitrogen radicals within bacteria in the presence of PA-824 which could augment host macrophage induced reactive radicals attack (Singh, et al., 2008).

SQ109 is a diamine analogue derived from the EMB pharmacophore, much more active than EMB and displays strong synergy with INH and RIF (Fig. 7 c) (Protopopova, et al., 2005). In spite of high structural similarity there seems to be some mechanistic divergence between EMB and SQ109 avoiding issues of cross resistance.

DNA dependent process inhibitors: Moxifloxacin and gatifloxacin, fluoroquinolones targeting DNA gyrases, are favoured candidates for shortening TB treatment due to their lowest MIC's and hence highest bactericidal activities (Fig. 7 a) (Ji, et al., 1998). They are in advanced stages of clinical trials but the main concern is possibility of resistance due to the wide spread use of fluoroquinolones for other infections (Conde, et al., 2009). Rifapentine, belonging to the RIF family, is another molecule in clinical trials which has been favoured due to its synergy with moxifloxacin which might aid in shortening treatment duration. It also targets *Mtb* RNA polymerase like RIF, and has been hypothesised to act on latent bacilli and poses fewer drug-drug interactions unlike RIF.

Protein synthesis inhibitors: Linezolid belonging to the class of oxazolidinones is one of the few antibacterials targeting 50S subunit of the ribosome (Fig. 7 c) (Vera-Cabrera, et al., 2006). It binds to 23S rRNA inhibiting translations at an early phase preventing binding of formyl methionine tRNA. This distinct mechanism of protein synthesis inhibition makes it active against MDR strains of *Mtb*.

F<sub>0</sub>/F<sub>1</sub> ATPase inhibitor: TMC207, a diarylquinone, is a promising new mycobactericidal agent which shows equal activity against susceptible and drug resistant strains of *Mtb* (Fig. 7 e). It targets a novel pathway involving ATP synthesis drastically reducing possibilities of cross resistance (Andries, et al., 2005). It specifically targets the c subunit of membrane bound F<sub>0</sub> unit of ATP synthase and resistant strains harbour mutations in *AtpE* gene which synthesises this c subunit. It does not inhibit DNA gyrases indicating no commonality with fluoroquinolones.

These molecules represent some of the most advanced investigations in clinical trials but additionally, numerous initiatives have brought forth compounds in lead optimization as well as pre-clinical stages (StopTBPartnership, 2009). Encouragingly, most of these have been collaborative efforts between industry and academic institutions emphasizing the high success of this public-private partnership approach. More recently, novel compounds targeting *Mtb* pathways aiding its adaptation to the host environment have been identified paving way for a paradigm shift in TB drug discovery by establishing the host-pathogen interface as an important target (Bryk, et al., 2008; Lin, et al., 2009). Additionally studies aiming to improve efficacy of existing drugs like  $\beta$ -lactams and ethionamide have met with tremendous success against drug resistant strains as well (Hugonnet, et al., 2009; Willand, et al., 2009). Understanding the biology of persistent *Mtb* combined with development of more relevant models for this state would aid drug discovery move closer towards finding a lasting solution for this

age old problem. Nevertheless, keeping in mind the constant attrition in the drug discovery pipeline it is imperative to constantly feed it with new targets and molecules.

## 2 Aim of the study

The current high burden of tuberculosis worldwide has made it the focus of drug discovery initiatives in academia and industry. Drug resistance and persistence are pressing issues and have prompted research into novel targets which could be whole pathways or specific entities. The aim of this study is to evaluate one such target, Ag85C, by investigating the anti-mycobacterial activity of a panel of inhibitors, Ag85C- 1-4. Ag85C is a mycolyl transferase belonging to the highly conserved family of Ag85 complex proteins involved in the final steps of mycolic acid incorporation into the outer membrane of mycobacteria. INH, the most potent mycobactericidal drug targeting mycolic acid biosynthesis emphasises the essentiality of cell envelope for *Mtb* survival as well as its potential as a drug target. Ag85 proteins play a pivotal role in its biogenesis thus rendering Ag85C an attractive target for intervention.

The hits, Ag85C-1-4, against Ag85C were identified through nuclear magnetic resonance (NMR) screen of a small molecule library of 5000 compounds and based on binding to Ag85C. Ag85C-2-4 are analogues derived through structure activity relation (SAR) studies with Ag85C-1. Since these compounds bind to the active site domain of Ag85C and could hence interfere with cell envelope formation, their activity against *Mtb* in broth culture, inside macrophages and in granulomas in infected mouse lungs was examined. This also gives information about viable structural modifications of the starting moiety Ag85C-1 in terms of inhibitory potential against *Mtb*. Additionally the utility of Ag85C inhibitors in tackling drug resistance was examined. An MDR strain of *Mtb* resistant to INH and RIF was used to test the activity of compounds since this would give information about cross resistance patterns.

Detailed characterization of the functional impact of one of the analogues, Ag85C-3, was undertaken with the aim of identifying its modes of action. Ag85 complex catalyse the transfer of mycolic acids to the two main components of *Mtb* cell outer membrane namely, mAGP and TDM. Hence biochemical analysis of cell wall lipids with an emphasis on mycolic acid containing species was performed. These lipids also contribute to the structural integrity of the cell envelope of *Mtb* rendering it highly resistant to harsh treatments and environments. Therefore, possible effect of Ag85C inhibitor on permeability of the external envelope was investigated. Specificity is another major concern and this has been addressed by testing the compound against the *Mtb* mutant strain lacking Ag85C.

Further, to gain better understanding of mycobacterial pathways perturbed by the compound microarray based analysis of gene expression patterns upon Ag85C-3 treatment *in vitro* has also been done. This gives a more complete picture of the impact of Ag85C-3 and Ag85C inhibition on the signalling networks in *Mtb*. Some of the most promising hits which were

involved in iron homeostasis were investigated in detail to gain insights in to their probable role in toxicity and/or *Mtb* cell envelope modification. This information is invaluable for future strategies for compound modification in order to improve its efficacy.

### 3 Results

#### 3.1 *In vitro* anti-mycobacterial activity

The panel of compounds Ag85C-1-4 were found to bind to Ag85C as detected by NMR studies. Ag85C-1 is the starting structure and Ag85C-2-4 are the modifications derived through Structure activity relation (SAR) studies (Appendix 8.1 Fig. 24). These compounds also inhibited growth of the fast growing non-pathogenic species of mycobacteria, *Mycobacterium smegmatis* (*Msmeg*), as observed with qualitative assay (Schade, M. et al, unpublished data).

Ag85C protein with the other Ag85 complex proteins, Ag85A and B, play an important role in cell envelope synthesis of mycobacteria and consequently their survival. They are periplasmic transferases which catalyse the transfer of mycolic acids to its substrates to give rise to the final components, mAGP and TDM, of the mycolic acid rich outer membrane (Armitige, et al., 2000; Belisle, et al., 1997; Jackson, et al., 1999; Puech, et al., 2000). Hence, these compounds were evaluated for activity against pathogenic *Mtb* lab strain H37Rv grown in enriched liquid medium. A qualitative resazurin based assay relying on colorimetric detection of live versus dead bacteria was first used. This was followed by a quantitative assessment of transcriptional activity of bacteria which correlates with number of live bacteria.

##### 3.1.1 Qualitative assay of anti-mycobacterial activity

The resazurin based assay is a standard test to monitor anti microbial compounds (Gabrielson, et al., 2002; Yajko, et al., 1995). It is based on reduction of active blue colored compound resazurin to red fluorescent compound resarufin by enzymes in the electron transport system of living cells. Dead cells are unable to perform this conversion thus facilitating visual detection of inhibition. Log phase culture of *Mtb* was diluted in rich 7H9 medium and treated with varying concentrations of compounds in a 96 well plate format for 96 hours at 37°C. The blue 'alar blue' reagent containing resazurin was then added and incubated with the samples for another 24 hours at 37°C. The visual colour change was then captured on digital camera. Thus, this is an end point assay which gives an indication of the cumulative effect of the tested compounds on *Mtb*.

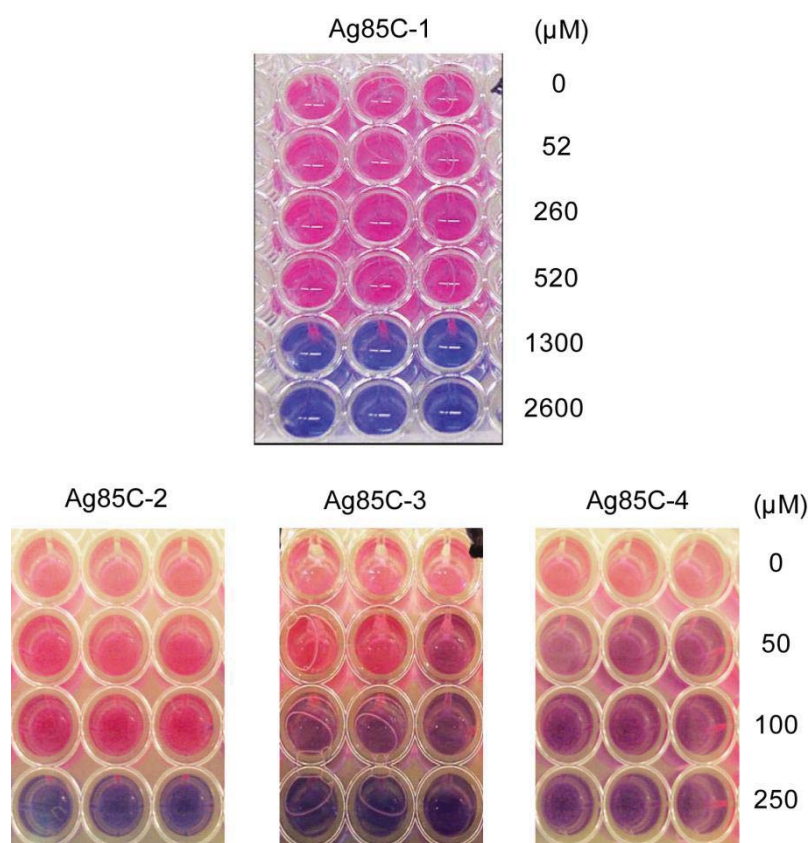


**Figure 8: Alamar blue assay.**

*Mtb* H37Rv from log phase culture was diluted 1:25 in 7H9 medium without detergent. 100μl of this suspension was added to 100μl of same medium containing the compounds Ag85C-1, 2, 3 and 4 at the indicated concentrations in 96 well plates and incubated at 37°C for 96 hours. 50μl of alamar blue substrate was added and colour change from pink (live bacteria) to blue (dead bacteria) monitored after 24 hours.

Ag85C-1, the starting compound, was first tested. It inhibited growth of *Mtb* at millimolar concentrations starting from 1.3mM (Fig. 8). Modified compounds, Ag85C- 2, 3 and 4, were then tested. They had improved activity with inhibitory concentrations in the micro molar range starting at 250μM for Ag85C-2, 100μM for Ag85C-3 and 50μM for Ag85C-4, thus, supporting the SAR studies (Fig. 8). Therefore, Ag85C-1-4 which bind to Ag85C also inhibit growth of *Mtb* in 7H9 medium.

### 3.1.2 Quantitative assay of anti-mycobacterial activity

Further detailed investigation of the inhibitory profile of the analogues, Ag85C-2-4, was performed due to their lower micromolar values of putative MIC. [<sup>3</sup>H]-uracil incorporation assay is a highly sensitive method to determine number of viable mycobacteria over time (Benitez, et al., 1974). It is based on incorporation of radioactive uracil into mRNA during transcription in living, dividing bacterial cells. The scintillation counts directly correlate with number of live bacteria in an actively growing population. Uptake of radiolabel by live bacteria was measured after compound treatment. Log phase culture of *Mtb* was treated with 50, 100 and 250 μM of compounds and fed with 1μCi of [<sup>3</sup>H]-uracil for 24 hours at 24, 72 and 120 hours



post treatment. Since the assay is performed over a period of 120 hours it gives additional information about the rate of inhibition over time.

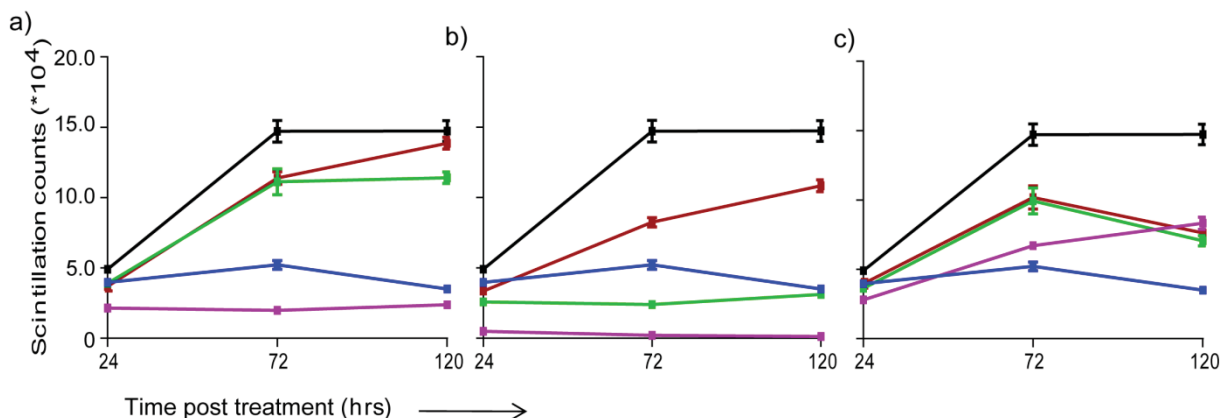


**Figure 9:** [<sup>3</sup>H]-Uracil incorporation assay

*Mtb* H37Rv from log phase culture was added at a density of 10<sup>7</sup> bacteria/ml to 100µl of 7H9 medium without detergent containing the indicated concentrations of compounds Ag85C-2, 3 and 4 in 96 well plates. 1µCi of [<sup>3</sup>H]-Uracil was added to each well 24 hours prior to each time point and plates frozen and fixed. Scintillation counts were then measured with TopCount (Perkin Elmer) (a) Ag85C-2 (b) Ag85C-3 (c) Ag85C-4. Untreated (■), 50µM (■), 100µM (■), 250µM (■) and Isoniazid-10µM (■). Average of hex-plicates for each condition was calculated with standard deviation and plotted.

Scintillation counts on the Y axis determine the number of bacteria and thus the degree of inhibition while the duration of treatment is plotted on the X axis in hours. Untreated bacteria (■) serve as the standard against which activity of each compound is measured. Ag85C-2 reduced scintillation counts by about 85% at 250µM both at 72 and 120 hours after treatment while lower concentrations did not have a significant effect (Fig. 9 a). Ag85C-3 was observed to be more potent since 100µM and 250µM showed reduction which began at 24 hours and persisted till later time points. 100µM caused a strong reduction of up to 80% at 120 hours and 250µM reduced counts up to 99% while 50µM had a smaller yet significant effect of 26% reduction (Fig. 9 b). Ag85C-4, on the other hand, showed an effect at 50, 100 and 250µM but only at the later time point of 120 hours post treatment (Fig. 9 c). INH, a first-line anti tuberculosis drug was used at 10µM as a positive control (Dover, et al., 2008).

Thus the analogues Ag85C-2-4 inhibited growth of *Mtb* in broth culture over a period of 120 hours. Each compound had a distinct pattern of inhibition with Ag85C-3 showing the strongest effect. These quantitative studies also correlated well with the qualitative alamar blue assay, reinforcing the latter as a reliable tool to screen potential lead compounds rapidly.

### 3.1.3 Activity against drug resistant strains

Emergence of drug resistance is one of the main concerns of public healthcare systems in developing countries since it could lead to potentially incurable cases of TB as well as increase the expenditure of therapy (Kaufmann and Parida, 2007; Nathan, et al., 2008). Inhibitors targeting molecules or pathways distinct from that of current TB drugs are urgently needed to

tackle this issue. In this context, the most active analogue, Ag85C-3, was tested against a clinical multi drug resistant (MDR) isolate of *Mtb*, SROB3023. MDR refers to resistance against INH and RIF irrespective of susceptibility to other first line or second line drugs. The simple colorimetric assay was used to observe activity of Ag85C-3 at 50, 100 and 250  $\mu$ M. INH at 100  $\mu$ g/ml was included to confirm resistance.

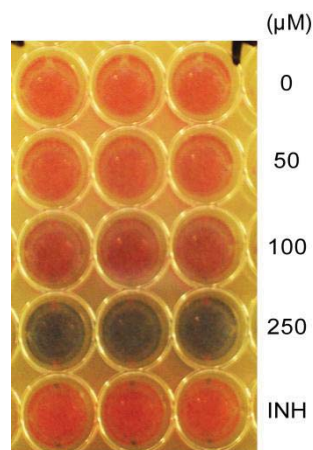


**Figure 10: Alamar blue assay with MDR *Mtb*.**

SROB3023 from log phase culture was diluted 1:25 in 7H9 medium without detergent. 100  $\mu$ l of this suspension was added to 100  $\mu$ l of same medium containing the compound Ag85C-3 at the indicated concentrations in 96 well plate and incubated at 37°C for 96 hours. 50  $\mu$ l of alamar blue substrate was added and colour change from pink (live bacteria) to blue (dead bacteria) monitored after 24 hours.

As shown in Figure 10, Ag85C-3 inhibited growth of the MDR strain at 100  $\mu$ M as indicated by slight colour change to purple while at 250  $\mu$ M the inhibition is complete. INH at 100  $\mu$ g/ml had no effect on this strain confirming its resistance pattern. Therefore, Ag85C-3 induced toxicity by a mechanism distinct from that employed by INH and RIF since the pattern of inhibition is identical to that observed with lab strain H37Rv. Ag85C-3 is thus an attractive starting molecule for research in to novel targets and pathways in TB drug discovery.

### 3.2 Growth of mycobacteria in macrophages

In the initial stage of infection, upon being inhaled, *Mtb* crosses the epithelial barriers of the alveoli to be taken up by host macrophages (Cosma, et al., 2003). Although macrophages are programmed to destroy invading pathogens, mycobacteria are able to circumvent microbicidal pathways and establish a safe niche inside macrophages (Kaufmann, 2001). Thus macrophages are the primary cells which harbour and promote infection. Signalling by these infected cells leads to formation of classical organized cellular structures called granulomas made up of T cells, dendritic cells, a few B cells and fibroblasts in addition to macrophages (Russell, 2007). TB pathogenesis progresses from these granulomas in lungs.

Since Ag85C-2-4 showed a direct effect on replicating *Mtb*, as a next step, their activity on phagocytosed bacteria was assessed. For this, an *ex vivo* model system was set up using primary mouse bone-marrow derived macrophages.

### 3.2.1 Toxicity

Ag85C-2-4 are hydrophobic molecules with low solubility in aqueous solutions and stock solutions are prepared in dimethyl sulfoxide. Hence, their toxic side effects were determined before testing on *Mtb* residing in primary macrophages. For this the simple MTT assay was used. It is based on reduction of yellow MTT (3-(4,5-Dimethylthiazol-2-yl)-2,5-diphenyltetrazolium bromide, a tetrazole) by enzymes in the electron transport system of live cells to purple formazan (Mosmann, 1983). Formazan has an absorbance peak at 550nm which is used to quantify its amounts.

Macrophages were generated from bone marrow derived monocytes obtained from C57BL/6 mice through standard differentiation protocols (Austin, et al., 1971). These were then treated with varying concentrations of compounds and incubated at 37°C for 48 and 96 hours. MTT was fed to these cells for 3 hours to facilitate production of formazan which was then measured. As shown, Ag85C-2, -3 and -4 did not have any cytotoxic side-effects on the macrophages at concentrations up to 100µM, higher concentrations were toxic (Fig. 11).

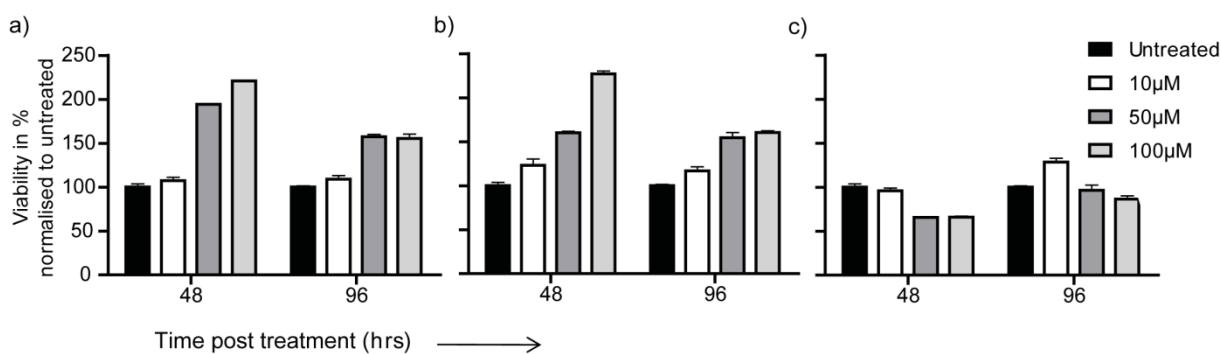


**Figure 11: MTT assay for toxicity.**

Primary macrophages obtained by differentiation of mouse bone marrow derived monocytes were plated at a density of  $3 \times 10^5$  cells/well in 48 well plate. The cells were incubated overnight at 37°C to allow complete adhesion. Compounds were then added at 10, 50 and 100µM and incubation continued. At 48 and 96 hours post treatment MTT was added to each well at 50µg/ml concentration for 3 hours to allow formation of purple formazan product. Cells were then solubilised in 100µl of dimethylsulfoxide and absorbance measured at 550nm. Viability was calculated in % with untreated sample taken as 100%. (a) Ag85C-2 (b) Ag85C-3 (c) Ag85C-4. Average of triplicates for each condition was calculated with standard deviation and plotted.

### 3.2.2 [<sup>3</sup>H]-Uracil incorporation assay

[<sup>3</sup>H]-Uracil incorporation by active bacteria was used to analyse effect of Ag85C-2, 3 and 4 on intracellular bacteria. This assay provides a much faster read-out of the impact of these compounds when compared with the conventional colony forming unit (CFU) assay. Primary

mouse bone marrow derived macrophages were infected with *Mtb* H37Rv at a multiplicity of infection (MOI) of 5 for 4 hours to allow complete phagocytosis. Compounds were added to media at 10, 50 and 100 $\mu$ M and tritiated uracil fed for 24 hours at 24, 72 and 120 hours post treatment. Thus this method measures effect of compounds on internalised bacteria and also provides kinetics of the inhibition, if any. In comparison transcriptional activity of macrophages is only to background levels.

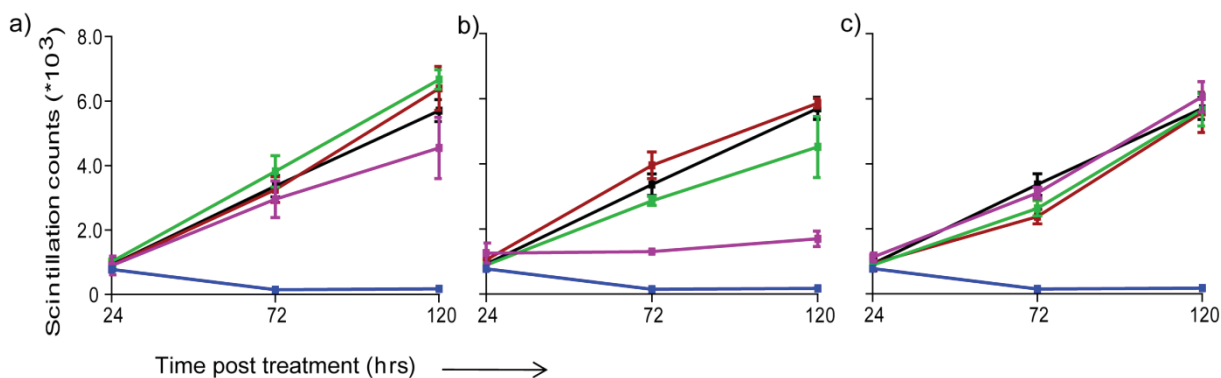


**Figure 12: Inhibition of *Mtb* residing in macrophages.**

Primary mouse bone marrow derived macrophages were infected with log-phase *Mtb* H37Rv at an MOI of 5:1. After 4 hours of incubation at 37 $^{\circ}$ C to allow complete phagocytosis, fresh medium was added with indicated concentrations of compounds Ag85C-2, 3 and 4. 1 $\mu$ Ci of [<sup>3</sup>H]-Uracil was added to each sample 24 hours prior to each time point and plates frozen and fixed. Scintillation counts were then measured with TopCount (Perkin Elmer) (a) Ag85C-2 (b) Ag85C-3 (c) Ag85C-4. Untreated (■), 10 $\mu$ M (■), 50 $\mu$ M (■), 100 $\mu$ M (■) and Isoniazid-100 $\mu$ M (■). Average of hex-plicates for each condition was calculated with standard deviation and plotted.

Infected cells which were not treated were the standard against which effect of Ag85C-2-4 was measured. Ag85C-3 showed a slight reduction in scintillation counts at 50 $\mu$ M after 120 hours of treatment while 10 $\mu$ M had no effect at any time points (Fig. 12 b). At 100 $\mu$ M the inhibition was about 40% at the earlier time point of 72 hours post treatment and was up to 70% after 120 hours. INH at 100 $\mu$ M was the positive control and reduced the scintillation counts close to 99%. Meanwhile Ag85C-2 and -4 had no effect on intracellular bacteria at these concentration ranges (Fig. 12 a & c). Ag85C-1 was tested at higher mill molar concentrations and did not show any effect as well (data not shown).

In conclusion, one of the analogues, Ag85C-3, did inhibit growth of *Mtb* inside resting macrophages, while the other two were inactive under these conditions. [<sup>3</sup>H]-Uracil incorporation thus provides a fast and reliable indication of activity of compounds in a cell-based infection model as well.

### 3.2.3 Colony forming unit measurement

The ability of Ag85C-3 to kill intracellular bacteria was confirmed by measuring number of colony forming units (CFU) of *Mtb* inside treated macrophages. Mouse bone marrow derived macrophages were infected with *Mtb* at a low MOI of 5 for 4 hours, washed with PBS to re-

move non-internalised bacteria and treated with Ag85C-3. 24, 72 and 120 hours post treatment cells were lysed, lysate dilutions plated out and colonies counted after 3 weeks of incubation at 37°C. 50 and 100µM of Ag85C-3 was used with INH at 50µM as the positive control. As shown in Figure 13, at a later time point of 120 hours post infection 100µM reduced CFU by about 40% while there was no effect at earlier time points and at a lower concentration of 50µM. INH cleared intracellular *Mtb* up to 99%.

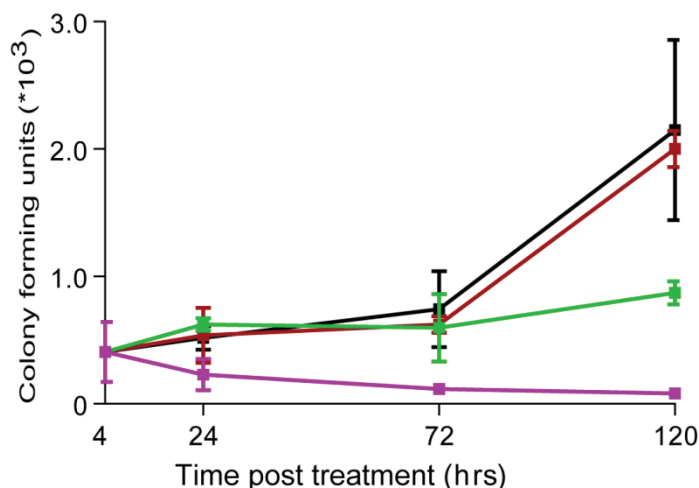


**Figure 13: Colony forming units (CFU) measurement.**

Primary mouse bone marrow derived macrophages were infected with log-phase *Mtb* H37Rv at an MOI of 5:1. After 4 hours of incubation at 37°C to allow complete phagocytosis cells were washed with PBS and fresh medium added with indicated concentrations of Ag85C-3. At each time point cells were lysed, dilutions prepared and plating done on 7H11 agar. CFU was measured after 3 weeks of incubation at 37°C. Untreated (■) 50µM (■) 100µM (■) and Isoniazid at 50µM (■). Average of triplicates for each treatment was calculated with standard deviation and plotted.

### 3.3 *In vivo* studies

Efficacy of Ag85C-3 in an *in vivo* model of TB infection was assessed to estimate its potential as a drug candidate. The mouse is one of the best established animal models of TB due to the ease of manipulation, availability of mutants and genetically altered strains and the wide range of reagents developed for analysis (Flynn, 2006). Mice are relatively resistant to *Mtb* leading to a contained infection. Infection of C57BL/6 mice via aerosol or intravenous routes displays a distinct profile with an initial acute phase of multiplication lasting up to 4 weeks arrested by the onset of adaptive response. The bacterial numbers then stabilize giving rise to the plateau phase with approximately one million CFU in the lungs. Within the acute phase of infection *Mtb* also disseminates to the spleen and liver after aerosol infection (Stewart, et al., 2003). Varied mouse strains, modes of infection and drug application have been developed to measure efficacy of drugs. In this study the resistant C57BL/6 mice were used with intranasal administration of compound. This experiment was done once with the aim of optimising parameters for future experiments.

Since aerosol is the more physiologically relevant means of infection, C57BL/6 mice were exposed to aerosolized *Mtb* H37Rv at 50-100 CFU/mouse. On the seventh day post infection dosage of Ag85C-3 and INH was started with Ag85C-3 administered at 0.5 and 1mM and INH at 100 $\mu$ M. Combination of Ag85C-3 and INH was also administered. The compounds were applied intranasal every alternate day for two weeks due to the expected direct access to lungs by the comparatively lower amounts of compound. One and three weeks after completion of treatment mice were sacrificed, lungs homogenized and dilutions plated out on 7H11 agar plates. CFUs visible after 21 days of incubation at 37°C were counted and plotted.

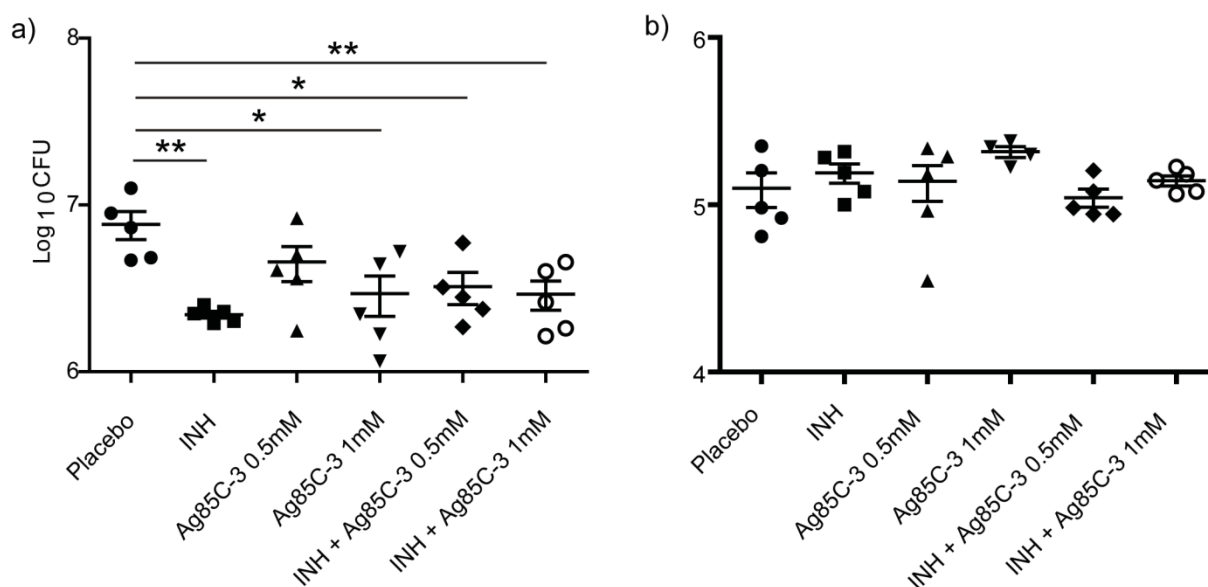


**Figure 14: Mouse model of TB infection.**

C57BL/6 mice in groups of five were exposed to aerosolized *Mtb* H37Rv at a density of 50-100 CFU per mouse. Dosage of compounds, Ag85C-3 at 0.5mM and 1mM and INH at 100 $\mu$ M, was started 7 days after infection and administered every alternate day for 2 weeks. Placebo refers to control group which were administered DMSO, the Ag85C-3 solvent. On day 28 and day 42 post infection mice were sacrificed, lungs homogenized and plated out. CFUs were observed after 21 days of incubation at 37°C and were counted. a) Day 28 CFU counts in logarithmic scale to base 10 b) Day 42 CFU counts in logarithmic scale to base 10. Average of 2 dilutions for each mouse was calculated and plotted, the mean value is indicated. `\*\*\*` indicates  $p < 0.01$  and `\*` indicates  $p < 0.05$  where  $p$  is significance calculated by Mann-Whitney test.

At the early time point of 28 days post infection which is one week after completion of compound administration a mild effect could be observed. INH at 100 $\mu$ M reduced CFU counts by 0.5 log units while Ag85C-3 at 1mM and in combination with INH reduced CFU counts by approximately 0.4 log units in each case (Fig. 24 a). But at the later time point of 42 days post-infection this reduction was no longer observed (Fig. 24 b). Moreover, the CFU counts was also lower than the earlier time point which suggests that probably in these mice the infection had not established itself normally or the initial inhaled CFU numbers itself were lower. Nevertheless, this data reveal that Ag85C-3 does have some effect on survival of *Mtb* inside mouse lungs and does not antagonise activity of INH. Additionally the comparatively

short duration of treatment might have caused the reduced phenotype and further optimisation of this set up is necessary for a more complete analysis.

Hence the panel of compounds, Ag85C-1-4, which bind to Ag85C at the active site also inhibited growth of broth cultured *Mtb*, though at differing concentration ranges and showed distinct patterns of inhibition over time. In the *ex vivo* system mimicking *Mtb* survival in its primary host cells, macrophages, they had varied effects with Ag85C-3 being the only active molecule. This again emphasizes the differences between the two systems used for testing activity. Ag85C-3 also decreased survival of *Mtb* in mouse lungs at early time points after treatment. Nevertheless, these experiments clearly demonstrated that the compounds under study which bind to Ag85C also inhibited growth of *Mtb* both directly as well as in the macrophage and mouse lung granuloma stage. The most potent analogue, Ag85C-3 also reduced growth of a MDR strain of *Mtb* underlining its utility as a novel inhibitor. To better characterize Ag85C-3, detailed investigation of its mode of action in whole *Mtb* cells was undertaken.

### 3.4 *Mtb* lipid analysis

Ag85 complex proteins function in the transfer of mycolic acids, major components of mycobacterial cell wall, to TMM and cell wall linked arabinogalactan-peptidoglycan to generate trehalose TDM (cord factor) and mAGP (Belisle, et al., 1997; Jackson, et al., 1999; Takayama, et al., 2005). Mycolic acids are very long chain  $\alpha$ -alkyl  $\beta$ -hydroxy fatty acids, the hallmark of *Mycobacteria*, and essential for maintaining integrity of its complex envelope (Marrakchi, et al., 2008). A disruption of its synthesis, for example, by the first line drug INH which targets the initial steps of mycolic acid synthesis pathway, leads to immediate death (Marrakchi, et al., 2000). INH is by far the strongest mycobactericidal compound available for treatment underlining the importance of cell wall to mycobacterial survival. Hence it could be that inhibition of the final steps in this pathway by Ag85C antagonists induces toxicity.

To analyse this, synthesis of mycolic acid containing lipids of *Mtb* cell wall was investigated during treatment with Ag85C-3. Sodium acetate labelled with [ $^{14}\text{C}$ ] was used as precursor to label mycolic acid species. Crude lipid extraction yielded loosely bound lipid extractibles containing TDM, TMM and phospholipids and delipidated cells which had the mAGP attached to their surface. These samples were then subjected to standard thin layer chromatography (TLC) accompanied with biochemical manipulation, where necessary, to assess the synthesis of lipids, visible as distinct bands. A systematic study of all the mycolic acid carrying species was performed to ascertain if Ag85C-3 had any impact on this pathway.

#### 3.4.1 TDM and TMM

TDM and TMM are found non-covalently attached to outer surface of *Mtb* cell envelope and numerous studies have implicated TDM as a virulence factor (Glickman, 2008). It induces granuloma like structures when administered to mice and also initiates pro-inflammatory response in macrophages (Indrigo, et al., 2002; Perez, et al., 2000). To measure amount of TDM and TMM synthesized during compound treatment, log phase cultures of *Mtb* were treated with 50 and 100 $\mu$ M of compound or left untreated for 48 hours. Then [ $^{14}$ C]-acetate was added and its incorporation into the lipid fraction allowed for 24 hours. The crude lipid extractible obtained was separated by TLC with Chloroform/Methanol/Water, 30:8:1, as solvent (Fig. 15 a) on a silica gel matrix. With this solvent TDM migrates with a retention factor ( $R_f$ ) of 0.81 while TMM has an  $R_f$  of about 0.48. Phospholipid bands are observed below TMM. The bands corresponding to TDM and TMM were densitometrically analysed by ImageQuant software.

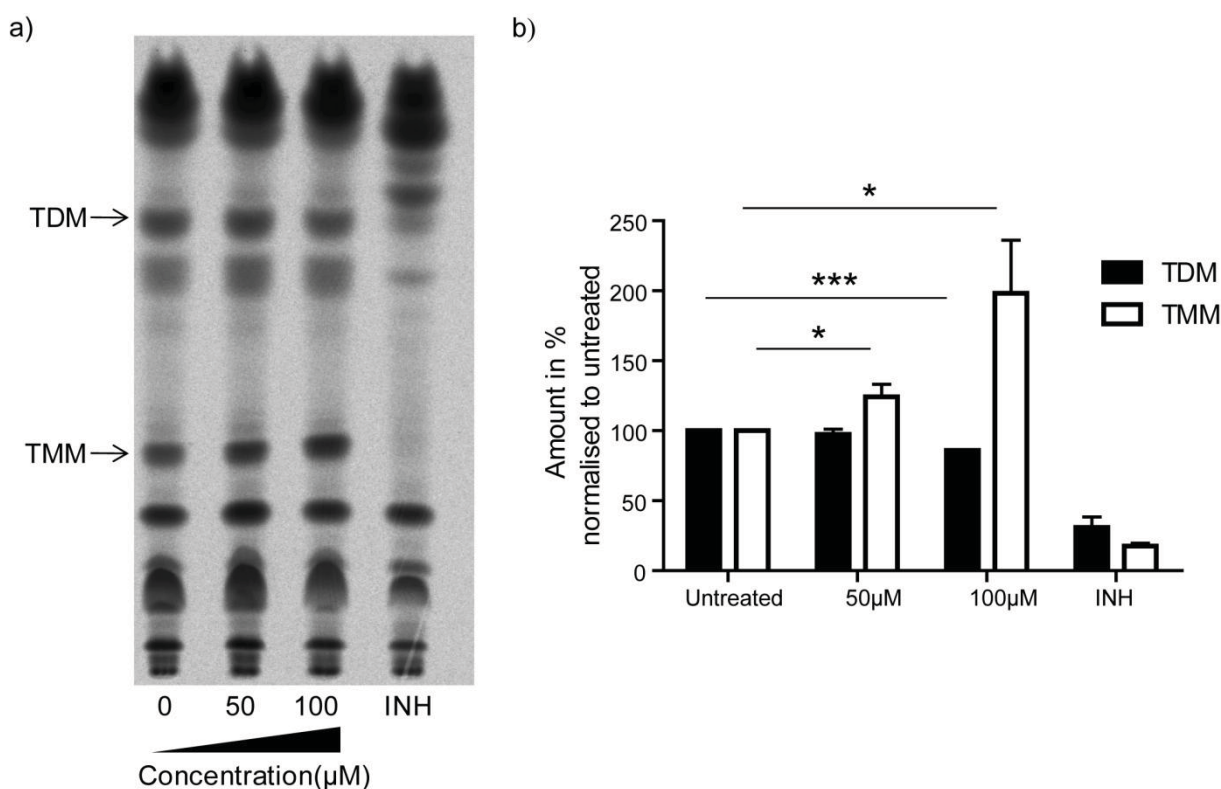


**Figure 15: Synthesis of TDM and TMM.**

*Mtb* H37Rv was grown in 7H9 medium without detergent to an  $OD_{580}$  of 0.3 to 0.4. Ag85C-3 was added to the culture at indicated concentrations and incubated at 37 $^{\circ}$ C with mild shaking for 48 hours. To label lipids [ $^{14}$ C]-acetate was added at a rate of 0.5 $\mu$ Ci/ml and incorporation allowed for 24 hours. Lipid extraction was then performed (a) TLC of lipid extractible fraction containing TDM and TMM with  $CHCl_3/CH_3OH/H_2O$  (30:8:1) (b) Intensity of TDM and TMM bands in TLC. Untreated is taken as 100%. Average value from 3 independent experiments was calculated with standard deviation and plotted. ‘\*’ indicates  $p < 0.05$ , ‘\*\*\*’ indicates  $p < 0.001$  where  $p$  denotes significance calculated by paired Student’s t-test. INH is Isoniazid at 10 $\mu$ M.

As shown in Figure 15 b, 100 $\mu$ M of Ag85C-3 reduced TDM synthesis by 14% accompanied by up to 100% increase in TMM while 50 $\mu$ M had no impact on TDM amounts but increased



TMM by about 25%. INH at 10 $\mu$ M reduced the amounts of both TDM and TMM since it affects the synthesis of mycolic acids at the earlier step of FAS-II cycle in mycolic acid biosynthesis. This strongly suggests inhibition of the mycolyl transferase step by Ag85C-3 since the substrate of the reaction, TMM, accumulated significantly while the product, TDM, was reduced. The extent of TDM reduction was small possibly due to a significant increase in number of bacteria treated with same amount of compound in this experimental set-up required to detect lipids. Thus 100 $\mu$ M is most likely a sub-optimal concentration where the inhibition is underway. At higher concentrations like 250 $\mu$ M the TDM band was completely abolished (data not shown). These results demonstrated that Ag85C-3 inhibited mycolyl transferase reaction catalysed by its target, Ag85C.

### 3.4.2 Free mycolic acids

Upon compound treatment it was observed that a band migrating very high with the solvent CHCl<sub>3</sub>/CH<sub>3</sub>OH (90:10) showed increased intensity (Fig. 16 c). It was speculated that it could be glycerol monomycolate (GMM), another mycolic acid containing moiety observed in extractable lipids. Consequently TLC was done with the solvent CHCl<sub>3</sub>/CH<sub>3</sub>OH (9:1) with purified glycerol monomycolate as standard (purified from extractable lipids of *Mtb* H37Rv by column chromatography). But it was observed that the band had an R<sub>f</sub> higher than GMM suggesting it could be a different lipid entity. Additionally, it was also observed that INH treatment abrogated this band indicating that this molecule contained mycolic acids (Fig. 16 c).

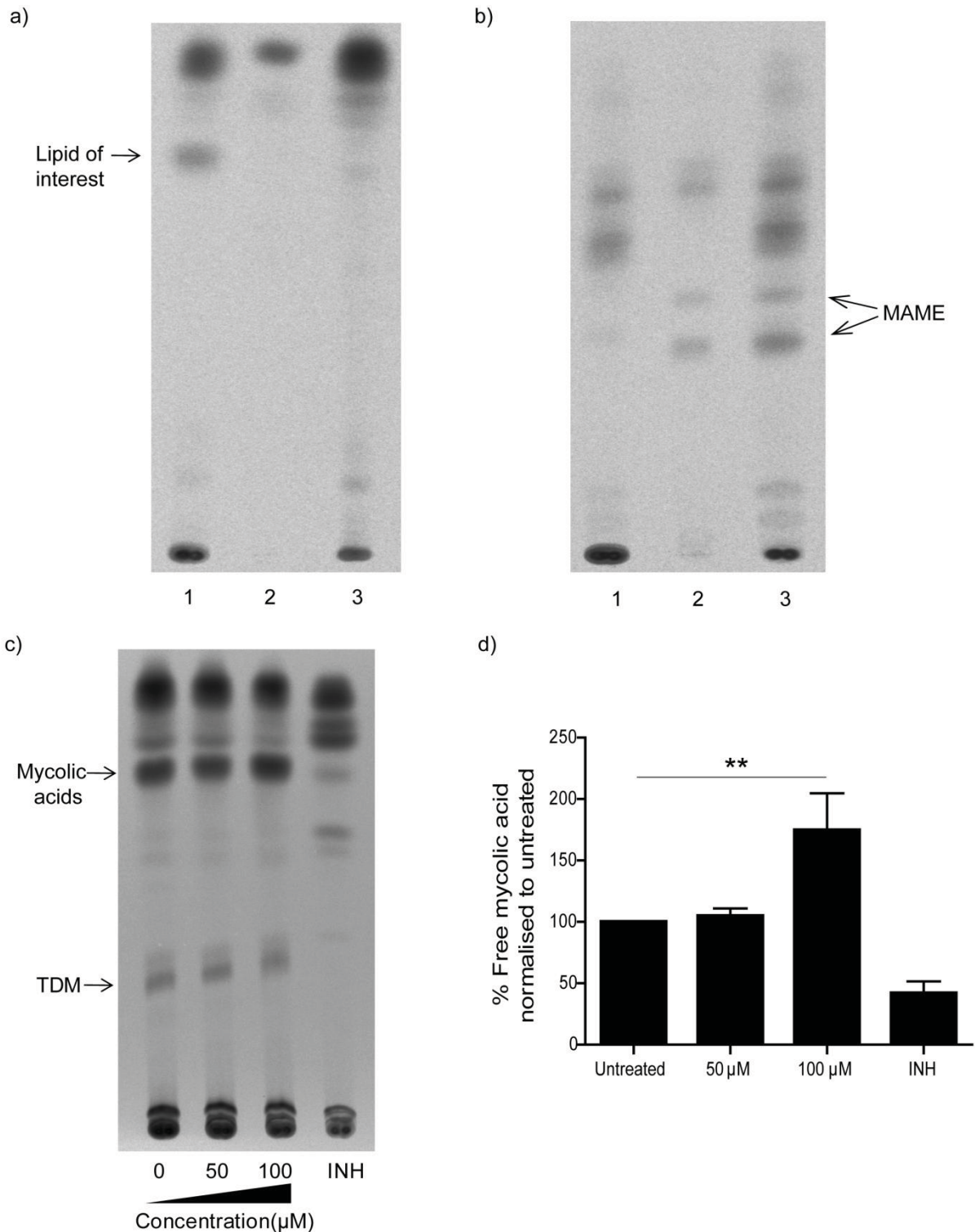


**Figure 16: Detection and quantification of free mycolic acids.**

Lipid extractible from *Mtb* H37Rv was left untreated (Lane 1), saponified and methylated (Lane 2) or methylated (Lane 3) (a) TLC of the treated samples run with the solvent  $\text{CHCl}_3/\text{CH}_3\text{OH}$  (9:1), the unknown lipid of interest is indicated (b) TLC of the treated samples run with  $\text{CH}_2\text{Cl}_2$  as solvent, Mycolic acid methyl esters (MAME) is indicated (c) TLC of lipid extractible from *Mtb* H37Rv treated with indicated concentrations of Ag85C-3 run with the solvent  $\text{CHCl}_3/\text{CH}_3\text{OH}$  (9:1) (d) Band intensity of free mycolic acids in the TLC, average value from 3 independent experiments was calculated with standard deviation and plotted. INH is Isoniazid at  $10\mu\text{M}$ . ‘\*\*\*’ indicates  $p < 0.01$  where  $p$  denotes significance calculated by paired Students t-test.

To resolve the identity of this species, a lipid extractible sample was taken and split into 3 parts, one untreated (Fig. 15 a & b, Lane 1), the second saponified and then methylated (Fig.

16 a & b, Lane 2), and the third only methylated (Fig. 16 a & b, Lane 3). Saponification refers to treatment with strong alkali to break ester bonds to release fatty acid moiety while methylation is treatment with highly reactive diazomethane species which methylates the free acyl moiety to yield methyl esters. Methyl esters of mycolic acids referred to as MAMEs (Mycolic acid methyl esters) have characteristic migration pattern with dichloromethane solvent. So if this molecule had mycolic acid esterified to an unknown substrate it would give rise to MAME in the second treatment. If it was free mycolic acid it would give rise to MAMEs in both the second and third treatments. Analysis of the sample clearly showed that the latter was true since MAME bands could be visualised in lanes 2 and 3 of Figure 16 b with dichloromethane as solvent. Further, the band of interest vanished when sample was methylated (Fig. 16 a, Lane 3) or saponified and methylated (Fig. 16 a, Lane 2) and run with Chloroform/Methanol (9:1) as solvent, clearly showing that it is indeed free mycolic acids.

Quantification of the free mycolic acid band intensity showed that there was an increase of up to 100% of free mycolic acids with 100 $\mu$ M of Ag85C-3 (Fig. 16 d). This is a surprising finding and could most likely be a consequence of the block in transferase reaction.

### 3.4.3 Time course analysis of TDM, TMM and free mycolic acid biosynthesis

Free mycolic acids have not been detected in log phase culture of *Mtb*. Hence it was surprising to observe them in lipid extractible of untreated and treated samples. Studies with *M. smegmatis* and *Mtb* biofilms have reported copious amounts of free mycolic acids which were also secreted externally (Ojha, et al., 2008).

The accumulated mycolic acids observed with 100 $\mu$ M of Ag85C-3 could either be degradation products from TDM and TMM or have previously uncharacterized role as precursors of these glycolipids. To better understand this, kinetic analysis of TDM, TMM and free mycolic acid synthesis in lipid extractible of *Mtb* H37Rv was undertaken. [ $^{14}$ C]- sodium acetate was fed to mid-log phase culture of *Mtb* and lipid extraction performed after 45 minutes (Lane 1), 1.5 hours (Lane 2), 3 hours (Lane 3), 6 hours (Lane 4) and 24 hours (Lane 5) respectively (Fig.17). The lipid extractible was run with two different solvent systems separately to visualise TMM, TDM and free mycolic acids.

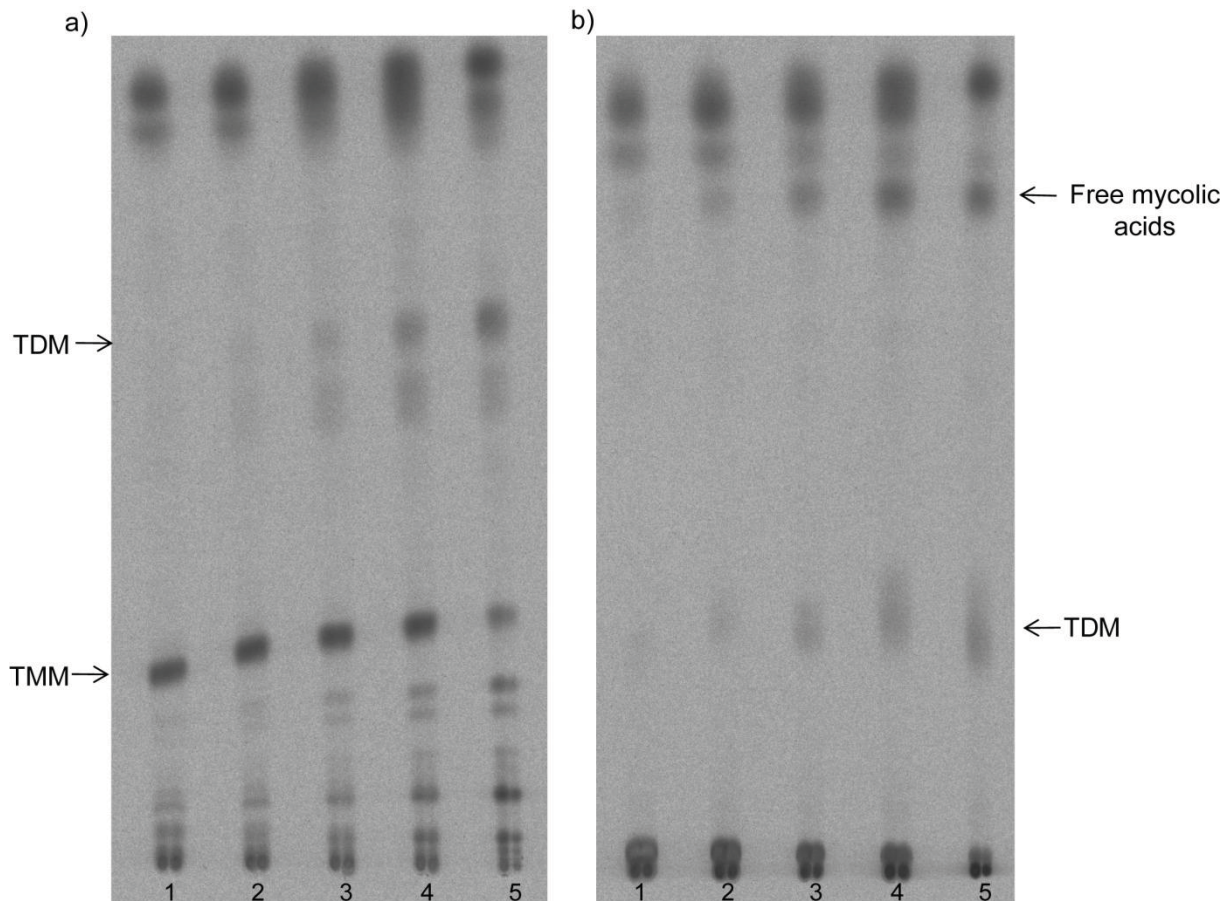


**Figure 17: Time course analysis of TMM, TDM and free mycolic acids.**

*Mtb* H37Rv was grown to an  $OD_{580}$  of 0.3-0.4 in 7H9 medium without detergent and [ $^{14}C$ ]- acetate added at the rate of  $0.5\mu Ci/ml$ . Culture was incubated at  $37^{\circ}C$  with mild shaking and after 45 minutes (Lane 1), 1.5 hours (Lane 2), 3 hours (Lane 3), 6 hours (Lane 4) and 24 hours (Lane 5) post labelling 10ml of culture was collected and standard lipid extraction performed. Lipid extractible was run on silica gel coated TLC with chloroform/methanol/ water (30:8:1) to visualise TDM and TMM (a) and with chloroform/methanol (9:1) to visualise free mycolic acids and TDM (b).

As shown in Figure 17 a, TMM appeared at the earliest time point of 45 minutes while TDM began to appear as a faint band 1.5 hours post labelling and after 3 hours it was clearly visible. Free mycolic acids also appeared as a faint band 1.5 hours post labelling strongly suggesting that they could be degradation products of TMM and/or TDM and not precursors (Fig. 17 b). Thus, accumulation of free mycolic acids with Ag85C-3 treatment might be a consequence of the drastic increase of TMM which then gets degraded in cell envelope. It could also be an indirect effect of modulation of mycolic acid biosynthesis pathway by Ag85C-3.

#### 3.4.4 Cell wall linked mycolic acids

The Ag85C mutant strain of *Mtb* showed a drastic 40% reduction in cell wall linked mycolic acids (Jackson, et al., 1999). Over-expression of Ag85A and B proteins in this mutant strain could partially rescue this phenotype (Puech, et al., 2000). This has led to the general assumption that Ag85C is more important for the synthesis of mAGP complex. The mAGP is responsible for the structural integrity of *Mtb* cell wall and reduction in its amounts leads to in-

creased permeability to hydrophobic and hydrophilic molecules (Jackson, et al., 1999). Therefore, the effect of Ag85C-3 on amounts of cell wall linked mycolic acids was studied.

*Mtb* cultures grown to mid-log phase were treated with 50 and 100 $\mu$ M of Ag85C-3, 10 $\mu$ M of INH or left untreated. Crude lipid extraction was performed and the remnant delipidated bacterial cells containing mAGP on its surface were analysed. Mycolic acid methyl esters (MAMEs) were obtained from these cells by extensive saponification and methylation procedures. TLC was then performed with the samples with petroleum ether/diethyl ether, 9:1, as solvent (Fig. 18 a). With this solvent three types of MAMEs, namely, alpha, methoxy and keto, representing the three types of mycolic acids found in *Mtb*, can be seen as distinct bands with alpha as the upper band, methoxy as the middle band and keto as the lowest.

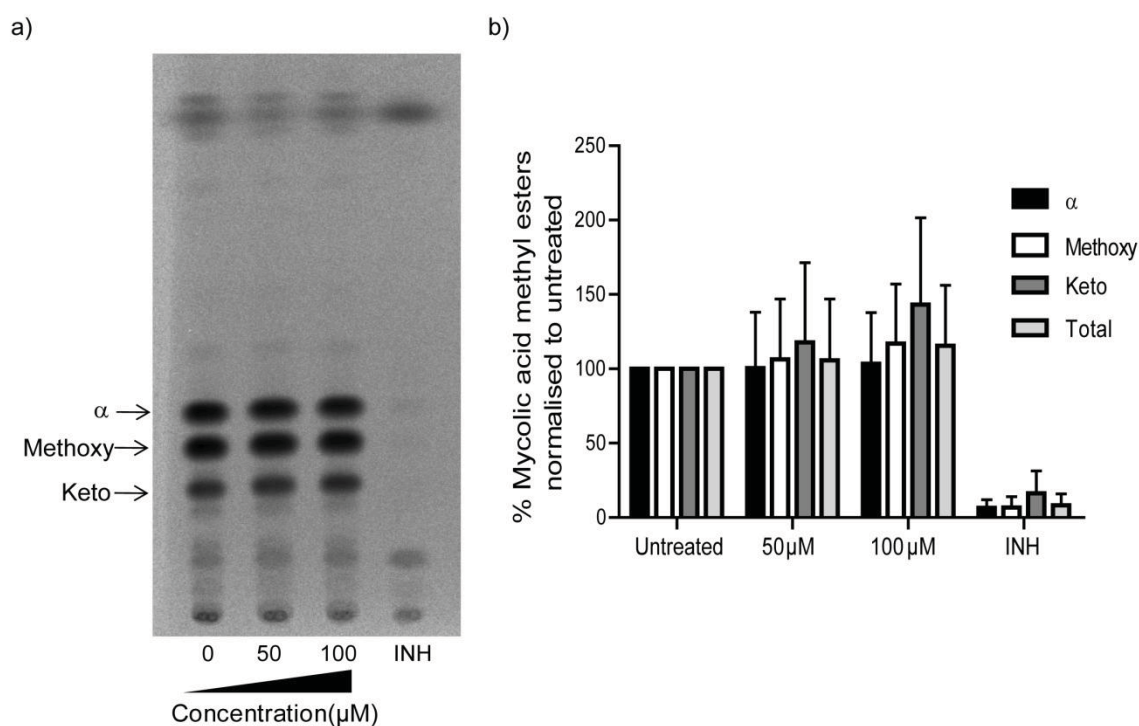


**Figure 18: Synthesis of arabinogalactan linked mycolic acids.**

*Mtb* H37Rv was grown in 7H9 medium without detergent to an  $OD_{580}$  of 0.3 to 0.4. Ag85C-3 was added to the culture at the indicated concentrations and incubated at 37 $^{\circ}$ C with mild shaking for 48 hours. To label lipids [ $^{14}$ C]-acetate was added at a rate of 0.5 $\mu$ Ci/ml and incorporation allowed for 24h. Lipid extraction was then performed (a) TLC of methyl esters of mycolic acid and fatty acids obtained after saponification and methylation of delipidated bacteria. TLC was run four times with petroleum ether/ diethyl ether (9:1) to resolve alpha, methoxy and keto mycolic acids (b) Band intensity of three types and total mycolic acids linked to the cell wall, average value from 3 independent experiments was calculated with standard deviation and plotted. INH is isoniazid at 10 $\mu$ M.

Quantification of the band intensities of individual MAMEs and total MAMEs showed no change upon treatment (Fig. 18 b) with untreated taken as 100%. INH, on the other hand, had a drastic effect on cell wall linked mycolic acids. Thus, Ag85C-3 has an effect only on TMM

to TMM transfer of mycolic acids to generate TDM while there is no impact on the transfer to AGP.

### 3.4.5 Total mycolic acids

Modulation of TDM and TMM could modify the total amounts of mycolic acids as a consequence of regulatory feed-back loops and thus amplify the actual differences. To resolve this, total mycolates synthesized during treatment was measured by saponification of the complete cell pellet from treated and untreated bacteria. The resultant mycolic acid acyl groups were methylated with diazomethane to give rise to methyl esters and subjected to TLC with dichloromethane as solvent. In this solvent system fatty acid methyl esters migrate above while MAMEs migrate as two bands below, namely alpha MAME as the upper band and oxygenated MAME (including both methoxy and keto MAMEs) as the lower band (Fig. 19 a).

Quantification of two types of MAMEs and total mycolates in cells showed that Ag85C-3 had no impact on mycolic acid synthesis machinery in the cell unlike INH which completely abrogated mycolic acids (Fig. 19 b). This reinforces the finding that Ag85C-3 specifically inhibits the final transfer step in mycolic acid biosynthesis catalysed by Ag85 complex.

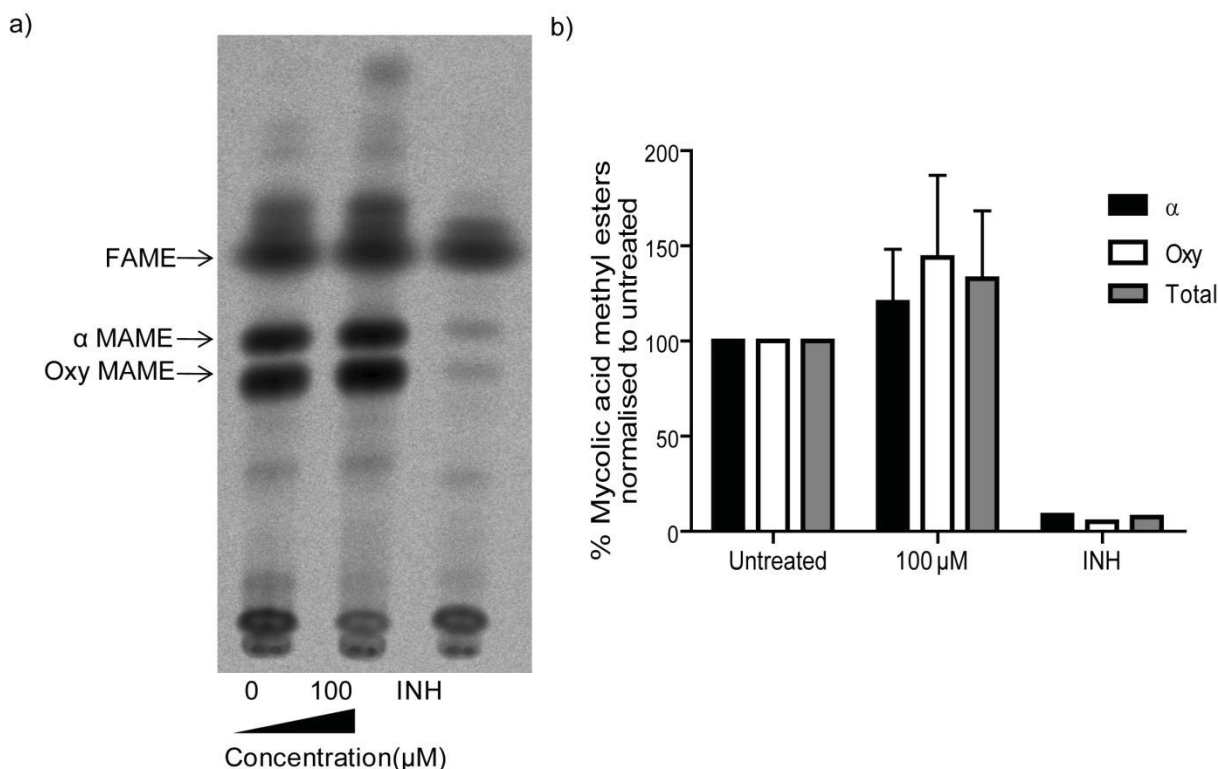


**Figure 19: Synthesis of total mycolic acids.**

*Mtb* H37Rv was grown in 7H9 medium without detergent to an  $OD_{580}$  of 0.3 to 0.4. Ag85C-3 was added to the culture at the indicated concentrations and incubated at 37°C with mild shaking for 48 hours. To label lipids [ $^{14}$ C]-acetate was added at a rate of 0.5  $\mu$ Ci/ml and incorporation allowed for 24h. The cell pellet was then autoclaved (a) TLC of methyl esters of mycolic acid and fatty acids obtained after saponification and methylation of complete cell pellet. TLC was run with dichloromethane as solvent to resolve alpha and oxygenated mycolic acids (b) Band intensity of two types and total mycolic acids in the cell, average value from 3 independent experiments was calculated with standard deviation and plotted. INH is isoniazid at 10  $\mu$ M

Complete analysis of the mycolic acid containing lipids of *Mtb* upon treatment with Ag85C-3 confirms that it blocks the activity of its target protein, Ag85C. The reduction in TDM amounts with a concomitant increase in TMM is strong evidence for a specific block at the mycolyl transferase step catalysed by the Ag85 complex proteins. Interestingly this also led to an accumulation of free mycolic acids which could either be a direct or indirect effect of the disruption of the mycolic acid synthesis pathway. The kinetics of free mycolic acid synthesis is similar to that of TDM suggesting that they do not have a precursory role in the mycolyl transferase reaction. Additionally, the total mycolic acid amounts are not modified by Ag85C-3 strengthening the proof for a block in transferase step. But, surprisingly, Ag85C-3 has no impact on the transfer of mycolic acids to covalently associated AGP which could be due to its distinct binding patterns to the possible different active site conformations of Ag85C. INH which blocks mycolic acid synthesis at the earlier biosynthetic FAS-II cycle reduced amounts of both TDM and TMM and also abrogated mAGP and total mycolic acids. Thus, the mode of Ag85C-3 disruption of the mycolic acid biosynthesis pathway is distinct from that of INH.

### 3.5 Permeability of cell wall

The modulation of cell wall glycolipid amounts by Ag85C-3 could perturb the integrity of the cell wall and hence its permeability to both hydrophilic and hydrophobic molecules. To investigate this aspect, radioactively labelled glycerol was used as a probe (Laneelle and Daffe, 2008). Glycerol is a small, organic molecule that is the preferred source of carbon and due to its neutral charge is taken up by both passive and facilitated diffusion.

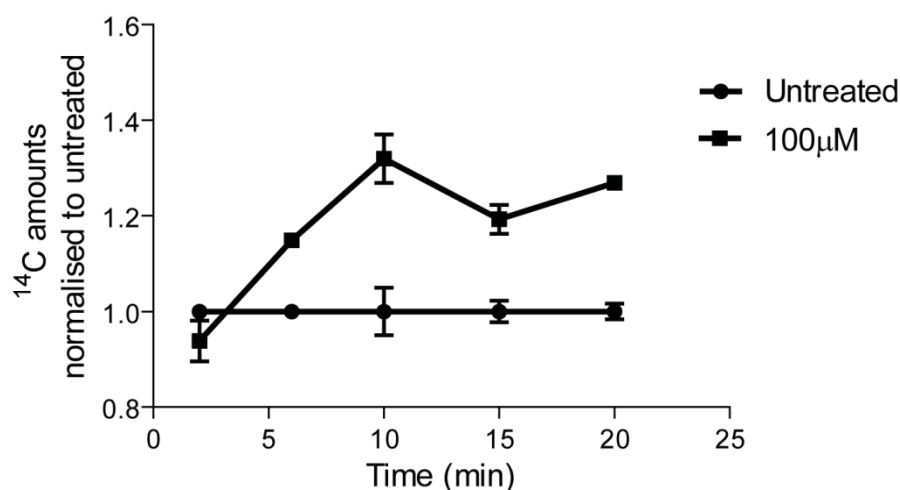


Figure 20: Cell wall permeability.

*Mtb* H37Rv mid-log phase culture was diluted in 7H9 medium without detergent at a density of  $7.5 \times 10^6$  bacteria/ml and incubated at 37°C for 24 hours. Ag85C-3 was then added at 100µM while the control culture was untreated and incubated at 37°C for 48 hours with mild shaking. [<sup>3</sup>H]-uracil was added at 0.5µCi/ml to normalise for cell number and cultures incubated for another 24 hours. An aliquot of the cell pellet was fixed for [<sup>3</sup>H] counts while 2µCi of [<sup>14</sup>C] glycerol was added to the remnant cell suspension. At 0, 2, 6, 10, 15 and 20 minutes after glycerol addition 100µl of cell suspension was collected and prepared for [<sup>14</sup>C] scintillation measurement. Each sample was normalised to total cell numbers and the counts of the untreated standard was taken as 1. Average from 2 measurements with standard deviation was calculated within a single representative experiment shown here.

*Mtb* treated with 100µM of Ag85C-3 and the untreated control were incubated with [<sup>14</sup>C] glycerol for short duration of time and processed for uptake measurements. The incorporation of [<sup>3</sup>H]-uracil prior to glycerol uptake was used to normalise the differing bacterial numbers between treated and untreated samples. As shown in Figure 20, the amount of [<sup>14</sup>C] counts relative to the untreated sample (which is taken as 1) is higher in the Ag85C-3 treated sample indicating increased permeability to glycerol. This shows that the integrity of the cell envelope is modified by Ag85C-3 through the changes in TDM, TMM and free mycolic acid amounts. Thus, the increased permeability of the cell wall could cause uncontrolled diffusion of substances including solvents in to the cell finally leading to cell death.

### 3.6 Inhibition of *Mtb* deficient in Ag85C

Specificity of a chemical inhibitor is a key issue while studying its mechanism. To understand if Ag85C is the sole target of the compound under study, tests were performed with an *Mtb* strain deficient in Ag85C protein, named MYC1554. This mutant was generated by transposon insertion in the Ag85C locus in a clinical isolate, Mt103, which led to abrogation of Ag85C protein. This led to 40% reduction of cell wall linked mycolic acids while TDM and TMM amounts remained unaffected (Jackson, et al., 1999). Hence Ag85 A, B and C proteins probably have a partially redundant role in TDM biosynthesis. Nevertheless, Ag85C-3 activity against MYC1554 and Mt103 was investigated.

#### 3.6.1 *In vitro* anti-mycobacterial assay

The strains, MYC1554 and Mt103, were tested for inhibition by Ag85C-3 with the qualitative colorimetric test and then with the quantitative [<sup>3</sup>H]-uracil incorporation assay. Qualitative readout from alamar blue colour change showed that growth of the mutant, MYC1554, and the wildtype, Mt103, was inhibited starting from 100µM, similar to the profile of the *Mtb* lab strain H37Rv (Fig. 21 a). Uptake of [<sup>3</sup>H]-uracil after treatment with 50, 100 and 250µM of Ag85C-3 was then measured to determine if the degree of inhibition was also similar in the mutant compared to its wild type, Mt103, and H37Rv. MYC1554 had a pattern of inhibition almost identical to H37Rv; 100µM reduced scintillation counts at 72 hours which went up to 70% after 120 hours of treatment (Fig. 21 c). In contrast, growth of Mt103 was inhibited to a



lesser degree at 100 $\mu$ M of Ag85C-3 (Fig. 21 b). 250 $\mu$ M had a sterilizing effect on both strains starting from 24 hours and persisting till 120 hours of treatment. INH at 10 $\mu$ M was the positive control in each case.

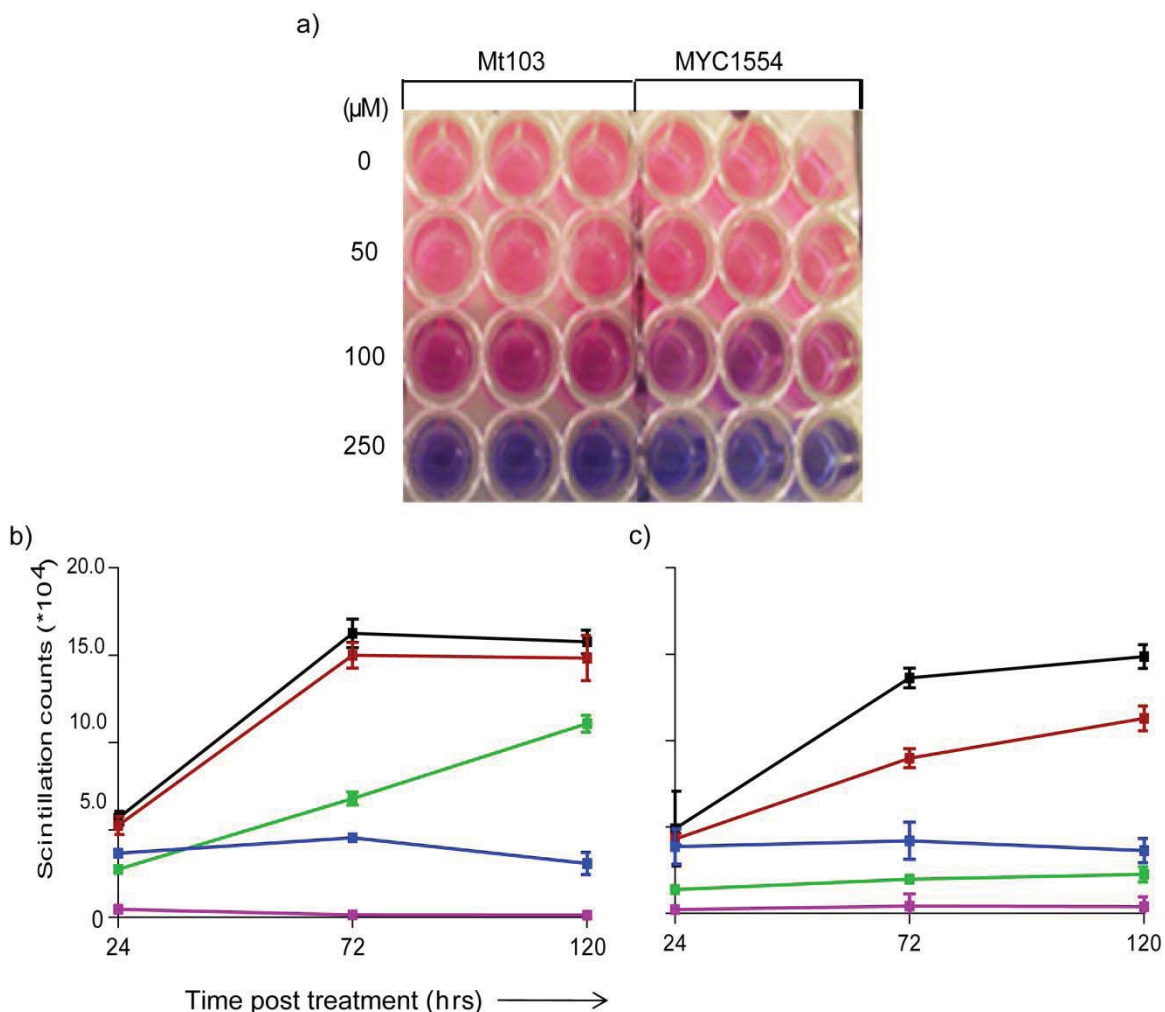


**Figure 21: Ag85C-3 activity on Ag85C mutant.**

Ag85C mutant, MYC1554, and its wild type background, Mt103, were grown to log phase and treated with indicated concentrations of Ag85C-3 to determine anti-mycobacterial activity (a) Alamar blue assay (b) [ $^3$ H]-Uracil incorporation assay with the wild type strain, Mt103 (c) [ $^3$ H]-Uracil incorporation assay with Ag85C mutant, MYC1554. Untreated (■), 50 $\mu$ M (■), 100 $\mu$ M (■), 250 $\mu$ M (■) and Isoniazid-10 $\mu$ M (■). Average of hex-plicates for each treatment was calculated with standard deviation and plotted.

Thus the mutant was as susceptible to Ag85C-3 as Mt103 and H37Rv, clearly indicating that the molecule is not specific to Ag85C. Its effect on survival of *Mtb* could be facilitated by interaction with the other two homologues, Ag85A and B or could be through yet undetected interacting partners.

### 3.6.2 TDM and TMM analysis

To investigate if Ag85C-3 induced survival defect in the mutant is due to an effect on the mycolyl transferase reaction TDM-TMM synthesis assays were performed. For this, the mutant, MYC1554 and the wild type, Mt103, were either treated with 100 $\mu$ M of Ag85C-3 or not treated for 48 hours. As described before, incorporation of radioactive [ $^{14}$ C] acetate for the

next 24 hours into the lipid extractable was monitored. Quantification of band intensities showed that there was a reduction in TDM amounts up to 50% in the mutant and up to 20% in the wild type strain (Fig. 22 a). The TMM amounts, on the other hand, did not change in the Ag85C mutant and the wild type strain unlike the increase observed in H37Rv. This could be because of a higher turnover of TMM in these clinical isolates. Moreover, the change in amount of free mycolic acids in the mutant and in the wild type was more drastic with up to 200-300% increase (Fig. 22 b). This also supports a high turnover scenario with larger amounts of free mycolic acids being produced as degradation products or side-products of the mycolyl transferase block.

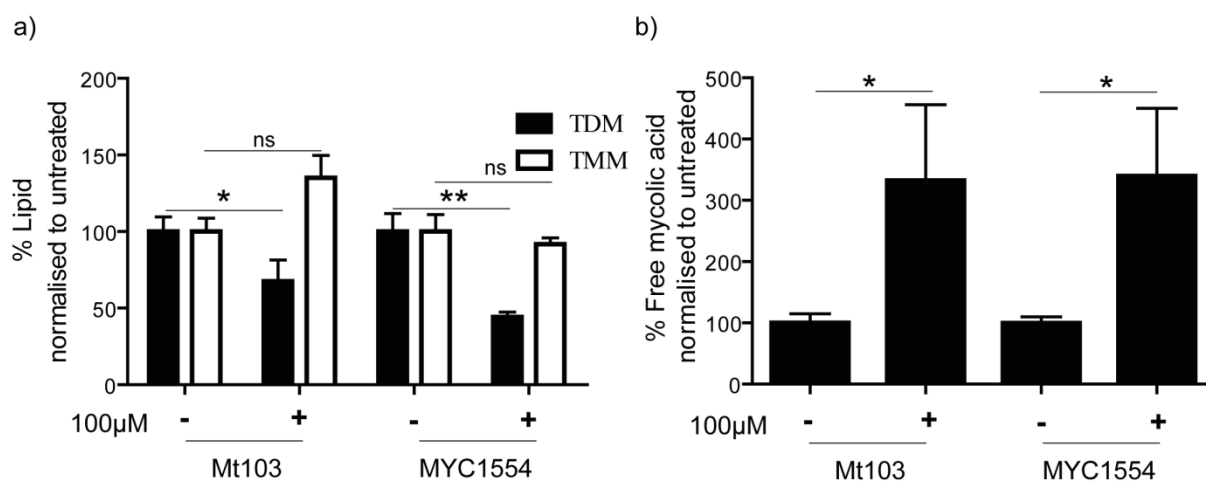


**Figure 22: Synthesis of TDM, TMM and free mycolic acids in Ag85C mutant.**

Ag85C mutant, MYC1554, and its wild type background, Mt103, were treated with 100µM of Ag85C-3 as described in Figure 14, lipid extraction done and TLC performed with lipid extractable (a) Band intensities of TDM and TMM in Mt103 (wild type) and MYC1554 (Ag85C mutant), untreated is taken to be 100% (b) Band intensity of free mycolic acids in Mt103 (wild type) and MYC1554 (Ag85C mutant), average of tetra-plicates for each treatment was calculated with standard deviation and plotted, untreated is taken to be 100%. ‘\*’ indicates  $p < 0.05$ , ‘\*\*\*’ indicates  $p < 0.01$  and ‘ns’ is non-significant with  $p > 0.05$  where  $p$  denotes significance calculated by paired Student’s t-test.

Thus, even in the absence of Ag85C protein Ag85C-3 inhibits growth of *Mtb* indicating that it is not specific to Ag85C and has other targets. Further, analysis of TDM and TMM abundance showed reduction of TDM in the mutant strain with Ag85C-3 treatment. This strongly suggests inhibition of the other two Ag85 proteins, Ag85A and B, leading to complete block in the transferase reaction. Hence, it could be that Ag85C-3 binds to the highly conserved active site of all the three Ag85 proteins leading to changes in cell envelope and consequently growth inhibition.

### 3.7 Gene expression analysis

The results of experiments with the Ag85C mutant strain establish that the other Ag85 proteins might also be targets of Ag85C-3. However it does not exclude other non-specific targets or pathways. These could either be direct and indirect effects of block in the mycolyl trans-

ferase step or be totally independent effects. To better understand this, whole genome level expression study was performed of *Mtb* treated with the compound *in vitro*. It is important to note that the regulatory role of mycolyl transferase reaction catalysed by Ag85 proteins has not been studied so far due to unavailability of a triple mutant and partial functional redundancy of the three proteins. Thus the availability of Ag85C-3 which inhibits this pathway as indicated by reduction of TDM and accumulation of TMM provides a valuable tool to understand impact of this pathway on general signalling networks of *Mtb*.

Microarray analysis of the transcriptional response of *Mtb* after treatment with Ag85C-3 was performed with custom made chips from Agilent technologies with probes against the complete list of annotated ORFs and intergenic regions in *Mtb* H37Rv (Cole, et al., 1998). An early time point of 48 hours was chosen with 50 and 100 $\mu$ M treatment. With a low cut off of 1.5 times fold change difference, up to 10 and 62 genes were up-regulated at 50 and 100 $\mu$ M, respectively with a common pool of 7 genes. Simultaneously, 7 and 29 genes were down-regulated at 50 and 100 $\mu$ M respectively with a common pool of 7 genes (Table 1). Interestingly, the most strongly regulated genes were transporters belonging to MMPL (Mycobacterial membrane protein large) family believed to play a role in lipid transport (Domenech, et al., 2005). Additionally most of the genes belonging to one of the mycobactin biosynthesis operons were up-regulated specifically at 100 $\mu$ M (Rodriguez, 2006). This was surprising since mycobactin synthesis is normally repressed in enriched medium. MprA (Mycobacterial persistence regulator A), part of the MprAB two component regulatory system, was the most notable transcription factor up-regulated at 100 $\mu$ M (He, et al., 2006; Zahrt, et al., 2003). Genes like Cyp132, AlkB, Cyp125 and LldD1 involved in fatty acid metabolism and general respiration were also up-regulated by the compound.

**Table 1: Regulation of *Mtb* genes with Ag85C-3 treatment.**

Total number of genes regulated after 50 and 100 $\mu$ M of Ag85C-3 treatment for 48 hours is tabulated according to functional categories described by Cole *et al.* (Cole, et al., 1998). ↓Represents down-regulation and ↑represents up-regulation.

Functional gene categories	Number of genes regulated			
	↓ 50 and 100 $\mu$ M	↓ 100 $\mu$ M	↑ 50 and 100 $\mu$ M	↑ 100 $\mu$ M
Lipid metabolism	-	7	1	4
Cell wall and cell processes	3	6	1	3
Intermediary metabolism and respiration	2	11	2	4
Information pathways	-	1	-	5
Regulatory proteins	1	3	-	1
PE/PPE	-	6	3	3
Conserved hypothetical	1	19	-	2
Insertions seqs and phages	-	2	-	-
	7	55	7	22

PPE proteins 50 and 51 were the most strongly down-regulated genes at both concentrations (Brennan and Delogu, 2002). Notably, IniB (Isoniazid inducible protein B) was down-regulated, again suggesting that mechanism of action is different from that of INH (Alland, et al., 2000). Pks11 (polyketide synthase 11), AcpM (acyl carrier protein M), Fas (fatty acid synthase) and Mas (multi functional mycocerosic acid synthase) were some of the general lipid biosynthesis genes down-regulated after treatment (Marrakchi, et al., 2008; Mathur and Kolatukudy, 1992). Ribosomal protein synthesis genes like RplL, RpsR2, RpsN2 and RpmB2 were also down-regulated possibly as a stress response.

### 3.7.1 MBT operon

Iron is an essential nutrient for most organisms and its uptake is tightly regulated at transcriptional level. *Mtb* acquires iron from its environment by synthesising mycobactins, siderophores with a distinct hydroxyphenyloxazoline ring moiety (Rodriguez, 2006). Two genetic loci named mbt-1 and mbt-2 have been implicated in the biosynthesis of mycobactins (Krithika, et al., 2006; Quadri, et al., 1998). The expression of genes belonging to these loci is under the control of the IdeR protein, an iron dependent transcription repressor (Rodriguez, et al., 2002).

Seven of the ten genes of the *mbt-1* locus, namely *MbtB*, *MbtC*, *MbtD*, *MbtE*, *MbtG*, *MbtH* and *MbtI*, were up-regulated in the range of 1.62-2.1 fold change values after treatment with 100 $\mu$ M of Ag85C-3 for 48 hours. This locus is primarily involved in the synthesis of mycobactin backbone structure composed of salicylic acid derived moiety. The *mbt-2* locus, which is necessary for attachment of long acyl chains to generate lipophilic mycobactins, remained unaffected by Ag85C-3. Further confirmation of these results was done with quantitative PCR against selected genes, *MbtG*, *MbtD* and *MbtJ*, of the *mbt-1* operon with the same samples. An increased expression up to 3 fold relative to untreated samples was observed for the 3 genes with this method which could be due to its high sensitivity (Fig. 23 c). *SigA* was the housekeeping gene used as the normalizing factor.

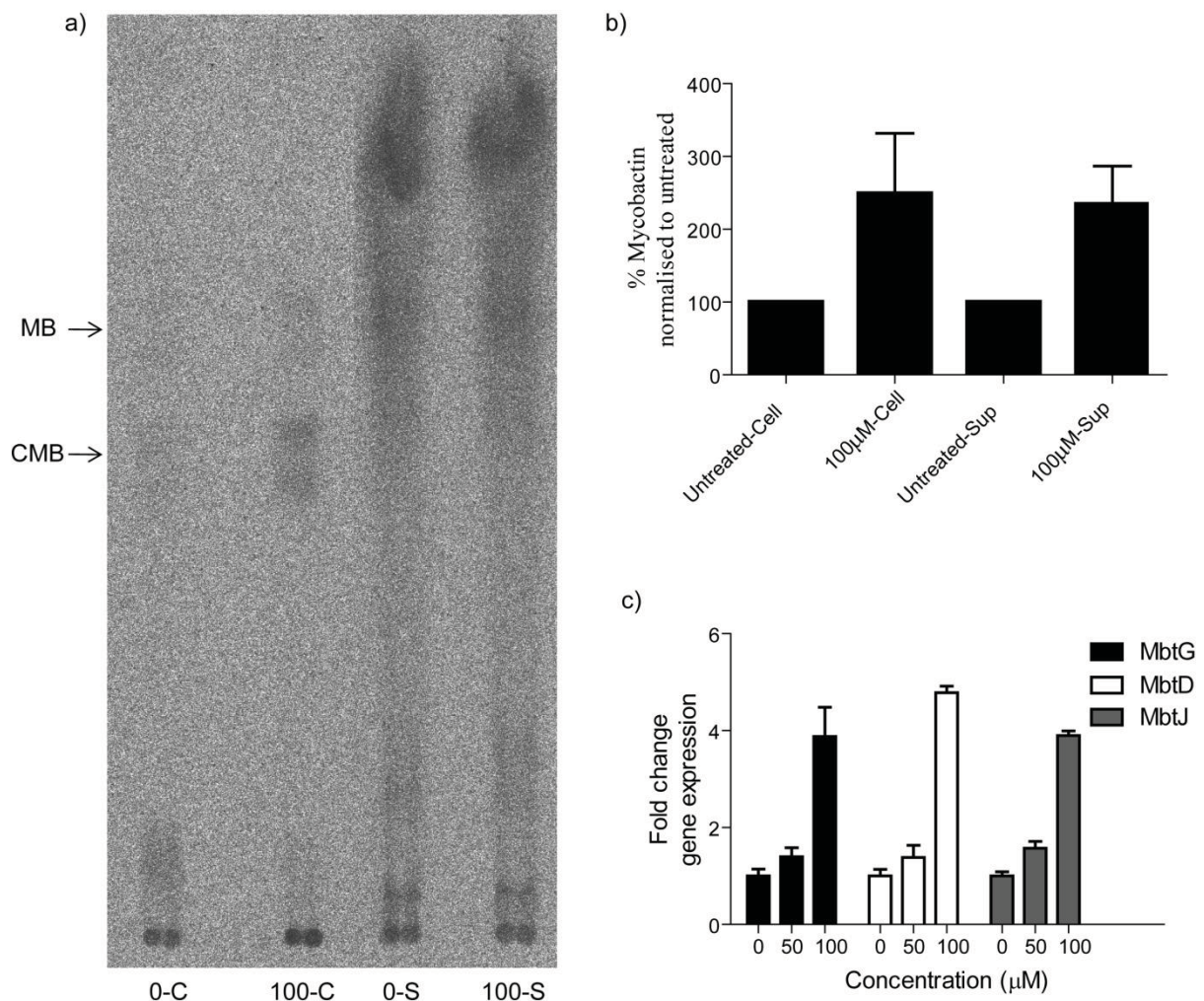


**Figure 23: Mycobactin synthesis:**

*Mtb* H37Rv mid-log phase culture was inoculated in 7H9 medium without detergent at a density of  $7.5 \times 10^6$  bacteria/ml and incubated at 37°C for 24 hours. Ag85C-3 was then added at 50 or 100µM while the control culture was untreated and incubated at 37°C for 48 hours with mild shaking. [ $^{14}\text{C}$ ]-salicylic acid was added at 0.5µCi/ml and cultures incubated for another 24 hours. Mycobactins were then extracted from the cell pellet and supernatant into chloroform after saturation with ferric chloride. These samples were then run on silica gel plate with petroleum ether/n-butanol/ethyl acetate (2:3:3). Gene expression level was determined through quantitative PCR as described in the next figure. a) TLC of mycobactin samples, 0-C is Untreated cell pellet; 100-C is Ag85C-3 100µM-cell pellet; 0-S is Untreated-culture filtrate; 100-S is Ag85C-3 100µM-culture filtrate b) Quantification of band intensities of total mycobactins, Cell is cell associated and Sup is culture filtrate, average of two independent experiments was calculated with standard deviation and plotted c) Quantitative PCR gene expression of MbtG, MbtD and MbtJ, average of triplicates for each treatment was calculated with standard deviation and plotted.

Functional impact of this up-regulation was investigated by measuring amounts of mycobactins, both cell-associated mycobactins and extracellular carboxy mycobactins in culture filtrate. For this, untreated and treated bacterial cultures were fed with radioactive [ $7\text{-}^{14}\text{C}$ ]-salicylic acid which is a common precursor of both carboxy and normal mycobactins for 24 hours. Cell pellets were treated with ethanol, saturated with ferric chloride and the mycobactins finally extracted into chloroform. Carboxy mycobactins in the culture filtrate were saturated with ferric chloride and then separately extracted into chloroform. These samples were then subjected to TLC with the solvent petroleum ether/n-butanol/ethyl acetate (2:3:3) (Fig. 23 a). Quantification of the distinct bands observed showed a marked increase in both mycobactin and carboxy mycobactins in *Mtb* treated with 100µM of Ag85C-3 (Fig. 23 b). Thus, genetic up-regulation of this operon also leads to increase in amounts of siderophores in the bacterial cells strongly suggesting a shift in the iron homeostasis within these cells. The higher amounts of mycobactins could either lead to accumulation of iron inside cells or be a stress response to reduced iron levels induced by modifications to cell envelope. Either scenario is detrimental to *Mtb* and might be an important mechanism by which Ag85C-3 induces toxicity.

### 3.7.2 MMPL transporter proteins

MMPLs are large transmembrane proteins belonging to the resistance, nodulation and division superfamily (RND superfamily) of transporters. 14 genes of this family have been identified in *Mtb* and postulated to play a role in the transport of lipids across the cell membrane (Domenech, et al., 2005). Two of these genes, namely MmpL6 and MmpL5, were found to be the most strongly up-regulated genes upon Ag85C-3 treatment. Quantitative PCR indicated an up-regulation of up to 70 fold for MmpL6 and up to 13 fold for MmpL5 with 100µM of Ag85C-3 (Fig. 24 a). The fact that MmpL5 is also regulated by iron levels in the environment strongly correlates with the *mbt-1* locus up regulation (Rodriguez, et al., 2002). MmpL6 protein, on the other hand, is reported to be truncated in H37Rv and hence considered non-functional. But the large up-regulation suggests a previously undeciphered function in *Mtb*

lipid metabolism. It could also be a general response to cell wall changes induced by Ag85C-3.

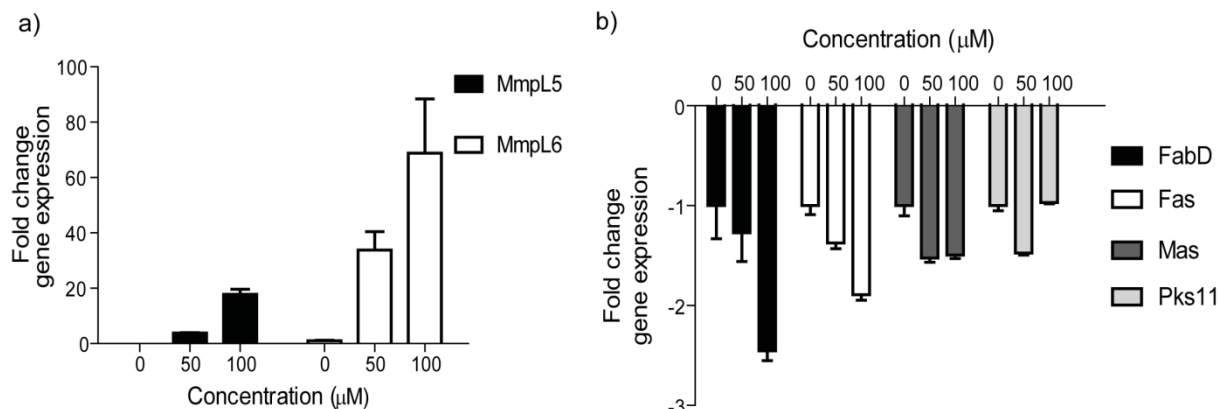


**Figure 24: Quantitative PCR analysis.**

*Mtb* H37Rv mid-log phase culture was inoculated in 7H9 medium without detergent at a density of  $7.5 \times 10^6$  bacteria/ml and incubated at 37°C for 24 hours. Ag85C-3 was then added at 50 or 100 μM while the control culture was untreated and incubated at 37°C for 48 hours with mild shaking. Cell pellets were collected and resuspended in 1ml TRIZOL for RNA extraction according to standard protocols. cDNA was synthesized from this RNA using random hexamers with standard protocols. Quantitative PCR reactions were set up with 1:150 dilution of the cDNA with readymade Sybergreen mix and 150nM gene primer mix in AB7000. SigA was used as the housekeeping standard control gene. Fold change expression relative to untreated control was calculated from the Ct values. i) Relative expression of MmpL genes. ii) Relative expression of lipid synthesis genes, FabD, Fas, Mas and Pks11. Average of triplicates for each treatment was calculated with standard deviation and plotted.

### 3.7.3 Lipid biosynthesis

Amongst the down-regulated genes in the microarray analysis were genes belonging to lipid synthesis pathways. These either belonged to general fatty acid synthesis genes like AcpM, FabD and Fas or to special PDIM/phenolic glycolipid pathways like Mas and Pks 11 (Guilhot, et al., 2008; Marrakchi, et al., 2008). However, quantitative PCR experiments showed that the degree of regulation was only up to 0.5 fold in the case of Fas and Mas while a slight down regulation up to 1.5 fold was observed with FabD and Pks 11 genes (Fig. 24 b). These results indicate that the basic lipid synthesis processes remain virtually unaffected after Ag85C-3 treatment unlike the concerted up regulation of fatty acid synthesis genes observed with INH treatment (Waddell, et al., 2004; Wilson, et al., 1999).

Thus, whole genome expression study provided novel insights into the mechanisms of Ag85C-3 activity against *Mtb*. The increase in mycobactin biosynthesis as indicated by up regulation of mbt-1 gene cluster, MmpL5 expression and accumulation of mycobactin molecules hints at perturbation of iron homeostasis within the treated bacterial cells which could also lead toxicity. Additionally, modulation of MmpL6 could point to its probable link to mycolic acid synthesis and transport. More detailed validation of other regulated genes would aid in developing a signature expression profile of this class of inhibitors.

## 4 Discussion

Tuberculosis (TB) drug discovery is in one of its most challenging phases in history due to the growing threat of extensively drug resistant (XDR) and multiple drug resistant (MDR) TB (Borgdorff and Small, 2009; Wright, et al., 2009). One of the main causes for the emergence of resistance is the 6-9 months long current regimen which encourages patient non-compliance especially in developing countries. Another concern is the lethal liaison between TB and AIDS which is the main contributing factor to the dramatic increase in infected individuals worldwide (Kaufmann and McMichael, 2005; WHO, 2009). This scenario calls for an urgent overhaul of the current regimen with new drugs which could shorten treatment duration as well as be synergistic with anti-retroviral therapy.

This study has focussed on Ag85C, a mycolyl transferase of *Mtb* as a drug target with a panel of chemical molecules identified through a small molecule library screen. The starting chemical moiety Ag85C-1 and its analogues Ag85C-2, Ag85C-3 and Ag85C-4 bound to Ag85C as detected by NMR (Schade, M. et al, unpublished data). Ag85C belongs to a family of three proteins, namely Ag85A, Ag85B and Ag85C, which are highly homologous to each other and conserved across mycobacterial species. They are secreted by *Mtb* with Ag85B being the most abundant protein in the culture filtrate and are immune-dominant antigens (Harth, et al., 1996; Wiker and Harboe, 1992). Belisle *et al.* (1997) elucidated their more fundamental physiological function as transferases of mycolic acids essential in the final critical steps of cell envelope biogenesis in mycobacteria. They demonstrated that all three Ag85 proteins transfer mycolic acids, building blocks of cell wall, to its terminal substrate trehalose monomycolate (TMM) to generate trehalose dimycolate (TDM) (Belisle, et al., 1997). TDM is non-covalently attached to the outer surface of cell wall while the arabinogalactan-peptidoglycan linked mycolic acids (mAGP) form the covalently attached structural framework. An *Mtb* strain with a deficiency in Ag85C showed a marked reduction of 40% in mAGP amounts suggesting that these proteins are also involved in transfer of mycolic acids to arabinogalactan-peptidoglycan multimer (Jackson, et al., 1999).

### 4.1 Activity of Ag85C antagonists

Ag85 proteins thus play a pivotal role in the assembly of mycobacterial cell wall which also makes them attractive targets from the drug discovery perspective. Other advantages include their uniqueness to mycobacteria which reduces the chances of cross reaction with host molecules. These proteins are located in the periplasmic space which also lowers the possibility of inhibitors being effluxed by drug efflux pumps. Initial studies identified 6-azido-6-deoxy-trehalose (ADT), one of many trehalose and TMM analogues, which blocked *in vitro* mycolyl



transferase activity, inhibited growth of *M. aurum* and reduced TDM, TMM and cell wall bound mycolates in treated bacteria (Belisle, et al., 1997). Rose *et al.* (2002) tested additional derivatives of trehalose based on 6, 6'-dideoxy trehalose against non-virulent *Mtb* H37Ra and a few clinical strains of *M. avium* (Rose, et al., 2002). They observed a wide range of activity which depended on the length of linked acyl chains. Another trehalose derivative which was a TDM mimic was synergistic with INH when tested against *M. smegmatis* suggesting that Ag85 blocking could enhance the activity of current anti-tuberculars (Wang, et al., 2004). More recently, phosphonate inhibitors of Ag85C were shown to be growth inhibitors of *M. aurum in vitro* (Gobec, et al., 2007). Though none of these molecules have a sufficiently low MIC to be considered a lead compound, they emphasize the relevance of Ag85 proteins as a novel target. In this context, detailed study of anti-mycobacterial potential of Ag85C-1, -2, -3 and -4 was undertaken with pathogenic *Mtb* as the model organism.

#### 4.1.1 Effect of Ag85C inhibition on *in vitro* *Mtb* culture

Resazurin based viability assay has been accepted as a standard qualitative test to measure anti-microbial activity (Gabrielson, et al., 2002). It is a simple, fast assay which relies on reduction of blue colored tetrazole substrate into pink product by respiratory dehydrogenases of live cells. The ease of this method makes it a convenient indicative test for large scale anti-mycobacterial studies (Yajko, et al., 1995). This assay has been used to assess biological activity of Ag85C-1-4 against *Mtb*. It was observed that all four molecules inhibited growth of *Mtb* in rich liquid medium, but at different concentrations (Fig. 8). The analogues with modifications to primary Ag85C-1 structure driven by SAR studies showed improved activity at micromolar concentration ranges compared to 1.3mM putative value of MIC for Ag85C-1. Ag85C-2, -3 and -4 had a putative MIC of 250 $\mu$ M, 100 $\mu$ M and 50 $\mu$ M, respectively. Thus, chemical binders of Ag85C had an impact on *Mtb* survival under growth inducive conditions. Moreover, structural improvements to the primary molecule led to increased activity indicating a broad chemical space which could be explored in the future. Similar experiments with *M. smegmatis*, *B. subtilis* and *E. coli* showed an effect on *M. smegmatis* and not on the other two representatives of gram positive and negative bacteria suggesting specificity for mycobacterial species (Schade, M. et al, unpublished data). Detailed characterization of the inhibitory properties of the analogues Ag85C-2-4 was performed with [<sup>3</sup>H]-Uracil incorporation assay to gain further insights in to their activity.

The uptake of radioactive uracil in to the mRNA during transcription has been used as a direct read out of bacterial numbers in an actively replicating population (Benitez, et al., 1974). Thus, scintillation counts are directly proportional to the number of bacteria and have been

used to follow cell numbers over time. Kinetics of inhibition showed that Ag85C-3 is the most potent of the three analogues with reduction of scintillation counts observed from 24 hours post-treatment at 100 and 250 $\mu$ M and close to 99% at 250 $\mu$ M after 120 hours (Fig. 9 b). This was more than the 77% inhibition observed with 10 $\mu$ M of INH, the positive control, after 120 hours. Though Ag85C-4 inhibited at 50 $\mu$ M, this effect was only observed at 120 hours post treatment and was only up to 50% inhibition (Fig. 9 c). Ag85C-2, on the other hand, had a strong effect only at 250 $\mu$ M while 100 $\mu$ M reduced counts by 20-30% after 120 hours of treatment (Fig. 9 a). The three analogues possessed distinct patterns of inhibition over time which could be due to the differences in their chemical structures. It thus gives us more information about the preferred functional group changes for improvement of inhibitory activity. These studies indicate that further modification of Ag85C-3 structure could yield more active antagonists of Ag85C.

The anti-mycobacterial activity of Ag85C-1-4 may not be attributable to Ag85C blockage alone, as genetic inactivation of Ag85A, B or C alone does not modify the growth kinetics of *Mtb* in liquid medium (Armitige, et al., 2000; Jackson, et al., 1999; Puech, et al., 2000). But a simultaneous antisense blockage of the three Ag85 enzymes using phosphorothioate-modified oligodeoxyribonucleotides (PS-ODN) diminished *Mtb* growth in liquid medium by 1.7 log colony forming units (CFU) while individual PS-ODNs only had a slight effect (Harth, et al., 2002). Hair pin extensions to these ODNs further improved their efficacy and reduced *Mtb* growth in THP1 macrophages as well (Harth, et al., 2007). These studies support the hypothesis that the three proteins are functionally redundant. Molecular analysis of the gene sequences identified a carboxylesterase conserved sequence which is necessary for catalysing the transesterification reaction (Belisle, et al., 1997). Analysis of crystal structures of all three proteins indicated an almost identical active site carrying the Ser-Asp/Glut-His catalytic triad (Anderson, et al., 2001; Ronning, et al., 2000; Ronning, et al., 2004). Since NMR analysis showed that Ag85C-1-4 bind to the active site and substrate binding domains as the artificial probe octylthioglucoside(OSG), these compounds may act through blocking Ag85A, B and C altogether, leading to growth inhibition (Schade, M. et al, unpublished data). This activity of Ag85C-1-4 is similar to that of previous trehalose derivative inhibitors which competitively bind to and block all three Ag85 proteins causing toxicity. This does not exclude induction of other non-specific pathways by the compounds in the whole *Mtb* cell. Functional investigation of these effects as discussed in section 4.2 has been carried out to approach these pertinent questions.

#### 4.1.1.1 Activity against MDR *Mtb*

One of the main concerns of current TB drug discovery initiatives is development of resistance and hence searches for lead compounds targeting novel pathways. Therefore, the most potent analogue, Ag85C-3, was tested against a multi-drug resistant (MDR) strain of *Mtb* with the colorimetric assay. An African clinical isolate of *Mtb*, SROB3023, which is resistant to both INH and RIF making it an MDR strain, was used. Ag85C-3 inhibited growth of this strain at 100 $\mu$ M with complete inhibition at 250 $\mu$ M, identical to the profile obtained with lab strain H37Rv (Fig. 8 & Fig. 10). Thus, Ag85C-3 has no cross resistance with two prominent mycobactericidal drugs, INH and RIF, making it attractive for development into a potential lead compound. Additionally, this also indicates that the pathways targeted by Ag85C-3 are distinct from those of INH and RIF. Studies with more MDR and also XDR strains could give additional information about cross-resistance patterns and thus probable targets of Ag85C-3. Nevertheless, direct inhibition of *Mtb* growth by the compounds raises the question about their effect and relevance in an infection scenario and this has been approached in *ex vivo* and *in vivo* models of TB.

#### 4.1.2 Activity in *ex vivo* infection model

Since *Mtb* resides mainly in the lung macrophages of infected individuals, the activity of the analogues in a primary mouse macrophage infection model was evaluated. *Mtb* can counter normal antimicrobial strategies deployed by macrophages upon its phagocytosis (Kaufmann, 2001). This includes blocking phagolysosomal fusion and neutralising reactive radicals released to kill the bacteria. From within its safe location inside these macrophages, *Mtb* modulates the immune response enabling it to survive and establish a chronic infection in most individuals (Cosma, et al., 2003). Thus, a molecule which retards the growth of *Mtb* directly should also be active against intracellular bacteria for it to be considered as a promising anti-mycobacterial compound. To address this aspect, an *ex-vivo* model with macrophages has been used. They were generated from bone-marrow cells of C57BL/6 mice using standard differentiation protocols (Austin, et al., 1971). Notably, none of the previously studied Ag85 inhibitors had been tested against intracellular mycobacteria in either primary macrophages or cell lines. Prior to testing their activity, toxicity of Ag85C-2-4 was evaluated since cytotoxicity is an essential parameter for any mammalian cell or animal based study of inhibitor molecules. Absorbance measurements of the product, purple formazan, produced by macrophage respiratory enzymes from yellow tetrazole MTT showed that up to 100 $\mu$ M of the three compounds was well tolerated (Fig. 11). Since the compounds were non-toxic, macrophages were treated with Ag85C-2, 3 and 4 post *Mtb* infection followed by a kinetic analysis of transcrip-

tional activity of *Mtb* with [<sup>3</sup>H]-Uracil uptake measurements. Ag85C-3 markedly reduced scintillation counts reflecting reduction of intracellular bacteria at 100µM while Ag85C-2 and Ag85C-4 had no effect (Fig. 12). Assessment of colony forming units further confirmed the activity of Ag85C-3 on phagocytosed *Mtb* at 100µM (Fig.13). The defective survival of *Mtb* inside macrophages upon Ag85C-3 treatment clearly shows that this molecule is active in an infection scenario and also hints that Ag85C inhibition could hinder the adaptation of *Mtb* to intracellular growth.

Previous studies have shown that though Ag85 complex proteins were detected in the phagosomes and cytosol of infected cells by immune-cytochemistry, only the Ag85A mutant had reduced survival in mouse and human macrophages while Ag85B and C mutants did not (Armitige, et al., 2000; Harth, et al., 1996; Jackson, et al., 1999). This defect was exacerbated in interferon gamma activated macrophages and was attributed to the decreased SOCS-1(Suppressor of cytokine signalling-1) activation by the Ag85A mutant in these cells (Katti, et al., 2008). However antisense blocking of the three genes together in *Mtb* inside human THP1 macrophages led to 0.3 to 0.4 log CFU reduction (Harth, et al., 2007). Comparative expression studies in human macrophages and liquid cultures have also indicated a differential expression pattern of the three genes in varied environments with increased expression of Ag85A in resting macrophages (Lee and Horwitz, 1995; Mariani, et al., 2000). Thus, Ag85C-3 might block all three Ag85 proteins with a pronounced effect on Ag85A leading to inhibition of growth inside primary mouse macrophages. There could also be non-specific activation of macrophage antimicrobial mechanisms by the compound. The observation that Ag85C-3 could retard growth of intracellular *Mtb* led to investigation of its activity in an animal model of infection.

#### **4.1.3 *In vivo* studies**

The mouse is the best established model for understanding TB pathogenesis as the result of cross-talk between host and pathogen. A large variety of reagents and tools have been developed to dissect cellular and immune response pathways in mice. *Mtb* infection via the aerosol or intravenous routes in mice leads to chronic infection with an initial acute phase of rapid replication followed by a plateau phase where the induced adaptive response contains the bacterial numbers for many months. But there are notable differences in the pathology of disease in mice when compared to human TB. The main points are the very high bacterial burden observed in mice even during the chronic infection stage and the absence of heterogeneity in granuloma structures (Flynn, 2006; Stewart, et al., 2003). In spite of this, mice have been extensively used for preclinical assessment of experimental compounds mainly because of the

relative ease in developing and establishing the mouse model. Initial studies used high intravenous doses of *Mtb* which was up to 50% of the lethal dose to infect the mice. These bacteria are taken up by spleen and liver macrophages thus representing the disseminated stage of infection.

More recently a low dose aerosol model of infection of mice was established for large scale screening of compounds. This system more closely resembles the primary stages of infection in humans where low numbers of inhaled bacteria establish infection accompanied with initiation of the adaptive response leading to positive tuberculin skin test (Kelly, et al., 1996). A modification of this model was used as a pilot study to determine if Ag85C inhibition had an effect whatsoever on lung resident *Mtb*. The compounds were administered via the intranasal route with the aim of expediting access to the bacteria. At the early time point of 28 days post infection a mild reduction of colony forming unit (CFU) counts was observed at 1mM dosage of Ag85C-3 and at 0.5mM and 1mM Ag85C-3 in combination with 0.1mM INH (Fig. 24). Thus, the compound does have an antimycobacterial effect in mice lungs and is active in combination with the first line anti-tubercular, INH. At the later time point of 42 days post infection this effect vanished probably due to rapid degradation of the compound. Therefore a continuous dose of compounds at higher concentrations via the more physiologically relevant oral route should be used in future experiments. Moreover, detailed understanding of the pharmacokinetics of the molecule is required for further optimisation of parameters.

Thus, the panel of molecules, Ag85C-1-4, which bind to the mycolyl transferase Ag85C, were also found to inhibit growth of *Mtb* in broth culture. This could be through simultaneous blocking of the three Ag85 proteins since they share a highly conserved active site and are partially redundant in function. Importantly, the most potent analogue, Ag85C-3, could also inhibit growth of the MDR strain SROB3023 in the same concentration ranges as observed for lab strain, H37Rv. Hence, the pathway/s being targeted by this compound is/are distinct from that of INH and RIF reducing the possibility of cross resistance development. Additionally, Ag85C-3 could retard the growth of *Mtb* residing in macrophages, the primary host cells of the pathogen. Preliminary studies also indicated that Ag85C-3 administration leads to a mild reduction in *Mtb* survival in lungs of infected mice at early time points after treatment. The potent anti-mycobacterial activity of Ag85C-3 in both liquid culture, macrophage infection model and in mouse lungs led to detailed functional investigation of its direct effect on *Mtb* cells.

## 4.2 Mechanisms of action

As periplasmic transferases, Ag85 complex proteins are necessary for terminal incorporation of mycolic acids to cell wall components, mAGP and TDM (Takayama, et al., 2005). Mycolic acids are long chain  $\alpha$ -alkyl  $\beta$ -hydroxy fatty acids with 80-90 carbon atoms and are the main structural components of the mycobacterial outer membrane. They are critical in establishing the characteristic low permeability of mycobacterial cell wall which makes it resistant to harsh treatments and antibiotics (Marrakchi, et al., 2008). INH, frontline antitubercular, induces bacterial death by disrupting biosynthesis of mycolic acids underlining their importance for *Mtb* survival (Dover, et al., 2008). Hence the impact of Ag85C-3 which binds to Ag85C, on the lipid composition of *Mtb* cell envelope was studied as a first step towards deciphering its mode of action.

### 4.2.1 Lipid analysis

The function of Ag85 proteins as mycolyl transferases, involved in the production of TDM and mAGP, the two most prominent mycolic acid carrying species, was discovered through *in vitro*, structural and mutant studies. TMM generated by unknown cytoplasmic transferase from trehalose-6-phosphate and mycolic acid-Pks13 is considered the common substrate of Ag85 proteins (Takayama, et al., 2005). They catalyze the transfer of a mycolic acyl group from one molecule of TMM to another TMM to give rise to TDM in periplasmic space (Belisle, et al., 1997). However, Ag85 B and C mutants showed no changes in amounts of TDM and TMM when compared with wild type strains (Jackson, et al., 1999; Puech, et al., 2002). Though initial experiments indicated a similar situation in Ag85A mutant, recent studies indicate that this strain might have slightly lesser amount of TDM (Katti, et al., 2008; Puech, et al., 2002). This suggests that the proteins are redundant for this arm of the reaction. The Ag85C mutant had reduced amounts of mAGP which is the strongest proof for its role in transfer of mycolic acids to the polysaccharide (Jackson, et al., 1999). Ag85A and B mutants, on the other hand, had no defects in mAGP and could only partially rescue the Ag85C mutant suggesting partial redundancy of these proteins in this second arm of the transferase reaction (Puech, et al., 2002). The initial trehalose analogue ADT is the only chemical inhibitor of Ag85 proteins which was probed for effect on cell wall lipids (Belisle, et al., 1997). It reduced amounts of TMM, TDM and mAGP in *M. aurum* hinting that a complete block of this step in the pathway could lead to drastic changes in amounts of mycolic acid carrying species. Therefore, a detailed analysis of *Mtb* lipids with an emphasis on TDM, TMM, mAGP and total mycolic acids has been performed to understand Ag85C-3 induced toxicity.

#### 4.2.1.1 TDM and TMM

Analysis of TDM and TMM biosynthesis in Ag85C-3 treated *Mtb* was performed by radiolabelling lipids using [ $^{14}\text{C}$ ] - sodium acetate precursor which is highly sensitive to minor perturbations. Quantification of TDM and TMM synthesis was done by feeding treated and untreated bacteria with radiolabel, extraction of loosely bound lipids and separation and visual detection with TLC. Measurement of band intensity showed that TDM amounts reduced by 14% with 100 $\mu\text{M}$  of Ag85C-3 with a concomitant 100% increase of TMM relative to the untreated samples (Fig.15 b). This established a direct effect of Ag85C-3 on the mycolyl transferase reaction since previous studies have shown TMM to be the substrate and TDM, the product of this reaction (Belisle, et al., 1997). This again points to the scenario where all three Ag85 proteins are blocked by Ag85C-3 since single mutants do not show a significant defect in TDM or TMM amounts (Jackson, et al., 1999; Puech, et al., 2002). INH reduced amounts of both TDM and TMM by close to 60% at 10 $\mu\text{M}$  (Fig. 14 b) (Dover, et al., 2008). Thus, even though Ag85C-3 targets cell wall biogenesis, the mechanism is distinct from that of standard cell wall modulator, INH. This could explain susceptibility of the INH resistant MDR strain, SROB3023, to Ag85C-3.

#### 4.2.1.2 Free mycolic acids

Interestingly, accumulation of free mycolic acids up to 100% in extractible lipids was observed with 100 $\mu\text{M}$  of Ag85C-3 (Fig.16 d). Free mycolic acids have not been detected in pellicle forming stationary *Mtb* cultures. But recent studies with *Mtb* and *Msmeg* biofilms *in vitro* showed that the extensive extracellular matrix observed in these structures were lipid rich particularly with free methoxy mycolic acids. Biofilm formation is dependent on mycolic acid biosynthesis and they harbour drug resistant persisters hinting that such a physiological state might be present in granulomas (Ojha, et al., 2008). Nevertheless, the high sensitivity of [ $^{14}\text{C}$ ] assay might have detected minor amounts of these molecules produced in log-phase cultures of *Mtb* used for testing Ag85C-3. Hence, to ascertain that the bands were truly free mycolic acids samples were subjected to biochemical manipulations like saponification and methylation procedures. This yielded typically two bands of  $\alpha$  and oxygenated mycolic acid methyl esters with standard TLC protocols which confirmed that it was free mycolic acids (Fig. 16 b). Thus, Ag85C-3 treatment increased amounts of free mycolic acids which might be a consequence of an imbalance in the amounts of mycolic acids due to a perturbation of transfer by Ag85C-3. These molecules could either be degradation products from accumulated TMM or be as yet unidentified precursors of this pathway. Time course analysis of synthesis of all mycolic acid containing species in the extractible lipids was performed to resolve this. It clearly

showed that while [ $^{14}\text{C}$ ] - acetate was incorporated into TMM from the earliest time point of 45 minutes, TDM and free mycolic acids were further downstream in the synthesis route (Fig. 17). Thus, the accumulated mycolic acids would most likely be degradation products or side-products of the block in enzymatic activity of Ag85 proteins. Since free mycolic acids are essential for the maintenance of biofilm like phenotype of *Mtb*, the excess amounts of free mycolic acids upon Ag85C-3 treatment might induce signalling pathways modifying the physiological state of *Mtb* leading to toxicity.

#### 4.2.1.3 Cell wall linked mAGP and total mycolic acids

In contrast to Ag85C inhibition by Ag85C-3, genetic inactivation of Ag85C showed no defect in TDM synthesis, but displayed a 40% reduction in the amount of cell wall linked mycolic acids (mAGP) (Jackson, et al., 1999). The Ag85A and B mutants, on the other hand, showed no reduction in cell wall linked mycolic acids and over expression of these proteins in the Ag85C mutant could only partially rescue the drastic phenotype indicating that the Ag85C might be more important for the synthesis of mAGP (Puech, et al., 2002). Hence modulation of mAGP synthesis by Ag85C-3 was determined. mAGP is found attached to outer surface of delipidated bacteria and were extracted by extensive biochemical manipulation of delipidated cells. Measurement of amount of radiolabel incorporation into the cell wall linked mycolic acids as indicated by band intensities of the three types of mycolic acid methyl esters revealed that Ag85C-3 treatment had no significant effect on transfer of mycolic acids to AGP (Fig. 18). This could be because the binding conformation of Ag85C-3 at the active site might be modulating only TMM to TMM transfer and not to cell wall linked AGP. Thus, Ag85C-3 mainly modified mycolic acid composition of the extractible compartment of cell envelope and not of the covalently associated one.

Disruption of mycolic acid biosynthesis pathways by certain drugs like INH led to upregulation of enzymes like KasA, FabD and AcpM which could then increase total mycolic acids as a feedback response (Waddell, et al., 2004; Wilson, et al., 1999). To exclude the possibility of an effect of Ag85C-3 on total mycolic acid biosynthesis, whole cells loaded with radiolabel precursor were saponified, methylated and analysed by TLC. There was no change in their amounts clearly indicating that Ag85C-3 is specifically affecting transfer of mycolic acids and not their synthesis. This is in contrast to INH which completely abrogated total mycolic acids (Fig. 19). Modification of TDM and TMM by Ag85C-3 could lead to changes in the composition and thus integrity of the cell envelope. The immediate aftermath of cell envelope perturbation is varied permeability which has been investigated as described below.



#### 4.2.2 Permeability

One of the main consequences of the complex architecture of mycobacterial cell wall is its very low permeability to both hydrophilic and even hydrophobic molecules. This is one of the main reasons for its renowned resistance to harsh treatments (Daffe, 2008). To overcome the lipid barrier to hydrophilic nutrient molecules required for their survival mycobacteria have porins like gram negative bacteria. Porins are water filled protein channels that non-specifically facilitate the influx of hydrophilic solutes. Though MspA has been identified as the major porin of non-pathogenic *Msmeg* a similar protein in *Mtb* has been not been detected (Niederweis, 2003). Nevertheless the need for transporters spanning outer membrane is well accepted.

Since Ag85C-3 modifies cell envelope glycolipid composition it could also change the permeability of the envelope to extrinsic molecules. This was investigated by measuring the uptake of the small hydrophilic molecule, glycerol. It is used as carbon source by mycobacteria and has been postulated to partially diffuse through the lipid barrier due to the sparse distribution of porins on *Mtb* envelope (Laneelle and Daffe, 2008). The continued accumulation of glycerol is dependent on glycerol metabolism and thus ATP production as demonstrated by arsenate mediated inhibition of this process. But uptake at earlier time points up to 25 minutes depends on the cell envelope integrity and reduction of mAGP leads to drastic increase in glycerol uptake (Jackson, et al., 1999). Hence, the increased [<sup>14</sup>C]-glycerol uptake by Ag85C-3 treated *Mtb* clearly established increased permeability of the membrane. The degree of increase is up to 30% which correlates with the low reduction of TDM amounts up to 14% (Fig. 20 & Fig.15 b). However, any change in permeability could lead to uncontrolled accumulation of solvents culminating in death of the bacteria. This could be one of the major mechanisms by which Ag85C-3 kills *Mtb*. Thus, modulation of cell wall components even by slight degrees can lead to drastic changes in survival.

#### 4.2.3 Specificity

Another aspect is the redundant role of Ag85 complex proteins in transfer of mycolic acids from TMM to another TMM by trans-esterification to generate TDM (Belisle, et al., 1997). To investigate if Ag85C-3 modified TDM amounts by a specific effect on Ag85C, it was tested against an *Mtb* strain lacking Ag85C, MYC1554. This strain was identified by screening a transposon library on clinical isolate Mt103 background based on insertion in Ag85C locus. It showed no defect in TDM amounts but cell wall linked mycolic acids were reduced up to 40% (Jackson, et al., 1999). Qualitative and quantitative anti-mycobacterial assays indicated that the mutant was equally susceptible to Ag85C-3 as the wild type (Fig. 21). Additionally,

analysis of extractible lipids showed that TDM synthesis was reduced in the mutant but TMM accumulation could not be observed (Fig. 22 a). This unchanged TMM amount was also observed in the wild type background and might be due to a higher turnover of TMM in these strains. This is supported by a much higher accumulation of free mycolic acids in these strains compared to H37Rv (Fig. 22 b).

Thus the mycolyl transferase reaction is blocked by Ag85C-3 even in the absence of Ag85C again suggesting that Ag85A and Ag85B might be inhibited by this molecule. To confirm this we first need to test the compound on the Ag85A and B single mutants and then a conditional knockdown of all three proteins. But it is important to emphasise that demonstration of an effect on mycolyl transferase activity does not exclude other putative targets which could also contribute to toxicity. A more large scale approach, through screening of a whole genome level over expression library or a mutagenesis library with the aim of picking up resistant strains or a whole genome level expression study as described below, would help identify all the possible targets of this compound.

#### 4.2.4 Gene expression analysis

An organism adapts to any change in its environment by modifying the expression of those genes which would aid in its survival and growth under the new conditions. Hence, mRNA levels would be a very good indication of signalling networks being evoked or suppressed upon stimulus. Based on this knowledge microarray analysis of *Mtb* response to a variety of perturbations including drug treatment has been performed. One of the most extensive studies performed by Boshoff *et al.* (2004) analysed *Mtb* response to drugs and growth inhibitory conditions using a data set of 430 microarray profiles. In addition to generating signature profiles for drugs or groups of drugs this kind of analysis helps in assigning target pathways to previously uncharacterized inhibitory molecules (Boshoff, et al., 2004). Individual studies looking into *Mtb* gene expression after INH, EMB, PA-824 and Benzothiazinones, to name a few, have also been performed to better understand their impact on *Mtb* (Makarov, et al., 2009; Manjunatha, et al., 2009; Wilson, et al., 1999). In this context, whole genome expression profiling of *in vitro* grown *Mtb* after treatment with Ag85C-3 was done for a complete functional characterization of the phenotype. Due to the partial redundancy of the Ag85 complex proteins and the absence of a triple mutant not much is known about the probable regulatory role of the mycoyl transferase reaction. Hence, gene regulation analysis after Ag85C-3 treatment is a useful tool to probe this aspect. Stringent analysis of expression levels based on fold change and P-value cut offs gave rise to a relatively short but robust list of 65 and 29 regulated genes with 50 and 100 $\mu$ M of Ag85C-3, respectively, after 48 hours of treatment.

The strongest up regulation was observed with proteins belonging to the *Mycobacteria* membrane protein large (MmpL) family, namely, MmpL6 and MmpL5 (Fig.24 a). MmpLs are transporter proteins with up to 12 transmembrane domains and is a subset of the larger resistance, nodulation and division (RND) superfamily of transporters (Jain, et al., 2008). In gram negative bacteria RND proteins primarily function as drug efflux pumps while in more closely related gram positive bacteria they serve as transporters for endogenous substrates. In mycobacteria most of the 14 MmpL genes are located in the vicinity of polyketide synthase genes suggesting that they could be involved in transport of the various polyketide derived products across plasma membrane. MmpL7 and 8 are the best characterized with their *Mtb* mutant strains showing defective transport and synthesis of PDIMs and SLs, respectively (Converse, et al., 2003; Cox, et al., 1999). Since none of the *Mtb* mmpL mutants displayed altered susceptibility to drugs, they have been hypothesized to function as putative lipid/polyketide transporters and not drug efflux pumps (Domenech, et al., 2005).

MmpL6 is a 42kDa truncated protein with only 5 transmembrane regions and is located in the variable TbD1 region in the *Mtb* genome (Domenech, et al., 2005). It is deleted in 'modern' strains of *Mtb* but is conserved in the ancestral strains and in *M. bovis* (Brosch, et al., 2002). The mutant strain of *Mtb* lacking this protein has no survival defects either in broth culture or in infected mice. The increased expression of up to 70 fold of MmpL6 with Ag85C-3 hints at a probable role in lipid transport specifically of mycolic acid or trehalose containing species (Fig. 24 a). The fact that it is located approximately 4Kbp. upstream of one of the trehalose biosynthesis operons, TreZ-X, further supports this hypothesis. MmpL5, on the other hand, has been linked to iron uptake due to its transcriptional control by the iron dependent IdeR repressor (Rodriguez, et al., 2002). It is associated with a predicted smaller transmembrane protein MmpS5 which could function like the MFPs associated with RND proteins in gram negative organisms. The *Mtb* mmpL5 mutant also did not display any growth defects *in vitro* and *in vivo* (Domenech, et al., 2005). Up regulation of both MmpL5 and MmpS5 with 100 $\mu$ M of Ag85C-3 suggests modification of iron regulation by this compound. It could also be that modulation of cell envelope components, specifically mycolic acid lipids, by Ag85C-3 might be causing non-specific effects on the regulation of these transmembrane proteins.

Another interesting gene cluster regulated by Ag85C-3 is the mycobactin synthesis locus, mbt-1. *Mtb* like any other organism depends on external sources for its iron and synthesises specialized iron chelators or siderophores called mycobactins for acquiring iron from outside. They are of two main types, the water insoluble membrane associated mycobactins and the water soluble secreted carboxymycobactins (Rodriguez, 2006). The structural core of the two

molecules is identical composed of a hydroxyphenyloxazoline ring derived from salicylic acid, two lysine residues and a polyketide fragment. They differ in the nature of the N-linked acyl chain which is a short carbonyl group in the case of carboxy mycobactins while it is a long lipidic chain in mycobactins (Snow, 1970). The ten gene MbtA-J or mbt-1 cluster is believed to be essential for the production of the core motif while the mbt-2 locus is involved in attachment of the fatty acyl chain as well as transport (Krithika, et al., 2006; Quadri, et al., 1998). The expression of these genes and thus mycobactin amounts is tightly coupled to iron availability and regulated by the IdeR repressor. IdeR is an iron dependent DNA binding protein and an essential gene (Rodriguez, et al., 2002). An *Mtb* strain lacking MbtB, a nonribosomal peptide synthase located in mbt-1 locus has reduced survival under iron limiting conditions and shows marked reduction in mycobactin and carboxy mycobactin amounts. It also cannot replicate in the human macrophage cell line, THP-1 (De Voss, et al., 2000).

Ag85C-3 treatment led to increased expression of seven genes in the mbt-1 locus as detected by microarray analysis which was confirmed by quantitative PCR validation with three genes (Fig. 23 c). This is unexpected since under iron rich conditions of 7H9 medium these genes would be normally repressed. Quantification of carboxymycobactins and mycobactins under same conditions showed a marked increase in their amounts in the presence of Ag85C-3 (Fig. 23 b). This could first be a stress response to outer membrane perturbations probably leading to lower association of membrane anchored mycobactins which results in reduced iron acquisition. Low iron amounts are toxic due to its essential role in the activity of enzymes involved in key processes ranging from respiration to DNA replication. The second possibility is an artificial induction of mycobactin synthesis by Ag85C-3 which then leads to unwarranted accumulation of iron within *Mtb*. Iron in excess is also toxic to cells due to its ability to generate reactive oxygen radicals from normal products of aerobic metabolism by the Fenton's reaction. Thus, iron modulation could be an additional mechanism by which Ag85C-3 induces death. It is also not clear if this is an indirect effect of the block in mycolic acid transfer or whether Ag85C-3 directly interacts with iron regulatory pathways. It does not appear to be an inhibition of IdeR repression since the other mycobactin synthesis genes of the mbt-2 cluster are not affected by Ag85C-3. It thus seems to be a specific up regulation of the mycobactin core synthesis machinery. More detailed studies including measurement of iron amounts upon Ag85C-3 treatment need to be performed to obtain a clearer picture of the underlying mechanism. Nevertheless, it is important to note that iron regulation in *Mtb* and thus mycobactin synthesis is considered an attractive target for intervention strategies due to its essentiality for survival in the host.

Ag85C-3 treatment also led to down regulation of some of the lipid synthesis genes like Fas, and Mas. Fas, AcpM and FabD are involved in the initial steps of fatty acid biosynthesis which gives rise to 16-18 carbon atom carrying lipids (Marrakchi, et al., 2008). A stress on the mycolic acid synthesis pathway by INH, for example, leads to upregulation of these genes (Wilson, et al., 1999). Mas, on the other hand, is a part of the PDIM/PGL locus involved in the synthesis of the mycocerosate carrying virulence lipids (Guilhot, et al., 2008). Quantitative PCR experiments showed that the expression was down regulated but the degree of regulation was lesser than the 1.5 fold change shown by microarray analysis suggesting that these pathways were not significantly modulated by the compound (Fig. 24 b). Other prominent groups of genes regulated by Ag85C-3 are the PE/PPE proteins which have been postulated to play a role in pathogenesis and virulence (Brennan and Delogu, 2002). Proteins involved in intermediary metabolism like GltA1, RubB and AlkB were found to be up regulated probably as a stress response to Ag85C-3 treatment. Additionally, ribosomal proteins like RpsR2, RpsN2 and RpmB2 were down regulated pointing to a repression of transcriptional activity and thus general metabolism in response to the compound induced stress.

Therefore, whole genome expression studies proved invaluable for obtaining deeper insights into signalling pathways and molecules being modulated by Ag85C-3. This could either be indirect effects of the block in mycolyl transferase reaction catalysed by Ag85C or be other direct effects of the compound. It is important to note that an inhibitory molecule would be more effective if it targets more than one pathway since the probability of resistance development is lower in these cases.

## 5 Conclusions and Outlook

In summary, our findings show that small molecule mediated inhibition of Ag85C induces toxicity in *Mtb* growing in liquid medium, inside macrophages and in lungs of mice. A multi drug resistant *Mtb* clinical isolate was found to be susceptible to Ag85C-3, the most potent of these molecules, highlighting the relevance of Ag85C as a novel target. Ag85C-3 specifically blocked the mycolyl transferase reaction catalysed by Ag85 proteins as indicated by reduced TDM and increased TMM. It also induced an unexpected accumulation of free mycolic acids while cell wall linked mycolic acid (mAGP) amounts remained unchanged. This disruption of mycolic acid biogenesis is distinct from that of classical cell wall inhibitor and first line anti tubercular drug, INH which abrogated TDM, TMM, free mycolic acids and mAGP. The distinct mechanism could explain susceptibility of the INH resistant MDR strain to this compound.

As a consequence of mycolic acid perturbations by Ag85C-3, the permeability of *Mtb* cell wall is altered leading to death. But additional mechanisms could be underway as indicated by up regulation of siderophore synthesis and membrane transporter genes detected by whole genome expression analysis. Since iron acquisition and homeostasis is crucial in the survival of any organism, modification of mycobactin production by Ag85C-3 could be another reason for its toxic effect on *Mtb*. Moreover, this molecule is not specific to Ag85C alone and could be blocking all three Ag85 proteins since treatment of an Ag85C deficient mutant strain leads to TDM reduction and growth defect.

Thus, Ag85C and its inhibitor, Ag85C-3 are promising starting points for development of future intervention strategies against TB. The current long duration therapy needs to be modified to enhance patient compliance and prevent further emergence of resistance. Drug resistant TB is another major concern and requires new molecules to be employed in the clinics at the earliest. Since Ag85C-3 blocks cell wall biosynthesis at an essential but distinct step from that of INH and EMB it could be extremely useful as a lead compound to counter strains resistant against these 2 antibiotics. Further testing with MDR and XDR strains would help in establishing its activity in this scenario. Synergy with other anti-tubercular drugs needs to be ascertained to determine its utility in combination therapy. Also, optimisation of Ag85C-3 structure is required to lower its MIC to nanomolar concentration ranges. These modifications should also enhance its aqueous solubility which would enable more physiologically relevant *in vivo* studies with higher concentrations administered via the oral route. Another important question is the efficacy of these compounds against non-replicating, dormant *Mtb*. Simplified

*in vitro* systems based on the Wayne hypoxia model and/or nutrient starvation can be used to address this aspect.

Small molecule antagonists like Ag85C-3 are also useful tools to understand the regulatory role of Ag85 complex and thus the complex biology of *Mtb*. Though it has been established that Ag85C-3 does inhibit mycolyl transferase activity of Ag85C and probably the other Ag85 complex proteins as well, a clear link between this and regulation of mycobactin biosynthesis or MmpL protein expression has not been elucidated. More detailed experiments like addition of exogenous TMM and/or free mycolic acids mimicking Ag85 complex block and subsequent analysis of mycobactin synthesis need to be performed. Further, comparison with a transient triple gene knockdown of Ag85A, B and C would also be essential for validation of the proposed regulatory role of Ag85 complex proteins. Thus Ag85C-3 also enables better understanding of pathways linked to and involved in cell wall biogenesis in *Mtb*.

## 6 Materials and methods

### 6.1 Methods

#### 6.1.1 Alamar blue assay

*Mtb* H37Rv was propagated in Middlebrook 7H9 broth supplemented with 10% ADC, 0.25 % glycerol, and 0.1 % Tween-80 to an OD of 1.0 at 580nm at 37°C. Stock solutions of the compounds were made in DMSO and aliquots stored at -20°C, this was used in all the following experiments. The compounds were diluted with 7H9 medium lacking Tween-80 to various working concentrations ranging from 50µM to 250µM and distributed in 100µl aliquots into the wells of a 96-well plate. An aliquot (100µl) of bacterial culture diluted at 1:25 ratio in 7H9 medium lacking Tween-80 and containing about  $2 \times 10^6$  bacteria was added per well. The plates were sealed and incubated at 37°C for 96 hours after which 50µl of freshly prepared 1:1 mixture of 10X Alamar Blue reagent containing resazurin and 20% Tween-80 were added to each well. Plates were incubated for additional 24 hours at 37° C. Hygromycin at a concentration of 100µg/ml was the positive control. Plates were read by visual inspection for colour change from blue (in wells containing no metabolic activity – dead *Mtb*) to pink in wells containing live *Mtb*. The images were captured with digital camera.

#### 6.1.2 [<sup>3</sup>H]-Uracil Incorporation Assay

*Mtb* H37Rv bacteria from mid-exponential growth phase were collected by sedimentation and resuspended in phosphate buffer saline (PBS). Single cell suspension was made by five to six forced passages through a 0.40µm needle. *Mtb* cell density was measured by spectrophotometer (OD<sub>580</sub> 0.1 =  $5 \times 10^7$  bacteria/ml) by diluting it at 1:10 ratio in 10% paraformaldehyde (PFA). Bacteria were then added at a density of  $10^7$  bacteria/ml to 100µl of 7H9 medium without Tween-80, with or without the desired concentrations of compounds in a 96 well plate and incubated at 37°C. The time points for measurement were 24, 72 and 120 hours post-treatment. 24 hours prior to each time point 1µCi of [<sup>3</sup>H]-Uracil was added to each well and the plate frozen at -80°C after the duration. The plates were fixed by adding 100µl of 10% paraformaldehyde to each well and harvested with Filtermate Harvester. The scintillation counts were then measured with TopCount scintillation counter. The average scintillation count from hex plicates was calculated for each treatment condition and plotted with standard deviation using Graphpad Prism 5.0.

#### 6.1.3 MTT toxicity assay

Bone marrow cells were extracted from the tibia and femur of C57BL/6 female mice aged 8-12 weeks and seeded in culture dishes ( $\sim 5 \times 10^6$  cells per dish). The differentiation into macro-



phages was performed as described. The macrophages were seeded in 48 well plate at a density of  $3 \times 10^5$  cells/well in triplicate and incubated at 37°C with 5% CO<sub>2</sub> overnight for complete adhesion to the surface. The cells were washed once with PBS and fresh medium added with or without the desired concentration of compound and incubated at 37°C with 5% CO<sub>2</sub>. 2-3 hours prior to each time point 50µg/ml MTT was added from a stock solution of 5mg/ml in 1X PBS. The supernatant was removed and adherent cells lysed in 100µl 100% DMSO and absorbance measured at 550nm with spectrophotometer. DMSO at concentrations present in the compound dilutions is used as control if necessary. The average absorbance from triplicates was calculated for each treatment and plotted with standard deviation using Graphpad Prism 5.0. The untreated samples were taken as 100%.

#### 6.1.4 [<sup>3</sup>H]-Uracil Incorporation Assay during macrophage infection

Primary bone marrow macrophages were obtained from C57BL/6 mice as described in 6.1.3. Cells were then seeded in 96-well plates at a density of  $5 \times 10^4$  cells per well in DMEM medium containing 10% fetal calf serum, 10 mM HEPES (pH from 6.5 to 7.5) 1 mM sodium pyruvate, and 1% L-glutamine, and incubated overnight at 37° C and 5% CO<sub>2</sub> for adhesion.

*Mtb* H37Rv bacteria from mid-exponential growth phase were collected and single cell suspension prepared by five to six forced passages through a 0.40 µm needle. *Mtb* cell density was measured by spectrophotometer (OD<sub>580</sub> 0.1 =  $5 \times 10^7$  bacteria/ml) by diluting it at 1:10 ratio in 10% PFA. Infection of macrophages was performed at 5 bacilli per macrophage (5:1) in hex plicate wells. Macrophages were incubated for 4 h at 37° C and then 10µl of fresh medium with working concentrations of compound was added to each well. 24 hours before each time point (24, 72 and 120 hours post treatment) 1µCi of [<sup>3</sup>H]-Uracil was added to each well and incorporation allowed. Then the whole plate was frozen away at -80°C. The plates were fixed, harvested and scintillation counts measured. The average scintillation count from hex plicates was calculated for each treatment condition and plotted with standard deviation using Graphpad Prism 5.0. Significance, *p*, for treatment and across time points was calculated using 2-way ANNOVA analysis.

#### 6.1.5 Colony forming unit (CFU) assay

Primary bone marrow macrophages were obtained from C57BL/6 mice as described in 6.1.3. *Mtb* H37Rv bacteria from mid-exponential growth phase were collected and single cell suspension prepared by five to six forced passages through a 0.40 µm needle. *Mtb* cell density was measured by spectrophotometer (OD<sub>580</sub> 0.1 =  $5 \times 10^7$  bacteria/ml) by diluting it at 1:10 ratio in 10% PFA. Infection of macrophages was performed at 5 bacilli per macrophage (5:1) in triplicate wells. Macrophages were incubated with *Mtb* for 4 h at 37° C to allow complete

phagocytosis and washed twice with PBS to remove non-phagocytosed bacteria. 100µl of fresh medium with or without the desired dilution of compound was added to each well. The plates were incubated at 37°C for 24, 72 and 120 hours post treatment. At each time point the supernatant was removed and the cells lysed with 30 µl of PBS containing 0.5% TritonX-100. Dilutions were made in PBS containing 0.05% Tween-80 and 30 µl plated out on 7H11 agar plates. After 3-4 weeks of incubation at 37°C, CFU were counted. The average CFU value from triplicates was calculated and plotted with standard deviation using Graphpad Prism 5.0.

#### **6.1.6 *In vivo* experiments**

8-12 week old C57BL/6 female mice were distributed into 6 groups per time point with 5 mice per group: Placebo, 0.5mM Ag85C-3 treated, 1mM Ag85C-3 treated, 0.1mM INH treated, 0.5mM Ag85C-3 with 0.1mM INH treated and 1mM Ag85C-3 with 0.1mM INH treated. A control group of 5 mice were included to verify initial dose of infection. Infection of mice was performed using a Glas-Col inhalation exposure system. An aliquot of frozen H37Rv *Mtb* stock culture was thawed and diluted (as determined in titration experiments performed for every infection stock) with water such that each mouse would receive 50-100 CFU. On day 1, control group were sacrificed, lungs removed and homogenized in PBST buffer. Dilutions were prepared and plated out on 7H11 agar plates. Mice were anaesthetized and then compounds administered intranasal. 8 doses were given over a period of 2 weeks. Mice were sacrificed at day 28 and day 42 after infection by cervical dislocation. Lungs were transferred into sterile sample bags containing 1 ml PBS/Tween solution (PBST). Organs were homogenized in the sample bags by smashing and after serial dilution in PBST, 50 µl were plated on 7H11-agar plates containing ampicillin and cyclohexamide which were sealed with parafilm and wrapped in aluminum foil. After 3-4 weeks of incubation at 37°C, CFU were counted. The CFU value calculated as average of two dilutions for each mouse, plotted with Graphpad Prism v.5.0 and the significance, *p*, calculated using non-parametric Mann Whitney test.  $p < 0.05$  is denoted by '\*' while  $p < 0.01$  is denoted by '\*\*' and  $p < 0.001$  is denoted by '\*\*\*'.

#### **6.1.7 TDM and TMM synthesis assay**

*Mtb* H37Rv organisms were allowed to grow to mid-exponential growth phase in 7H9 complete medium at 37°C with shaking and optical density measurements made at 580nm. The culture was diluted in 10ml of 7H9 medium without Tween-80 such that the OD was 0.01 and then allowed to grow at 37°C without shaking till the culture reached log phase ( $OD_{580} = 0.3-0.4$ ). Ag85C-3 was then added at the desired concentrations and incubated at 37°C without shaking while the control culture was not treated. After 48 hours [<sup>14</sup>C]-sodium acetate was

added to the medium at a concentration of 0.5 $\mu$ Ci/ml and the cultures were grown for another 24 hours with shaking at 37°C. The bacteria were then collected by sedimentation and lipid extraction initiated with CH<sub>3</sub>OH/CHCl<sub>3</sub> (2:1) solvent for 12 hours. The supernatant was transferred to a fresh tube and evaporated with nitrogen to yield the lipid extractible. CHCl<sub>3</sub>/CH<sub>3</sub>OH (2:1) solvent was added to the bacterial residue for another 12 hours to extract remanant extractible lipids and the supernatant transferred to the same lipid extractible containing tube. This was repeated once more to completely delipidate the bacterial residue.

For the analysis of TDM and TMM these lipid extractible samples were loaded on silica-gel coated plates and subjected to TLC with CHCl<sub>3</sub>/CH<sub>3</sub>OH/H<sub>2</sub>O (60:16:2) as solvent. The plates were exposed to phosphor plates and the band intensities measured with Typhoon image analyzer and ImageQuant software. For normalization the total lane intensity was used and then the values compared against the untreated sample taken as 100%.

#### **6.1.8 Detection and analysis of free mycolic acids**

Extractible lipids obtained as described in 6.1.7 were loaded on silica-gel coated plates and subjected to TLC with CHCl<sub>3</sub>/CH<sub>3</sub>OH (9:1) solvent. To ascertain the nature of the lipid band migrating close to the solvent front, purified glycerol monomycolate (GMM) was used as standard but the unknown band migrated higher. To resolve this issue, one lipid extractible sample was analysed in detail. It was split into three parts, one part left untreated and the second part saponified with 800 $\mu$ l of 1:7 mixture of 40% KOH: 3-methoxyethanol (20ml for every 1g of starting material) at 110°C for 3 hours. The saponified product was then acidified with a few drops of 20% H<sub>2</sub>SO<sub>4</sub> and washed with twice the volume of diethyl ether. The upper organic phase was collected in a fresh tube and the washes repeated twice more. This organic phase was then washed thrice with 1ml of water and the lower aqueous phase discarded each time. The organic phase was dried and then methylated with freshly prepared diazomethane. Briefly, prepare 3ml of 40% KOH in 15ml of diethyl ether in a stoppered flask. To this add 1g of N-nitroso-N-methyl urea very slowly in small quantities and allow the reaction to be complete as visualized by yellow coloration. Carefully transfer the upper organic phase (containing diazomethane) to a fresh stoppered flask with a few pellets of KOH (water adsorbant). A few drops of this reactive species was added to the saponified products and allowed to sit on the bench for 15-20 minutes for complete methylation. The sample was dried and contained methyl esters of mycolic acids (MAME) and fatty acids (FAME). The third part was only methylated as described above.

The three parts were loaded on silica-gel coated plates and TLC with CHCl<sub>3</sub>/CH<sub>3</sub>OH (9:1) and dichloromethane as solvents separately. CHCl<sub>3</sub>/CH<sub>3</sub>OH (9:1) resolves the unknown band

and TDM while dichloromethane resolves MAME and FAME bands. For quantification of free mycolic acid in samples they were loaded on silica-gel coated plates and subjected to thin layer chromatography with  $\text{CHCl}_3/\text{CH}_3\text{OH}$  (9:1) as solvent, exposed to phosphor plates and bands analyzed with Typhoon image analyzer and ImageQuant software. For normalization the total lane intensity was used and then the values compared against the untreated sample taken as 100%.

### 6.1.9 Time course analysis of TMM, TDM and free mycolic acids

*Mtb* H37Rv organisms were allowed to grow to mid-exponential growth phase in 7H9 complete medium at 37°C with shaking and optical density measurements made at 580nm. The culture was diluted in 50ml of 7H9 medium without Tween-80 such that the OD was 0.01 and then allowed to grow at 37°C without shaking till the culture reached log phase ( $\text{OD}_{580}=0.3-0.4$ ). [ $^{14}\text{C}$ ]-sodium acetate was added to the medium at a concentration of 0.5 $\mu\text{Ci/ml}$  and 10ml each of culture taken after 45 minutes, 1.5 hours, 3 hours, 6 hours and 24 hours after addition of radiolabel. The bacteria were then collected by sedimentation from each 10ml culture and lipid extraction initiated with  $\text{CH}_3\text{OH}/\text{CHCl}_3$  (2:1), solvent for 12 hours. The supernatant was transferred to a fresh tube and evaporated with nitrogen to yield the lipid extractible.  $\text{CHCl}_3/\text{CH}_3\text{OH}$  (2:1) solvent was added to the bacterial residue for another 12 hours to extract remanant extractible lipids and the supernatant transferred to the same lipid extractible containing tube. This was repeated once more to completely delipidate the bacterial residue.

The lipid extractible samples were then analysed for TMM, TDM and free mycolic acids. To resolve TDM and TMM, the samples whose volumes were normalised to scintillation counts, were loaded on silica-gel coated plates and subjected to TLC with  $\text{CHCl}_3/\text{CH}_3\text{OH}/\text{H}_2\text{O}$  (60:16:2) as solvent. To resolve TDM and free mycolic acids samples were loaded on silica-gel coated plates and subjected to TLC with  $\text{CHCl}_3/\text{CH}_3\text{OH}$  (90:10) as solvent. The plates were exposed to phosphor plates and bands visualised with image analyzer.

### 6.1.10 mAGP synthesis assay

The delipidated cells obtained after lipid extraction in 6.1.6 were analysed to measure the amount of cell wall linked mycolic acids. The delipidated cells were dried and weighed. Saponification and methylation was performed on the cells as described in 5.1.7. Saponification extracted the mycolic acids exposed at the outer surface of the delipidated cells while methylation converted them to TLC resolvable methyl esters. The dried samples containing MAMEs and FAMEs were run on silica gel coated plates with petroleum ether/ diethyl ether (9:1) four times to completely resolve the three types of MAMEs found in *Mtb*, namely  $\alpha$ , methoxy and keto. The plate was exposed to phosphor plates and bands analyzed with Ty-

phoon image analyzer and ImageQuant software. Normalisation was done to the weight of the delipidated cells and untreated sample was taken as 100%.

#### **6.1.11 Mycolic acid synthesis assay**

*Mtb* H37Rv organisms were grown and subjected to Ag85C-3 treatment as described in 6.1.6. The bacteria were then collected by sedimentation and the whole cell pellet autoclaved at 120°C and high pressure. The pellet was saponified to extract all the mycolic acids from the cell and then methylated to obtain MAMEs as described in 5.1.7. The dried samples containing MAMEs and FAMEs were analysed with TLC with dichloromethane as solvent. The plates were exposed to phosphor plate and bands analyzed with Typhoon image analyzer and ImageQuant software. The FAME bands served as the normalisation control for quantification of the total MAMEs and the untreated sample was taken as 100%.

#### **6.1.12 Data analysis for lipid synthesis assays**

Average value of lipid amounts expressed in % from 3 independent experiments was calculated and plotted with standard deviation using Graphpad prism 5.0. Significance,  $p$ , was calculated with paired two-tailed Student's t-test where  $p < 0.05$  is denoted by '\*' while  $p < 0.01$  is denoted by '\*\*' and  $p < 0.001$  is denoted by\*\*\*'.

#### **6.1.13 Purification of TDM, TMM and GMM**

Extractibel lipids from *Mtb* H37Rv were dissolved in methanol and the mycolic acid lipid enriched precipitate was collected and weighed. The precipitate was dissolved in minimal volume of chloroform and loaded on 50X weight of florisil packed in a glass column. Elution was performed with the following solvents in a step-wise manner: 1)CHCl<sub>3</sub> 2) CHCl<sub>3</sub>/CH<sub>3</sub>OH (99:1) 3) CHCl<sub>3</sub>/CH<sub>3</sub>OH (95:5) 4) CHCl<sub>3</sub>/CH<sub>3</sub>OH (90:10) 5) CHCl<sub>3</sub>/CH<sub>3</sub>OH (85:15) 6) CHCl<sub>3</sub>/CH<sub>3</sub>OH (80:20) 7) CHCl<sub>3</sub>/CH<sub>3</sub>OH/H<sub>2</sub>O (65:25:4). All the fractions were dried, run on silica gel plate and revealed with anthrone to visualize the glycolipids. Fraction 3, 5 and 7 were used for purifying GMM, TDM and TMM, respectively. For this, the fractions were run on silica gel plate and the band corresponding to the lipid scrapped out, dissolved in CHCl<sub>3</sub>/CH<sub>3</sub>OH (2:1) and purified with florisil column using the same solvent as the elution step.

#### **6.1.14 Permeability of *Mtb* cell wall**

*Mtb* H37Rv organisms were allowed to grow to mid-exponential growth phase in 7H9 complete medium at 37°C with shaking and optical density measurements made at 580nm. The culture was diluted in 10ml of 7H9 medium without Tween-80 such that the cell density was  $7.5 \times 10^6$  bacteria /ml. The cultures were incubated at 37°C without shaking overnight and then

Ag85C-3 added at 100 $\mu$ M while the control culture was not treated. Incubation was performed at 37°C with mild shaking. After 48 hours of treatment 0.5 $\mu$ Ci/ml of [<sup>3</sup>H]-Uracil was added and cultures incubated at 37°C with mild shaking for 24 hours. [<sup>3</sup>H]-Uracil incorporation is measured to normalise for total cell number. The culture was centrifuged at 4000 rpm for 10 minutes and the bacterial pellet resuspended in 10ml of PBS. 1ml of this suspension was collected separately in eppendorf tube, spun down at 13,000rpm for 10 minutes and the cell pellet fixed in 100 $\mu$ l of 10% paraformaldehyde overnight at 37°C. [<sup>3</sup>H]-Uracil incorporation in this fixed cell pellet was measured to normalise for total cell number. The remnant suspension was centrifuged and cell pellet suspended in 600 $\mu$ l of PBS. This is the starting suspension for [<sup>14</sup>C]-glycerol uptake measurements. 2 $\mu$ Ci of [<sup>14</sup>C]-glycerol was added to each sample and 100 $\mu$ l immediately transferred to eppendorf tube. This is immediately spun down at 13,000 rpm for 2 minutes, supernatant discarded and snap frozen on dry ice. This is time-point 0 and similar sample collection was performed after 2, 6, 10, 15 and 20 minutes of [<sup>14</sup>C]-glycerol addition. The frozen pellets were fixed in 100 $\mu$ l of 10% paraformaldehyde for 24 hours at 37°C. The scintillations were measured by adding the fixed samples to 3ml of scintillation fluid and counted with Tri-Carb liquid scintillation analyzer. Normalisation was done to the [<sup>3</sup>H] counts and permeability expressed relative to the untreated sample.

#### 6.1.15 Gene expression analysis

*Mtb* H37Rv organisms were allowed to grow to mid-exponential growth phase in 7H9 complete medium at 37°C with shaking and optical density measurements made at 580nm. The culture was diluted in 10ml of 7H9 medium without Tween-80 such that the cell density was 7.5\*10<sup>6</sup> bacteria /ml. The cultures were incubated at 37°C without shaking overnight and then Ag85C-3 added at desired concentrations. Incubation was performed at 37°C with mild shaking. At 48 hours post treatment 5ml of each sample was centrifuged at 4000rpm for 10 minutes to obtain the cell pellet. Supernatant was discarded and the pellet resuspended in remnant medium.

1ml of trizol was added to each sample and total RNA isolated by the TRIZOL reagent RNA preparation method using glycogen as carrier. Briefly, cells were resuspended in 1 ml TRIZOL, shock frozen and stored at -80°C. Cells in TRIZOL were thawed and further processed for total RNA isolation as described by the manufacturer. The amount of RNA was determined by OD<sub>260/280</sub> measurement using a NanoDrop 1000 spectrophotometer. The RNA size, integrity and the amount of total RNA were measured with a Bioanalyzer 2100 with a RNA Nano 6000 microfluidics kit. *Mtb* microarrays were designed with eArray software in conjunction with OligoWiz as 4x44K custom arrays including all open reading frames and

intergenic regions (IGR) from the whole genome of *Mtb* H37Rv (<http://genolist.pasteur.fr/TubercuList/>). Each ORF and IGR was covered at least by several specific oligonucleotides.

Microarray experiments were performed as dual-color hybridizations. In order to compensate specific effects of the dyes and to ensure statistically relevant data analysis, a color-swap dye-reversal was performed. RNA labeling was performed with the two color Quick Amp Labeling Kit using FullSpectrum MultiStart Primer for T7 IVT RNA amplification as random T7 labeling. In brief, mRNA was reverse transcribed and amplified using a FullSpectrum MultiStart-T7-promotor primer and was labeled either with Cyanine 3-CTP or Cyanine 5-CTP. Alternatively, the total RNA samples were amplified with the TransPlex Whole Transcriptome Amplification Kit and labeled with BioPrime Plus Array CGH Indirect Genomic Labeling System as WTA BioPrime indirect. In brief, a library was generated by strand displacement reaction using phi-29 polymerase and quasi-random primers followed by 17 PCR cycles. The resultant cDNA library was labeled with Klenow polymerase in an indirect reaction using aminoallyl nucleotides and subsequent chemical NHS-ester Cy-dye coupling. After precipitation, purification and quantification, of each labelled cRNA (random T7 labelling) or cDNA (WTA BioPrime indirect labelling) the samples were hybridized to custom 44k microarrays according to the supplier's protocol. Scanning of microarrays was performed with 5  $\mu$ m resolution and extended mode using a DNA microarray laser scanner. Raw microarray image data were extracted and analyzed with the Image Analysis / Feature Extraction software G2567AA. The extracted MAGE-ML files were further analyzed on reporter level with the Rosetta Resolver Biosoftware, Build 7.1. Ratio profiles comprising single hybridizations were combined in an error-weighted fashion to create ratio experiments. A 2-fold change expression cut-off for ratio experiments was applied together with anti-correlation of ratio profiles rendering the microarray analysis highly significant (P-value > 0.01), robust and reproducible. Additionally, data derived from the different labelling procedures (random T7 labelling and WTA BioPrime indirect labelling) were compared and combined. Only results derived from both labelling methods were considered as relevant for further verification. The data presented in this publication have been deposited in NCBI's Gene Expression Omnibus (GEO, <http://www.ncbi.nlm.nih.gov/geo/>) and are accessible through GEO Series accession number GSE17424.

#### **6.1.16 cDNA synthesis and quantitative PCR**

*Mtb* RNA samples obtained as described above in 6.1.15 were subjected to DNase digestion with 1.5 units of DNase enzyme and 1.5 $\mu$ g of RNA in 1X DNase buffer at room temperature

for 15 minutes. The reaction was stopped by addition of 2.5mM EDTA and heating at 65°C for 10 minutes. 1µg of DNase digested RNA was incubated with xxµM of Random hexamer mix and 0.5mM dNTP mix for 5 minutes at 65°C and immediately transferred on to ice. To this, 40 units of RNAeasy™, 200 units of Superscript Reverse Transcriptase™ and 0.05mM DTT was added in 1X cDNA synthesis buffer and incubated at 55°C for 60-75 minutes. The reaction was stopped by heat denaturation of samples at 70°C for 15 minutes. The resultant cDNA mix was diluted 1:10 times in distilled H<sub>2</sub>O and stored at -20°C.

For quantitative PCR, 1:10 dilution of the cDNA mix was added to 1X Syber green mix with 0.15µM forward and reverse primers specific for each gene separately and subjected to the FAST qPCR protocol installed in the AB Prism 7900H. SigA was used as the housekeeping gene and the fold change gene expression was calculated using the comparative  $\Delta\Delta C_t$  method.

#### **6.1.17 Mycobactin synthesis assay**

Mtb H37Rv organisms were allowed to grow to mid-exponential growth phase in 7H9 complete medium at 37°C with shaking and optical density measurements made at 580nm. The culture was diluted in 10ml of 7H9 medium without Tween-80 such that the cell density was  $7.5 \times 10^6$  bacteria /ml. The cultures were incubated at 37°C without shaking overnight and then Ag85C-3 added at desired concentrations. Incubation was performed at 37°C with mild shaking. After 48 hours of treatment 0.5µCi/ml of [14C]-salicylic acid and 0.5µCi/ml of [3H]-Uracil were added and cultures incubated at 37°C with mild shaking for 24 hours. [3H]-Uracil incorporation is measured to normalise for total cell number. The culture was centrifuged at 4000 rpm for 10 minutes and the supernatant filtered through 0.22µm filter. The cell pellet was resuspended in 10ml of PBS and 1ml transferred to an eppendorf tube for [3H]-Uracil counts. Cells from 1ml were fixed with 10% PFA overnight at 37°C and scintillation counts measured with TriCarb. Mycobactin extraction was initiated from the remnant 9ml suspension by centrifugation at 4000rpm for 10 minutes, resuspension in 10ml 100% ethanol and incubation overnight at room temperature. The supernatant was filtered through 0.22µm filter, saturated with 2.2mM FeCl<sub>3</sub> (Stock solution-20mg/ml in ethanol) and washed with 1 volume H<sub>2</sub>O. Mycobactins were then extracted in to 10ml of CHCl<sub>3</sub> twice. Carboxymycobactins from FeCl<sub>3</sub> saturated (incubation with 0.6mM FeCl<sub>3</sub> overnight at room temperature) cell culture supernatant were extracted in to 1.5 volume chloroform. The organic extracts were dried, dissolved in 100-200µl of chloroform and equal volumes loaded on silica-gel coated TLC plate. TLC was run with petroleum ether/n-butanol/ethyl acetate (2:3:3) and exposed to phosphorimager screen. Band intensities were measured with AIDA Image analyzer and normalised to [<sup>3</sup>H] counts.



## 6.2 Materials

### 6.2.1 *Mtb* strains

Strain	Source
H37Rv- lab strain	American Type Culture Collection, USA
Mt103- clinical isolate	Prof. Brigitte Gicquel, Institute Pasteur, Paris, France.
MYC1554- Ag85C mutant on Mt103 background	Prof. Brigitte Gicquel, Institute Pasteur, Paris, France.

### 6.2.2 Mice

Mice were maintained under special pathogen free conditions with a 12 hour light cycle. C57BL/6 female mice, age 8-12 weeks obtained from Charles River Laboratories (Germany). Infected mice were kept in a biosafety level 3 facility under special pathogen free conditions in filter bonnet cages with food and water *ad libidum*.

### 6.2.3 Buffers and media

Buffer/Media	Composition
7H9 medium with Tween	4.7g 7H9 powder 100ml of ADC 5ml 20% Tween-80 4ml 50% Glycerol add to 1000ml with H <sub>2</sub> O
10% Paraformaldehyde (10% PFA) solution	100g PFA add to 1000ml with 1x PBS stir O/N at 50°C, keep dark
20% Tween-80	20ml Tween 80 in 100ml 1X PBS stir at RT
Mouse bone-marrow derived macrophage differentiation medium	DMEM medium plus: 0.2mM L-Glutamine 10% L929 conditioned

	<p>medium</p> <p>10% heat inactivated (1h 65°C) FCS</p> <p>5% heat inactivated horse serum</p> <p>10mM HEPES buffer</p> <p>1mM Sodium Pyruvate</p>
Macrophage infection medium	<p>DMEM medium plus:</p> <p>0.2mM L-Glutamine</p> <p>10% heat inactivated (1h 65°C) FCS</p> <p>5% heat inactivated horse serum</p> <p>10mM HEPES buffer</p> <p>1mM Sodium Pyruvate</p>
MTT stock solution	<p>5mg MTT powder</p> <p>in 1ml 1X PBS</p>
Cell lysis buffer/PBST (PBS/Triton X 100 solution)	<p>1ml Triton X 100</p> <p>add to 1000ml 1x PBS</p>
Dilution buffer/PBST (PBS/Tween solution)	<p>0.5ml Tween20</p> <p>add to 1000ml 1x PBS</p>

#### 6.2.4 Reagents

Reagents	Supplier
7H9 powder	<i>Difco</i>
Albumin-Dextrose-Catalase (ADC)	<i>BD Biosciences</i>
Dimethyl sulfoxide	<i>Fluka</i>
Hygromycin (50mg/ml)	<i>Roche</i>
Isonicotinic acid hydrazide/Isoniazid	<i>Sigma Aldrich</i>
Alamar blue (10X)	<i>Serotec</i>
Ferric chloride	<i>Sigma Aldrich</i>
Tween-80	<i>Sigma Aldrich</i>

Triton-X 100	<i>Sigma Aldrich</i>
Glycerol	<i>Sigma Aldrich</i>
MTT	<i>Sigma Aldrich</i>
FCS	<i>Gibco</i>
1xPBS	<i>Gibco</i>
Dulbecco's modified eagle medium (DMEM)	<i>Gibco</i>
L-Glutamine	<i>Gibco</i>
HEPES-1M	<i>PAA</i>
Sodium pyruvate-100mM	<i>Biochrom AG</i>
Deionised H <sub>2</sub> O	<i>Gibco</i>
TRIZOL	<i>Invitrogen</i>
Quick Amp Labeling Kit	<i>Agilent Technologies</i>
FullSpectrum MultiStart Primer for T7 IVT RNA Amplification	<i>BioCat GmBH</i>
TransPlex Whole Transcriptome Amplification Kit	<i>Sigma-Aldrich</i>
BioPrime Plus Array CGH Indirect Genomic Labeling System	<i>Invitrogen</i>
Sybergreen 2X	<i>Applied Biosystems</i>
Random hexamer primer mix (0.2 µg/µl)	<i>Fermentas</i>
DNase I Amplification Grade (1 U/µl)	<i>Invitrogen</i>
SuperScript III Reverse Transcriptase (200 U/µl)	<i>Invitrogen</i>
RNase OUT-Recombinant Ribonuclease inhibitor (40 U/µl)	<i>Invitrogen</i>
[5,6- <sup>3</sup> H]-Uracil-1mCi/ml, 31.9Ci/mmol	<i>Perkin Elmer</i>
[1,2- <sup>14</sup> C]-Sodium acetate-100µCi/ml, 53.9mCi/mmol	<i>Perkin Elmer</i>
[ <sup>14</sup> C(U)]-Glycerol- 100µCi/ml, 142.7mCi/mmol	<i>Perkin Elmer</i>
[7- <sup>14</sup> C]-Salicylic acid-100µCi/ml, 47mCi/mmol	<i>Perkin Elmer</i>
Methanol	<i>Fluka/ Merck</i>
Chloroform	<i>Sigma-Aldrich/Merck</i>
3-methoxyethanol	<i>Merck</i>
Diethylether	<i>Merck</i>
Dichloromethane	<i>Merck</i>
Ethanol	<i>Merck</i>

### 6.2.5 Instruments/Softwares

<b>Instrument/Software</b>	<b>Manufacturer</b>
Novaspec Spectrophotometer	<i>Pharmacia Biotech</i>

Innova 4200 Incubator Shaker	<i>New Brunswick Scientific</i>
Steri-Cycle CO <sub>2</sub> Incubator	<i>Thermo Forma</i>
Digital Camera-SP 350	<i>Olympus</i>
Galaxy 6D centrifuge	<i>VWR</i>
Filtermate harvester	<i>Perkin Elmer</i>
TopCount NXT Microplate scintillation and luminescence counter	<i>Packard Biosciences</i>
Tri-Carb 2800TR Liquid scintillation analyzer	<i>Perkin Elmer</i>
Typhoon 9400 Imaging system	<i>GE Healthcare Lifesciences</i>
ImageQuant image analysis software	<i>GE Healthcare Lifesciences</i>
FLA 3000 Fluorescent image analyzer	<i>Fujifilm</i>
BAS Reader v. 3.14	<i>Raytest</i>
Aida Image Analyzer v4.03	<i>Raytest</i>
NanoDrop 1000 spectrophotometer	<i>Kisker</i>
Bioanalyzer 2100	<i>Agilent Technologies</i>
DNA microarray laser scanner	<i>Agilent Technologies</i>
Image Analysis / Feature Extraction software G2567AA v.A.9.5.1	<i>Agilent Technologies</i>
Rosetta Resolver Biosoftware, Build 7.1	<i>Rosetta Biosoftware</i>
7900HT Fast Real-Time PCR system	<i>Applied Biosystems</i>
Sequence detection system (SDS) v.2.2.2	<i>Applied Biosystems</i>

### 6.2.6 RT-PCR Primers

<b>Gene</b>	<b>Primer pairs</b>
MbtG	Fwd-5'-ggatgtcggtttccctacc-3' Rev-5'-ggtggcgatcagatacgact-3'
MbtD	Fwd-5'-gatctcgggtgctgattccat -3' Rev-5'-agtttcgcgacaagtccatc -3'
MbtJ	Fwd-5'-acatcctggctgctgcatt -3' Rev-5'-atacgtgcgctaaccaatcc -3'
MmpL6	Fwd-5'-gcagcatcttctcggtatcc -3' Rev-5'-tccttgaatcgggaaatcag -3'
MmpL5	Fwd-5'-cgacattcagtcacaacatcg -3'

	Rev-5'-aactcctcgacatcgaccac -3'
Fas	Fwd-5'-atcgatgttcggtccactc -3' Rev-5'-gcaccaggttgggaatgtag -3'
FabD	Fwd-5'-ttccacaccgattcatgg -3' Rev-5'-ggagaccaggtgtccatc -3'
Mas	Fwd-5'-catcaggtgcataacgttgc -3' Rev-5'-tctgctcaaaggtgatgtcg -3'
Pks11	Fwd-5'-acatcatgggttgggatgac -3' Rev-5'-catcaagaacgtggtgacg -3'
SigA	Fwd-5'-cctccggtgatttcgtctgg -3' Rev-5'-cagcgtaccttgccgatct -3'

## References

- Abou-Zeid, C.; Ratliff, T. L.; Wiker, H. G.; Harboe, M.; Bennedsen, J. and Rook, G. A. (1988): Characterization of fibronectin-binding antigens released by *Mycobacterium tuberculosis* and *Mycobacterium bovis* BCG, *Infect Immun* 56 [12], pp. 3046-51.
- Alland, D.; Steyn, A. J.; Weisbrod, T.; Aldrich, K. and Jacobs, W. R., Jr. (2000): Characterization of the *Mycobacterium tuberculosis* *iniBAC* promoter, a promoter that responds to cell wall biosynthesis inhibition, *J Bacteriol* 182 [7], pp. 1802-11.
- Anderson, D. H.; Harth, G.; Horwitz, M. A. and Eisenberg, D. (2001): An interfacial mechanism and a class of inhibitors inferred from two crystal structures of the *Mycobacterium tuberculosis* 30 kDa major secretory protein (Antigen 85B), a mycolyl transferase, *J Mol Biol* 307 [2], pp. 671-81.
- Andries, K.; Verhasselt, P.; Guillemont, J.; Gohlmann, H. W.; Neefs, J. M.; Winkler, H.; Van Gestel, J.; Timmerman, P.; Zhu, M.; Lee, E.; Williams, P.; de Chaffoy, D.; Huitric, E.; Hoffner, S.; Cambau, E.; Truffot-Pernot, C.; Lounis, N. and Jarlier, V. (2005): A diarylquinoline drug active on the ATP synthase of *Mycobacterium tuberculosis*, *Science* 307 [5707], pp. 223-7.
- Armitige, L. Y.; Jagannath, C.; Wanger, A. R. and Norris, S. J. (2000): Disruption of the genes encoding antigen 85A and antigen 85B of *Mycobacterium tuberculosis* H37Rv: effect on growth in culture and in macrophages, *Infect Immun* 68 [2], pp. 767-78.
- Asselineau, J. and Lederer, E. (1950): Structure of the mycolic acids of *Mycobacteria*, *Nature* 166 [4227], pp. 782-3.
- Austin, P. E.; McCulloch, E. A. and Till, J. E. (1971): Characterization of the factor in L-cell conditioned medium capable of stimulating colony formation by mouse marrow cells in culture, *J Cell Physiol* 77 [2], pp. 121-34.
- Axelrod, S.; Oschkinat, H.; Enders, J.; Schlegel, B.; Brinkmann, V.; Kaufmann, S. H.; Haas, A. and Schaible, U. E. (2008): Delay of phagosome maturation by a mycobacterial lipid is reversed by nitric oxide, *Cell Microbiol* 10 [7], pp. 1530-45.
- Banerjee, A.; Dubnau, E.; Quemard, A.; Balasubramanian, V.; Um, K. S.; Wilson, T.; Collins, D.; de Lisle, G. and Jacobs, W. R., Jr. (1994): *inhA*, a gene encoding a target for isoniazid and ethionamide in *Mycobacterium tuberculosis*, *Science* 263 [5144], pp. 227-30.
- Barry, C. E., 3rd; Boshoff, H. I.; Dartois, V.; Dick, T.; Ehrt, S.; Flynn, J.; Schnappinger, D.; Wilkinson, R. J. and Young, D. (2009): The spectrum of latent tuberculosis: rethinking the biology and intervention strategies, *Nat Rev Microbiol*.

- Bartz, Q. R.; Ehrlich, J.; Mold, J. D.; Penner, M. A. and Smith, R. M. (1951): Viomycin, a new tuberculostatic antibiotic, *Am Rev Tuberc* 63 [1], pp. 4-6.
- Baulard, A. R.; Betts, J. C.; Engohang-Ndong, J.; Quan, S.; McAdam, R. A.; Brennan, P. J.; Loch, C. and Besra, G. S. (2000): Activation of the pro-drug ethionamide is regulated in mycobacteria, *J Biol Chem* 275 [36], pp. 28326-31.
- Belisle, J. T.; Vissa, V. D.; Sievert, T.; Takayama, K.; Brennan, P. J. and Besra, G. S. (1997): Role of the major antigen of *Mycobacterium tuberculosis* in cell wall biogenesis, *Science* 276 [5317], pp. 1420-2.
- Benitez, P.; Medoff, G. and Kobayashi, G. S. (1974): Rapid radiometric method of testing susceptibility of mycobacteria and slow-growing fungi to antimicrobial agents, *Antimicrob Agents Chemother* 6 [1], pp. 29-33.
- Bernstein, J.; Lott, W. A.; Steinberg, B. A. and Yale, H. L. (1952): Chemotherapy of experimental tuberculosis. V. Isonicotinic acid hydrazide (nydrazid) and related compounds, *Am Rev Tuberc* 65 [4], pp. 357-64.
- Bertozzi, C.R. and Schelle, M.W. (2008): Sulfated Metabolites from *Mycobacterium tuberculosis*: Sulfolipid-1 and Beyond, Reyrat, Mamadou Daffe and Jean-Marc, *The Mycobacterial Cell Envelope* pp. 291-305, ASM Press, Washington, DC.
- Betts, J. C.; Lukey, P. T.; Robb, L. C.; McAdam, R. A. and Duncan, K. (2002): Evaluation of a nutrient starvation model of *Mycobacterium tuberculosis* persistence by gene and protein expression profiling, *Mol Microbiol* 43 [3], pp. 717-31.
- Bhowruth, V.; Alderwick, L. J.; Brown, A. K.; Bhatt, A. and Besra, G. S. (2008): Tuberculosis: a balanced diet of lipids and carbohydrates, *Biochem Soc Trans* 36 [Pt 4], pp. 555-65.
- Bloch, K. and Vance, D. (1977): Control mechanisms in the synthesis of saturated fatty acids, *Annu Rev Biochem* 46, pp. 263-98.
- Borgdorff, M. W. and Small, P. M. (2009): Scratching the surface of ignorance on MDR tuberculosis, *Lancet* 373 [9678], pp. 1822-4.
- Boshoff, H. I.; Myers, T. G.; Copp, B. R.; McNeil, M. R.; Wilson, M. A. and Barry, C. E., 3rd (2004): The transcriptional responses of *Mycobacterium tuberculosis* to inhibitors of metabolism: novel insights into drug mechanisms of action, *J Biol Chem* 279 [38], pp. 40174-84.
- Brennan, M. J. and Delogu, G. (2002): The PE multigene family: a 'molecular mantra' for mycobacteria, *Trends Microbiol* 10 [5], pp. 246-9.
- Brennan, P. J. and Nikaido, H. (1995): The envelope of mycobacteria, *Annu Rev Biochem* 64, pp. 29-63.

- Brosch, R.; Gordon, S. V.; Marmiesse, M.; Brodin, P.; Buchrieser, C.; Eiglmeier, K.; Garnier, T.; Gutierrez, C.; Hewinson, G.; Kremer, K.; Parsons, L. M.; Pym, A. S.; Samper, S.; van Soolingen, D. and Cole, S. T. (2002): A new evolutionary scenario for the *Mycobacterium tuberculosis* complex, *Proc Natl Acad Sci U S A* 99 [6], pp. 3684-9.
- Bryk, R.; Gold, B.; Venugopal, A.; Singh, J.; Samy, R.; Pupek, K.; Cao, H.; Popescu, C.; Gurney, M.; Hotha, S.; Cherian, J.; Rhee, K.; Ly, L.; Converse, P. J.; Ehrt, S.; Vandal, O.; Jiang, X.; Schneider, J.; Lin, G. and Nathan, C. (2008): Selective killing of nonreplicating mycobacteria, *Cell Host Microbe* 3 [3], pp. 137-45.
- Camacho, L. R.; Constant, P.; Raynaud, C.; Laneelle, M. A.; Triccas, J. A.; Gicquel, B.; Daffe, M. and Guilhot, C. (2001): Analysis of the phthiocerol dimycocerosate locus of *Mycobacterium tuberculosis*. Evidence that this lipid is involved in the cell wall permeability barrier, *J Biol Chem* 276 [23], pp. 19845-54.
- Camacho, L. R.; Ensergueix, D.; Perez, E.; Gicquel, B. and Guilhot, C. (1999): Identification of a virulence gene cluster of *Mycobacterium tuberculosis* by signature-tagged transposon mutagenesis, *Mol Microbiol* 34 [2], pp. 257-67.
- Cole, S. T.; Brosch, R.; Parkhill, J.; Garnier, T.; Churcher, C.; Harris, D.; Gordon, S. V.; Eiglmeier, K.; Gas, S.; Barry, C. E., 3rd; Tekaia, F.; Badcock, K.; Basham, D.; Brown, D.; Chillingworth, T.; Connor, R.; Davies, R.; Devlin, K.; Feltwell, T.; Gentles, S.; Hamlin, N.; Holroyd, S.; Hornsby, T.; Jagels, K.; Krogh, A.; McLean, J.; Moule, S.; Murphy, L.; Oliver, K.; Osborne, J.; Quail, M. A.; Rajandream, M. A.; Rogers, J.; Rutter, S.; Seeger, K.; Skelton, J.; Squares, R.; Squares, S.; Sulston, J. E.; Taylor, K.; Whitehead, S. and Barrell, B. G. (1998): Deciphering the biology of *Mycobacterium tuberculosis* from the complete genome sequence, *Nature* 393 [6685], pp. 537-44.
- Cole, S. T.; Eiglmeier, K.; Parkhill, J.; James, K. D.; Thomson, N. R.; Wheeler, P. R.; Honore, N.; Garnier, T.; Churcher, C.; Harris, D.; Mungall, K.; Basham, D.; Brown, D.; Chillingworth, T.; Connor, R.; Davies, R. M.; Devlin, K.; Duthoy, S.; Feltwell, T.; Fraser, A.; Hamlin, N.; Holroyd, S.; Hornsby, T.; Jagels, K.; Lacroix, C.; Maclean, J.; Moule, S.; Murphy, L.; Oliver, K.; Quail, M. A.; Rajandream, M. A.; Rutherford, K. M.; Rutter, S.; Seeger, K.; Simon, S.; Simmonds, M.; Skelton, J.; Squares, R.; Squares, S.; Stevens, K.; Taylor, K.; Whitehead, S.; Woodward, J. R. and Barrell, B. G. (2001): Massive gene decay in the leprosy bacillus, *Nature* 409 [6823], pp. 1007-11.
- Conde, M. B.; Efron, A.; Loredó, C.; De Souza, G. R.; Graca, N. P.; Cezar, M. C.; Ram, M.; Chaudhary, M. A.; Bishai, W. R.; Kritski, A. L. and Chaisson, R. E. (2009): Moxiflox-



- acin versus ethambutol in the initial treatment of tuberculosis: a double-blind, randomised, controlled phase II trial, *Lancet* 373 [9670], pp. 1183-9.
- Connolly, L. E.; Edelstein, P. H. and Ramakrishnan, L. (2007): Why is long-term therapy required to cure tuberculosis?, *PLoS Med* 4 [3], p. e120.
- Constant, P.; Perez, E.; Malaga, W.; Laneelle, M. A.; Saurel, O.; Daffe, M. and Guilhot, C. (2002): Role of the pks15/1 gene in the biosynthesis of phenolglycolipids in the *Mycobacterium tuberculosis* complex. Evidence that all strains synthesize glycosylated p-hydroxybenzoic methyl esters and that strains devoid of phenolglycolipids harbor a frameshift mutation in the pks15/1 gene, *J Biol Chem* 277 [41], pp. 38148-58.
- Converse, S. E.; Mougous, J. D.; Leavell, M. D.; Leary, J. A.; Bertozzi, C. R. and Cox, J. S. (2003): MmpL8 is required for sulfolipid-1 biosynthesis and *Mycobacterium tuberculosis* virulence, *Proc Natl Acad Sci U S A* 100 [10], pp. 6121-6.
- Cook, G. M.; Berney, M.; Gebhard, S.; Heinemann, M.; Cox, R. A.; Danilchanka, O. and Niederweis, M. (2009): Physiology of mycobacteria, *Adv Microb Physiol* 55, pp. 81-182, 318-9.
- Cosma, C. L.; Sherman, D. R. and Ramakrishnan, L. (2003): The secret lives of the pathogenic mycobacteria, *Annu Rev Microbiol* 57, pp. 641-76.
- Cox, J. S.; Chen, B.; McNeil, M. and Jacobs, W. R., Jr. (1999): Complex lipid determines tissue-specific replication of *Mycobacterium tuberculosis* in mice, *Nature* 402 [6757], pp. 79-83.
- Crick, D. C. and Brennan, P. J. (2008): Biosynthesis of the Arabinogalactan-Peptidoglycan Complex of *Mycobacterium Tuberculosis*, Reyrat, Mamadou Daffe and Jean-Marc, *The Mycobacterial Cell Envelope* pp. 25-41, ASM Press, Washington,DC.
- Daffe, M. and Laneelle, M. A. (1988): Distribution of phthiocerol diester, phenolic mycosides and related compounds in mycobacteria, *J Gen Microbiol* 134 [7], pp. 2049-55.
- Daffe, M.; Laneelle, M. A.; Asselineau, C.; Levy-Frebault, V. and David, H. (1983): [Taxonomic value of mycobacterial fatty acids: proposal for a method of analysis], *Ann Microbiol (Paris)* 134B [2], pp. 241-56.
- Daffe, Mamadou (2008): The Global Architecture of the Mycobacterial Cell Envelope, Daffe, M. and Reyrat, J.M., *The Mycobacterial Cell Envelope* pp. 3-13, ASM Press, Washington,DC.
- De Voss, J. J.; Rutter, K.; Schroeder, B. G.; Su, H.; Zhu, Y. and Barry, C. E., 3rd (2000): The salicylate-derived mycobactin siderophores of *Mycobacterium tuberculosis* are essential for growth in macrophages, *Proc Natl Acad Sci U S A* 97 [3], pp. 1252-7.

- DeBarber, A. E.; Mdluli, K.; Bosman, M.; Bekker, L. G. and Barry, C. E., 3rd (2000): Ethionamide activation and sensitivity in multidrug-resistant *Mycobacterium tuberculosis*, *Proc Natl Acad Sci U S A* 97 [17], pp. 9677-82.
- Dockrell, H.M.; Gorak-Stolinska, P. and Rodrigues, L.C. (2008): BCG Vaccination: Epidemiology and Immunology, Kaufmann, S. H. and van Helden, P., *Handbook of Tuberculosis: Clinical, Diagnostics, Therapy and Epidemiology* pp. 245-76, WILEY-VCH, Weinheim.
- Domenech, P.; Reed, M. B. and Barry, C. E., 3rd (2005): Contribution of the *Mycobacterium tuberculosis* MmpL protein family to virulence and drug resistance, *Infect Immun* 73 [6], pp. 3492-501.
- Dorhoi, A. and Kaufmann, S. H. (2009): Fine-tuning of T cell responses during infection, *Curr Opin Immunol* 21 [4], pp. 367-77.
- Dover, L. G.; Alderwick, L.; Bhowruth, V.; Brown, A.K.; Kremer, L. and Besra, G. S. (2008): Antibiotics and New Inhibitors of the Cell Wall, Daffe, M. and Reyrat, J.M., *The Mycobacterial Cell Envelope* pp. 107-133, ASM Press, Washington, DC.
- Fernandes, N. D. and Kolattukudy, P. E. (1996): Cloning, sequencing and characterization of a fatty acid synthase-encoding gene from *Mycobacterium tuberculosis* var. *bovis* BCG, *Gene* 170 [1], pp. 95-9.
- Flynn, J. L. (2006): Lessons from experimental *Mycobacterium tuberculosis* infections, *Microbes Infect* 8 [4], pp. 1179-88.
- Flynn, J. L. and Chan, J. (2001): Immunology of tuberculosis, *Annu Rev Immunol* 19, pp. 93-129.
- Gabrielson, J.; Hart, M.; Jarelov, A.; Kuhn, I.; McKenzie, D. and Mollby, R. (2002): Evaluation of redox indicators and the use of digital scanners and spectrophotometer for quantification of microbial growth in microplates, *J Microbiol Methods* 50 [1], pp. 63-73.
- Gagneux, S. and Small, P. M. (2007): Global phylogeography of *Mycobacterium tuberculosis* and implications for tuberculosis product development, *Lancet Infect Dis* 7 [5], pp. 328-37.
- Geijtenbeek, T. B.; Van Vliet, S. J.; Koppel, E. A.; Sanchez-Hernandez, M.; Vandenbroucke-Grauls, C. M.; Appelmelk, B. and Van Kooyk, Y. (2003): Mycobacteria target DC-SIGN to suppress dendritic cell function, *J Exp Med* 197 [1], pp. 7-17.
- Gilleron, M.; Jackson, M.; Nigou, J. and Puzo, G. (2008): Structure, Biosynthesis and Activities of the Phosphatidyl-myo-Inositol-Based Lipoglycans, Reyrat, Mamadou Daffe

- and Jean-Marc, *The Mycobacterial Cell Envelope* pp. 75-107, ASM Press, Washington, DC.
- Glickman, M. S.; Cahill, S. M. and Jacobs, W. R., Jr. (2001): The Mycobacterium tuberculosis *cmaA2* gene encodes a mycolic acid trans-cyclopropane synthetase, *J Biol Chem* 276 [3], pp. 2228-33.
- Glickman, M. S.; Cox, J. S. and Jacobs, W. R., Jr. (2000): A novel mycolic acid cyclopropane synthetase is required for cording, persistence, and virulence of Mycobacterium tuberculosis, *Mol Cell* 5 [4], pp. 717-27.
- Glickman, M.S. (2008): Cording, cord factors and Trehalose Dimycolate, Daffe, M. and Reyrat, J.M., *The Mycobacterial Cell Envelope* pp. 63-75, ASM Press, Washington, DC.
- Gobec, S.; Plantan, I.; Mravljak, J.; Svajger, U.; Wilson, R. A.; Besra, G. S.; Soares, S. L.; Appelberg, R. and Kikelj, D. (2007): Design, synthesis, biochemical evaluation and antimycobacterial action of phosphonate inhibitors of antigen 85C, a crucial enzyme involved in biosynthesis of the mycobacterial cell wall, *Eur J Med Chem* 42 [1], pp. 54-63.
- Gonzalo Asensio, J.; Maia, C.; Ferrer, N. L.; Barilone, N.; Laval, F.; Soto, C. Y.; Winter, N.; Daffe, M.; Gicquel, B.; Martin, C. and Jackson, M. (2006): The virulence-associated two-component PhoP-PhoR system controls the biosynthesis of polyketide-derived lipids in Mycobacterium tuberculosis, *J Biol Chem* 281 [3], pp. 1313-6.
- Guidry, T. V.; Hunter, R. L., Jr. and Actor, J. K. (2007): Mycobacterial glycolipid trehalose 6,6'-dimycolate-induced hypersensitive granulomas: contribution of CD4+ lymphocytes, *Microbiology* 153 [Pt 10], pp. 3360-9.
- Guilhot, C.; Chalut, C. and Daffe, M. (2008): Biosynthesis and Roles of Phenolic Glycolipids and Related Molecules in *Mycobacterium tuberculosis*, Daffe, M. and Reyrat, J.M., *The Mycobacterial Cell Envelope* pp. 273-291, ASM Press, Washington, DC.
- Harth, G.; Horwitz, M. A.; Tabatadze, D. and Zamecnik, P. C. (2002): Targeting the Mycobacterium tuberculosis 30/32-kDa mycolyl transferase complex as a therapeutic strategy against tuberculosis: Proof of principle by using antisense technology, *Proc Natl Acad Sci U S A* 99 [24], pp. 15614-9.
- Harth, G.; Lee, B. Y.; Wang, J.; Clemens, D. L. and Horwitz, M. A. (1996): Novel insights into the genetics, biochemistry, and immunocytochemistry of the 30-kilodalton major extracellular protein of Mycobacterium tuberculosis, *Infect Immun* 64 [8], pp. 3038-47.

- Harth, G.; Zamecnik, P. C.; Tabatadze, D.; Pierson, K. and Horwitz, M. A. (2007): Hairpin extensions enhance the efficacy of mycolyl transferase-specific antisense oligonucleotides targeting *Mycobacterium tuberculosis*, *Proc Natl Acad Sci U S A* 104 [17], pp. 7199-204.
- He, H.; Hovey, R.; Kane, J.; Singh, V. and Zahrt, T. C. (2006): MprAB is a stress-responsive two-component system that directly regulates expression of sigma factors SigB and SigE in *Mycobacterium tuberculosis*, *J Bacteriol* 188 [6], pp. 2134-43.
- Hoffmann, C.; Leis, A.; Niederweis, M.; Plitzko, J. M. and Engelhardt, H. (2008): Disclosure of the mycobacterial outer membrane: cryo-electron tomography and vitreous sections reveal the lipid bilayer structure, *Proc Natl Acad Sci U S A* 105 [10], pp. 3963-7.
- Hugonnet, J. E.; Tremblay, L. W.; Boshoff, H. I.; Barry, C. E., 3rd and Blanchard, J. S. (2009): Meropenem-clavulanate is effective against extensively drug-resistant *Mycobacterium tuberculosis*, *Science* 323 [5918], pp. 1215-8.
- Indrigo, J.; Hunter, R. L., Jr. and Actor, J. K. (2002): Influence of trehalose 6,6'-dimycolate (TDM) during mycobacterial infection of bone marrow macrophages, *Microbiology* 148 [Pt 7], pp. 1991-8.
- Indrigo, J.; Hunter, R. L., Jr. and Actor, J. K. (2003): Cord factor trehalose 6,6'-dimycolate (TDM) mediates trafficking events during mycobacterial infection of murine macrophages, *Microbiology* 149 [Pt 8], pp. 2049-59.
- Jackson, M.; Raynaud, C.; Laneelle, M. A.; Guilhot, C.; Laurent-Winter, C.; Ensergueix, D.; Gicquel, B. and Daffe, M. (1999): Inactivation of the antigen 85C gene profoundly affects the mycolate content and alters the permeability of the *Mycobacterium tuberculosis* cell envelope, *Mol Microbiol* 31 [5], pp. 1573-87.
- Jain, M.; Chow, E.D. and Cox, J. S. (2008): The MmpL protein family, Daffe, M. and Reyrat, J.M., *The Mycobacterial Cell Envelope* pp. 201-211, ASM Press, Washington D.C.
- Jarlier, V. and Nikaïdo, H. (1994): Mycobacterial cell wall: structure and role in natural resistance to antibiotics, *FEMS Microbiol Lett* 123 [1-2], pp. 11-8.
- Ji, B.; Lounis, N.; Maslo, C.; Truffot-Pernot, C.; Bonnafous, P. and Grosset, J. (1998): In vitro and in vivo activities of moxifloxacin and clinafloxacin against *Mycobacterium tuberculosis*, *Antimicrob Agents Chemother* 42 [8], pp. 2066-9.
- Kang, P. B.; Azad, A. K.; Torrelles, J. B.; Kaufman, T. M.; Beharka, A.; Tibesar, E.; DesJardin, L. E. and Schlesinger, L. S. (2005): The human macrophage mannose receptor directs *Mycobacterium tuberculosis* lipoarabinomannan-mediated phagosome biogenesis, *J Exp Med* 202 [7], pp. 987-99.

- Katti, M. K.; Dai, G.; Armitige, L. Y.; Marrero, C. R.; Daniel, S.; Singh, C. R.; Lindsey, D. R.; Dhandayuthapani, S.; Hunter, R. L. and Jagannath, C. (2008): The Delta fbpA mutant derived from *Mycobacterium tuberculosis* H37Rv has an enhanced susceptibility to intracellular antimicrobial oxidative mechanisms, undergoes limited phagosome maturation and activates macrophages and dendritic cells, *Cell Microbiol* 10 [6], pp. 1286-303.
- Kaufmann, S. H. (2000): Is the development of a new tuberculosis vaccine possible?, *Nat Med* 6 [9], pp. 955-60.
- Kaufmann, S. H. (2001): How can immunology contribute to the control of tuberculosis?, *Nat Rev Immunol* 1 [1], pp. 20-30.
- Kaufmann, S. H. (2003): Immune response to tuberculosis: experimental animal models, *Tuberculosis (Edinb)* 83 [1-3], pp. 107-11.
- Kaufmann, S. H. (2005): Recent findings in immunology give tuberculosis vaccines a new boost, *Trends Immunol* 26 [12], pp. 660-7.
- Kaufmann, S. H. (2007): The contribution of immunology to the rational design of novel anti-bacterial vaccines, *Nat Rev Microbiol* 5 [7], pp. 491-504.
- Kaufmann, S. H. and McMichael, A. J. (2005): Annulling a dangerous liaison: vaccination strategies against AIDS and tuberculosis, *Nat Med* 11 [4 Suppl], pp. S33-44.
- Kaufmann, S. H. and Parida, S. K. (2007): Changing funding patterns in tuberculosis, *Nat Med* 13 [3], pp. 299-303.
- Kelly, B. P.; Furney, S. K.; Jessen, M. T. and Orme, I. M. (1996): Low-dose aerosol infection model for testing drugs for efficacy against *Mycobacterium tuberculosis*, *Antimicrob Agents Chemother* 40 [12], pp. 2809-12.
- Koch, R (1882): Die Aetiologie der Tuberculose., *Berliner klin. Wochenschr.* 19, pp. 221-230.
- Konno, K.; Feldmann, F. M. and McDermott, W. (1967): Pyrazinamide susceptibility and amidase activity of tubercle bacilli, *Am Rev Respir Dis* 95 [3], pp. 461-9.
- Krithika, R.; Marathe, U.; Saxena, P.; Ansari, M. Z.; Mohanty, D. and Gokhale, R. S. (2006): A genetic locus required for iron acquisition in *Mycobacterium tuberculosis*, *Proc Natl Acad Sci U S A* 103 [7], pp. 2069-74.
- Kurosawa, H. (1952): The isolation of an antibiotic produced by a strain of streptomycetes K-300, *Yokohama Med Bull* 3 [6], pp. 386-99.
- Kwara, A.; Flanigan, T. P. and Carter, E. J. (2005): Highly active antiretroviral therapy (HAART) in adults with tuberculosis: current status, *Int J Tuberc Lung Dis* 9 [3], pp. 248-57.

- Laneelle, M. A. and Daffe, M. (2008): Transport assays and permeability in pathogenic Mycobacteria, Parish, T., Mycobacteria Protocols pp. 143-151, Humana Press, Totowa, NJ.
- Lee, B. Y. and Horwitz, M. A. (1995): Identification of macrophage and stress-induced proteins of Mycobacterium tuberculosis, J Clin Invest 96 [1], pp. 245-9.
- Lee, J. S.; Krause, R.; Schreiber, J.; Mollenkopf, H. J.; Kowall, J.; Stein, R.; Jeon, B. Y.; Kwak, J. Y.; Song, M. K.; Patron, J. P.; Jorg, S.; Roh, K.; Cho, S. N. and Kaufmann, S. H. (2008): Mutation in the transcriptional regulator PhoP contributes to avirulence of Mycobacterium tuberculosis H37Ra strain, Cell Host Microbe 3 [2], pp. 97-103.
- Lehmann, J. (1946): p-aminosalicylic acid in the treatment of tuberculosis, Lancet 1, pp. 15-16.
- Lin, G.; Li, D.; de Carvalho, L. P.; Deng, H.; Tao, H.; Vogt, G.; Wu, K.; Schneider, J.; Chidawanyika, T.; Warren, J. D.; Li, H. and Nathan, C. (2009): Inhibitors selective for mycobacterial versus human proteasomes, Nature 461 [7264], pp. 621-6.
- Maggi, N.; Pasqualucci, C. R.; Ballotta, R. and Sensi, P. (1966): Rifampicin: a new orally active rifamycin, Chemotherapy 11 [5], pp. 285-92.
- Makarov, V.; Manina, G.; Mikusova, K.; Mollmann, U.; Ryabova, O.; Saint-Joanis, B.; Dhar, N.; Pasca, M. R.; Buroni, S.; Lucarelli, A. P.; Milano, A.; De Rossi, E.; Belanova, M.; Bobovska, A.; Dianiskova, P.; Kordulakova, J.; Sala, C.; Fullam, E.; Schneider, P.; McKinney, J. D.; Brodin, P.; Christophe, T.; Waddell, S.; Butcher, P.; Albrethsen, J.; Rosenkrands, I.; Brosch, R.; Nandi, V.; Bharath, S.; Gaonkar, S.; Shandil, R. K.; Balasubramanian, V.; Balganes, T.; Tyagi, S.; Grosset, J.; Riccardi, G. and Cole, S. T. (2009): Benzothiazinones kill Mycobacterium tuberculosis by blocking arabinan synthesis, Science 324 [5928], pp. 801-4.
- Malone, L.; Schurr, A.; Lindh, H.; Mc, Kenzie D.; Kiser, J. S. and Williams, J. H. (1952): The effect of pyrazinamide (aldinamide) on experimental tuberculosis in mice, Am Rev Tuberc 65 [5], pp. 511-8.
- Manjunatha, U.; Boshoff, H. I. and Barry, C. E. (2009): The mechanism of action of PA-824: Novel insights from transcriptional profiling, Commun Integr Biol 2 [3], pp. 215-8.
- Manjunatha, U. H.; Boshoff, H.; Dowd, C. S.; Zhang, L.; Albert, T. J.; Norton, J. E.; Daniels, L.; Dick, T.; Pang, S. S. and Barry, C. E., 3rd (2006): Identification of a nitroimidazo-oxazine-specific protein involved in PA-824 resistance in Mycobacterium tuberculosis, Proc Natl Acad Sci U S A 103 [2], pp. 431-6.

- Mariani, F.; Cappelli, G.; Riccardi, G. and Colizzi, V. (2000): Mycobacterium tuberculosis H37Rv comparative gene-expression analysis in synthetic medium and human macrophage, *Gene* 253 [2], pp. 281-91.
- Marrakchi, H.; Bardou, F.; Laneelle, M. A. and Daffe, M. (2008): A Comprehensive overview of Mycolic Acid Structure and Biosynthesis, Daffe, M. and Reyrat, J.M., *The Mycobacterial Cell Envelope* pp. 41-63, ASM Press, Washington,DC.
- Marrakchi, H.; Ducasse, S.; Labesse, G.; Montrozier, H.; Margeat, E.; Emorine, L.; Charpentier, X.; Daffe, M. and Quemard, A. (2002): MabA (FabG1), a Mycobacterium tuberculosis protein involved in the long-chain fatty acid elongation system FAS-II, *Microbiology* 148 [Pt 4], pp. 951-60.
- Marrakchi, H.; Laneelle, G. and Quemard, A. (2000): InhA, a target of the antituberculous drug isoniazid, is involved in a mycobacterial fatty acid elongation system, FAS-II, *Microbiology* 146 ( Pt 2), pp. 289-96.
- Mathur, M. and Kolattukudy, P. E. (1992): Molecular cloning and sequencing of the gene for mycocerosic acid synthase, a novel fatty acid elongating multifunctional enzyme, from Mycobacterium tuberculosis var. bovis Bacillus Calmette-Guerin, *J Biol Chem* 267 [27], pp. 19388-95.
- Matsumoto, M.; Hashizume, H.; Tomishige, T.; Kawasaki, M.; Tsubouchi, H.; Sasaki, H.; Shimokawa, Y. and Komatsu, M. (2006): OPC-67683, a nitro-dihydro-imidazooxazole derivative with promising action against tuberculosis in vitro and in mice, *PLoS Med* 3 [11], p. e466.
- McKinney, J. D.; Honer zu Bentrup, K.; Munoz-Elias, E. J.; Miczak, A.; Chen, B.; Chan, W. T.; Swenson, D.; Sacchettini, J. C.; Jacobs, W. R., Jr. and Russell, D. G. (2000): Persistence of Mycobacterium tuberculosis in macrophages and mice requires the glyoxylate shunt enzyme isocitrate lyase, *Nature* 406 [6797], pp. 735-8.
- Mdluli, K.; Slayden, R. A.; Zhu, Y.; Ramaswamy, S.; Pan, X.; Mead, D.; Crane, D. D.; Musser, J. M. and Barry, C. E., 3rd (1998): Inhibition of a Mycobacterium tuberculosis beta-ketoacyl ACP synthase by isoniazid, *Science* 280 [5369], pp. 1607-10.
- Middlebrook, G, Dubos, R.J, Pierce,C (1947): Virulence and morphological characteristics of mammalian tubercle bacilli., *Journal of experimental medicine* 86, pp. 175-184.
- Mitchison, D. A. (2004): Antimicrobial therapy of tuberculosis: justification for currently recommended treatment regimens, *Semin Respir Crit Care Med* 25 [3], pp. 307-15.
- Mosmann, T. (1983): Rapid colorimetric assay for cellular growth and survival: application to proliferation and cytotoxicity assays, *J Immunol Methods* 65 [1-2], pp. 55-63.

- Nathan, C.; Gold, B.; Lin, G.; Stegman, M.; de Carvalho, L. P.; Vandal, O.; Venugopal, A. and Bryk, R. (2008): A philosophy of anti-infectives as a guide in the search for new drugs for tuberculosis, *Tuberculosis (Edinb)* 88 Suppl 1, pp. S25-33.
- Niederweis, M. (2003): Mycobacterial porins--new channel proteins in unique outer membranes, *Mol Microbiol* 49 [5], pp. 1167-77.
- Odriozola, J. M.; Ramos, J. A. and Bloch, K. (1977): Fatty acid synthetase activity in *Mycobacterium smegmatis*. Characterization of the acyl carrier protein-dependent elongating system, *Biochim Biophys Acta* 488 [2], pp. 207-17.
- Ojha, A. K.; Baughn, A. D.; Sambandan, D.; Hsu, T.; Trivelli, X.; Guerardel, Y.; Alahari, A.; Kremer, L.; Jacobs, W. R., Jr. and Hatfull, G. F. (2008): Growth of *Mycobacterium tuberculosis* biofilms containing free mycolic acids and harbouring drug-tolerant bacteria, *Mol Microbiol* 69 [1], pp. 164-74.
- Park, H. D.; Guinn, K. M.; Harrell, M. I.; Liao, R.; Voskuil, M. I.; Tompa, M.; Schoolnik, G. K. and Sherman, D. R. (2003): Rv3133c/dosR is a transcription factor that mediates the hypoxic response of *Mycobacterium tuberculosis*, *Mol Microbiol* 48 [3], pp. 833-43.
- Perez, R. L.; Roman, J.; Roser, S.; Little, C.; Olsen, M.; Indrigo, J.; Hunter, R. L. and Actor, J. K. (2000): Cytokine message and protein expression during lung granuloma formation and resolution induced by the mycobacterial cord factor trehalose-6,6'-dimycolate, *J Interferon Cytokine Res* 20 [9], pp. 795-804.
- Portevin, D.; De Sousa-D'Auria, C.; Houssin, C.; Grimaldi, C.; Chami, M.; Daffe, M. and Guilhot, C. (2004): A polyketide synthase catalyzes the last condensation step of mycolic acid biosynthesis in mycobacteria and related organisms, *Proc Natl Acad Sci U S A* 101 [1], pp. 314-9.
- Protopopova, M.; Hanrahan, C.; Nikonenko, B.; Samala, R.; Chen, P.; Gearhart, J.; Einck, L. and Nacy, C. A. (2005): Identification of a new antitubercular drug candidate, SQ109, from a combinatorial library of 1,2-ethylenediamines, *J Antimicrob Chemother* 56 [5], pp. 968-74.
- Puech, V.; Bayan, N.; Salim, K.; Leblon, G. and Daffe, M. (2000): Characterization of the in vivo acceptors of the mycoloyl residues transferred by the corynebacterial PS1 and the related mycobacterial antigens 85, *Mol Microbiol* 35 [5], pp. 1026-41.
- Puech, V.; Guilhot, C.; Perez, E.; Tropis, M.; Armitige, L. Y.; Gicquel, B. and Daffe, M. (2002): Evidence for a partial redundancy of the fibronectin-binding proteins for the



- transfer of mycoloyl residues onto the cell wall arabinogalactan termini of *Mycobacterium tuberculosis*, *Mol Microbiol* 44 [4], pp. 1109-22.
- Quadri, L. E.; Sello, J.; Keating, T. A.; Weinreb, P. H. and Walsh, C. T. (1998): Identification of a *Mycobacterium tuberculosis* gene cluster encoding the biosynthetic enzymes for assembly of the virulence-conferring siderophore mycobactin, *Chem Biol* 5 [11], pp. 631-45.
- Raviglione, M. C. and Smith, I. M. (2007): XDR tuberculosis--implications for global public health, *N Engl J Med* 356 [7], pp. 656-9.
- Reece, S. T. and Kaufmann, S. H. (2008): Rational design of vaccines against tuberculosis directed by basic immunology, *Int J Med Microbiol* 298 [1-2], pp. 143-50.
- Reed, M. B.; Domenech, P.; Manca, C.; Su, H.; Barczak, A. K.; Kreiswirth, B. N.; Kaplan, G. and Barry, C. E., 3rd (2004): A glycolipid of hypervirulent tuberculosis strains that inhibits the innate immune response, *Nature* 431 [7004], pp. 84-7.
- Rodriguez, G. M. (2006): Control of iron metabolism in *Mycobacterium tuberculosis*, *Trends Microbiol* 14 [7], pp. 320-7.
- Rodriguez, G. M.; Voskuil, M. I.; Gold, B.; Schoolnik, G. K. and Smith, I. (2002): *ideR*, An essential gene in *mycobacterium tuberculosis*: role of *IdeR* in iron-dependent gene expression, iron metabolism, and oxidative stress response, *Infect Immun* 70 [7], pp. 3371-81.
- Ronning, D. R.; Klabunde, T.; Besra, G. S.; Vissa, V. D.; Belisle, J. T. and Sacchettini, J. C. (2000): Crystal structure of the secreted form of antigen 85C reveals potential targets for mycobacterial drugs and vaccines, *Nat Struct Biol* 7 [2], pp. 141-6.
- Ronning, D. R.; Vissa, V.; Besra, G. S.; Belisle, J. T. and Sacchettini, J. C. (2004): *Mycobacterium tuberculosis* antigen 85A and 85C structures confirm binding orientation and conserved substrate specificity, *J Biol Chem* 279 [35], pp. 36771-7.
- Rose, J. D.; Maddry, J. A.; Comber, R. N.; Suling, W. J.; Wilson, L. N. and Reynolds, R. C. (2002): Synthesis and biological evaluation of trehalose analogs as potential inhibitors of mycobacterial cell wall biosynthesis, *Carbohydr Res* 337 [2], pp. 105-20.
- Russell, D. G. (2007): Who puts the tubercle in tuberculosis?, *Nat Rev Microbiol* 5 [1], pp. 39-47.
- Rustad, T. R.; Harrell, M. I.; Liao, R. and Sherman, D. R. (2008): The enduring hypoxic response of *Mycobacterium tuberculosis*, *PLoS One* 3 [1], p. e1502.

- Sacchetti, J. C.; Rubin, E. J. and Freundlich, J. S. (2008): Drugs versus bugs: in pursuit of the persistent predator *Mycobacterium tuberculosis*, *Nat Rev Microbiol* 6 [1], pp. 41-52.
- Salomon, J. A.; Lloyd-Smith, J. O.; Getz, W. M.; Resch, S.; Sanchez, M. S.; Porco, T. C. and Borgdorff, M. W. (2006): Prospects for advancing tuberculosis control efforts through novel therapies, *PLoS Med* 3 [8], p. e273.
- Schatz, A.; Bugie, E. and Waksman, S. A. (1944): Streptomycin, a substance exhibiting antibiotic activity against gram-positive and gram-negative bacteria, *Proc. Soc. Exp. Biol. Med.* 55, pp. 66-69.
- Schnappinger, D.; Ehrt, S.; Voskuil, M. I.; Liu, Y.; Mangan, J. A.; Monahan, I. M.; Dolganov, G.; Efron, B.; Butcher, P. D.; Nathan, C. and Schoolnik, G. K. (2003): Transcriptional Adaptation of *Mycobacterium tuberculosis* within Macrophages: Insights into the Phagosomal Environment, *J Exp Med* 198 [5], pp. 693-704.
- Singh, R.; Manjunatha, U.; Boshoff, H. I.; Ha, Y. H.; Niyomrattanakit, P.; Ledwidge, R.; Dowd, C. S.; Lee, I. Y.; Kim, P.; Zhang, L.; Kang, S.; Keller, T. H.; Jiricek, J. and Barry, C. E., 3rd (2008): PA-824 kills nonreplicating *Mycobacterium tuberculosis* by intracellular NO release, *Science* 322 [5906], pp. 1392-5.
- Snow, G. A. (1970): Mycobactins: iron-chelating growth factors from mycobacteria, *Bacteriol Rev* 34 [2], pp. 99-125.
- Stewart, G. R.; Robertson, B. D. and Young, D. B. (2003): Tuberculosis: a problem with persistence, *Nat Rev Microbiol* 1 [2], pp. 97-105.
- StopTBPartnership (2009): Pipeline-Working group on New TB drugs <http://www.newtbdrugs.org/pipeline.php>
- Stover, C. K.; Warren, P.; VanDevanter, D. R.; Sherman, D. R.; Arain, T. M.; Langhorne, M. H.; Anderson, S. W.; Towell, J. A.; Yuan, Y.; McMurray, D. N.; Kreiswirth, B. N.; Barry, C. E. and Baker, W. R. (2000): A small-molecule nitroimidazopyran drug candidate for the treatment of tuberculosis, *Nature* 405 [6789], pp. 962-6.
- Takayama, K. and Kilburn, J. O. (1989): Inhibition of synthesis of arabinogalactan by ethambutol in *Mycobacterium smegmatis*, *Antimicrob Agents Chemother* 33 [9], pp. 1493-9.
- Takayama, K.; Wang, C. and Besra, G. S. (2005): Pathway to synthesis and processing of mycolic acids in *Mycobacterium tuberculosis*, *Clin Microbiol Rev* 18 [1], pp. 81-101.
- TBAlliance (2009): TB-HIV
- TBAlliance (2009): TB Drug Portfolio

- Telenti, A.; Philipp, W. J.; Sreevatsan, S.; Bernasconi, C.; Stockbauer, K. E.; Wieles, B.; Musser, J. M. and Jacobs, W. R., Jr. (1997): The emb operon, a gene cluster of *Mycobacterium tuberculosis* involved in resistance to ethambutol, *Nat Med* 3 [5], pp. 567-70.
- Thomas, J. P.; Baughn, C. O.; Wilkinson, R. G. and Shepherd, R. G. (1961): A new synthetic compound with antituberculous activity in mice: ethambutol (dextro-2,2'-(ethylenediimino)-di-1-butanol), *Am Rev Respir Dis* 83, pp. 891-3.
- Tsunekawa, H.; Miyachi, T.; Nakamura, E.; Tsukamura, M. and Amano, H. (1987): [Therapeutic effect of ofloxacin on 'treatment-failure' pulmonary tuberculosis], *Kekkaku* 62 [9], pp. 435-9.
- Ulrichs, T. and Kaufmann, S. H. (2006): New insights into the function of granulomas in human tuberculosis, *J Pathol* 208 [2], pp. 261-9.
- van den Boogaard, J.; Kibiki, G. S.; Kisanga, E. R.; Boeree, M. J. and Aarnoutse, R. E. (2009): New drugs against tuberculosis: problems, progress, and evaluation of agents in clinical development, *Antimicrob Agents Chemother* 53 [3], pp. 849-62.
- van Soolingen, D.; Qian, L.; de Haas, P. E.; Douglas, J. T.; Traore, H.; Portaels, F.; Qing, H. Z.; Enkhsaikan, D.; Nymadawa, P. and van Embden, J. D. (1995): Predominance of a single genotype of *Mycobacterium tuberculosis* in countries of east Asia, *J Clin Microbiol* 33 [12], pp. 3234-8.
- Ventura, M.; Canchaya, C.; Tauch, A.; Chandra, G.; Fitzgerald, G. F.; Chater, K. F. and van Sinderen, D. (2007): Genomics of Actinobacteria: tracing the evolutionary history of an ancient phylum, *Microbiol Mol Biol Rev* 71 [3], pp. 495-548.
- Vera-Cabrera, L.; Brown-Elliott, B. A.; Wallace, R. J., Jr.; Ocampo-Candiani, J.; Welsh, O.; Choi, S. H. and Molina-Torres, C. A. (2006): In vitro activities of the novel oxazolidinones DA-7867 and DA-7157 against rapidly and slowly growing mycobacteria, *Antimicrob Agents Chemother* 50 [12], pp. 4027-9.
- Voskuil, M. I.; Schnappinger, D.; Visconti, K. C.; Harrell, M. I.; Dolganov, G. M.; Sherman, D. R. and Schoolnik, G. K. (2003): Inhibition of respiration by nitric oxide induces a *Mycobacterium tuberculosis* dormancy program, *J Exp Med* 198 [5], pp. 705-13.
- Waddell, S. J.; Stabler, R. A.; Laing, K.; Kremer, L.; Reynolds, R. C. and Besra, G. S. (2004): The use of microarray analysis to determine the gene expression profiles of *Mycobacterium tuberculosis* in response to anti-bacterial compounds, *Tuberculosis (Edinb)* 84 [3-4], pp. 263-74.

- Wang, J.; Elchert, B.; Hui, Y.; Takemoto, J. Y.; Bensaci, M.; Wennergren, J.; Chang, H.; Rai, R. and Chang, C. W. (2004): Synthesis of trehalose-based compounds and their inhibitory activities against *Mycobacterium smegmatis*, *Bioorg Med Chem* 12 [24], pp. 6397-413.
- Wayne, L. G. and Hayes, L. G. (1996): An in vitro model for sequential study of shutdown of *Mycobacterium tuberculosis* through two stages of nonreplicating persistence, *Infect Immun* 64 [6], pp. 2062-9.
- Wehrli, W. (1983): Rifampin: mechanisms of action and resistance, *Rev Infect Dis* 5 Suppl 3, pp. S407-11.
- Welsh, K. J.; Abbott, A. N.; Hwang, S. A.; Indrigo, J.; Armitige, L. Y.; Blackburn, M. R.; Hunter, R. L., Jr. and Actor, J. K. (2008): A role for tumour necrosis factor-alpha, complement C5 and interleukin-6 in the initiation and development of the mycobacterial cord factor trehalose 6,6'-dimycolate induced granulomatous response, *Microbiology* 154 [Pt 6], pp. 1813-24.
- WHO (1993): WHO declares tuberculosis a global emergency, *Soz Praventivmed* 38 [4], pp. 251-2.
- WHO (2009): Global Tuberculosis Control 2009 [http://www.who.int/tb/publications/global\\_report/2009/pdf/full\\_report.pdf](http://www.who.int/tb/publications/global_report/2009/pdf/full_report.pdf)
- Wiker, H. G. and Harboe, M. (1992): The antigen 85 complex: a major secretion product of *Mycobacterium tuberculosis*, *Microbiol Rev* 56 [4], pp. 648-61.
- Willand, N.; Dirie, B.; Carette, X.; Bifani, P.; Singhal, A.; Desroses, M.; Leroux, F.; Willery, E.; Mathys, V.; Deprez-Poulain, R.; Delcroix, G.; Frenois, F.; Aumercier, M.; Locht, C.; Villeret, V.; Deprez, B. and Baulard, A. R. (2009): Synthetic EthR inhibitors boost antituberculous activity of ethionamide, *Nat Med* 15 [5], pp. 537-44.
- Wilson, M.; DeRisi, J.; Kristensen, H. H.; Imboden, P.; Rane, S.; Brown, P. O. and Schoolnik, G. K. (1999): Exploring drug-induced alterations in gene expression in *Mycobacterium tuberculosis* by microarray hybridization, *Proc Natl Acad Sci U S A* 96 [22], pp. 12833-8.
- Wright, A.; Zignol, M.; Van Deun, A.; Falzon, D.; Gerdes, S. R.; Feldman, K.; Hoffner, S.; Drobniewski, F.; Barrera, L.; van Soolingen, D.; Boulabhal, F.; Paramasivan, C. N.; Kam, K. M.; Mitarai, S.; Nunn, P. and Raviglione, M. (2009): Epidemiology of antituberculosis drug resistance 2002-07: an updated analysis of the Global Project on Anti-Tuberculosis Drug Resistance Surveillance, *Lancet* 373 [9678], pp. 1861-73.

- Yajko, D. M.; Madej, J. J.; Lancaster, M. V.; Sanders, C. A.; Cawthon, V. L.; Gee, B.; Babst, A. and Hadley, W. K. (1995): Colorimetric method for determining MICs of antimicrobial agents for *Mycobacterium tuberculosis*, *J Clin Microbiol* 33 [9], pp. 2324-7.
- Zahrt, T. C.; Wozniak, C.; Jones, D. and Trevett, A. (2003): Functional analysis of the *Mycobacterium tuberculosis* MprAB two-component signal transduction system, *Infect Immun* 71 [12], pp. 6962-70.
- Zhang, Y.; Heym, B.; Allen, B.; Young, D. and Cole, S. (1992): The catalase-peroxidase gene and isoniazid resistance of *Mycobacterium tuberculosis*, *Nature* 358 [6387], pp. 591-3.
- Zhang, Y.; Wade, M. M.; Scorpio, A.; Zhang, H. and Sun, Z. (2003): Mode of action of pyrazinamide: disruption of *Mycobacterium tuberculosis* membrane transport and energetics by pyrazinoic acid, *J Antimicrob Chemother* 52 [5], pp. 790-5.
- Zimhony, O.; Cox, J. S.; Welch, J. T.; Vilcheze, C. and Jacobs, W. R., Jr. (2000): Pyrazinamide inhibits the eukaryotic-like fatty acid synthetase I (FASI) of *Mycobacterium tuberculosis*, *Nat Med* 6 [9], pp. 1043-7.
- Zuber, B.; Chami, M.; Houssin, C.; Dubochet, J.; Griffiths, G. and Daffe, M. (2008): Direct visualization of the outer membrane of mycobacteria and corynebacteria in their native state, *J Bacteriol* 190 [16], pp. 5672-80.

**Anhang****Chemical structures of compounds**

The chemical structures of the Ag85C inhibitors, Ag85C-1-4 is shown below.

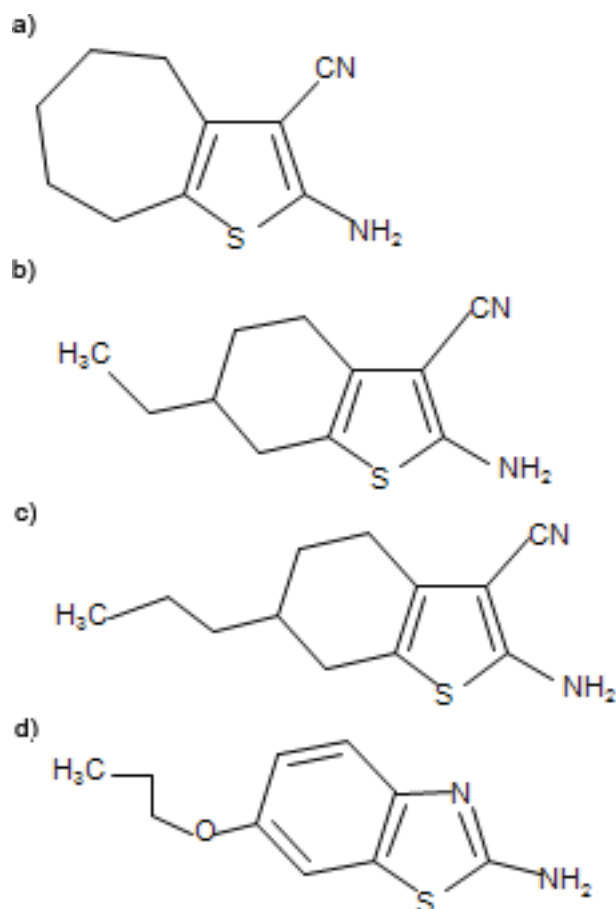


**Figure 25: Structure of Ag85C antagonists.**

a) Ag85C-1 b) Ag85C-2 c) Ag85C-3 d) Ag85C-4.

**Abbreviations**

Abbreviation	Expansion
TB	Tuberculosis
<i>Mtb</i>	<i>Mycobacterium tuberculosis</i>
Ag85	Antigen 85
Ag85C-1	Antigen85C inhibitor-1
Ag85C-2	Antigen85C inhibitor-2
Ag85C-3	Antigen85C inhibitor-3
Ag85C-4	Antigen85C inhibitor-4
NMR	Nuclear magnetic resonance
SAR	Structure activity relation
BCG	Bacille Calmette-Guérin

HIV	Human immunodeficiency virus
SM	Streptomycin
PAS	P-amino salicylic acid
INH	Isoniazid
PZA	Pyrazinamide
RIF	Rifampin
EMB	Ethambutol
MDR	Multidrug resistant
XDR	Extensively drug resistant
WHO	World Health Organisation
AIDS	Acquired immune deficiency syndrome
IL-12	Interleukin-12
TNF- $\alpha$	Tumour necrosis factor- $\alpha$
CCL5	Chemokines like (C-C) Ligand 5
MIP-1 $\alpha$	Macrophage inflammatory protein-1 $\alpha$
FAS	Fatty acid synthase
Pks	Polyketide synthase
TMM	Trehalose monomycolate
TDM	Trehalose dimycolate
mAGP	Mycolic acid linked to arabinogalactan peptidoglycan complex
PG	Peptidoglycan
AG	Arabinogalactan
LM	Lipomannan
PIM	Phosphatidyl-myo-inositol mannosides
ManLAM	Mannosylated lipoarabinomannan
PGL	Phenolic glycolipid
PDIM	Pthiocerol dimycocerosate
SL	Sulfolipid
PAMP	Pathogen associated molecular pattern
DC-SIGN	Dendritic cell-specific intercellular adhesion molecule 3 grabbing nonintegrin
TLR-2	Toll-like receptor-2
ETH	Ethionamide

MIC	Minimum inhibitory concentration
MTT	3-(4,5-Dimethylthiazol-2-yl)-2,5-diphenyltetrazolium bromide
MOI	Multiplicity of infection
CFU	Colony forming unit
TLC	Thin layer chromatography
MAME	Mycolic acid methyl esters
FAME	Fatty acid methyl esters
MBT/Mbt	Mycobactin
MmpL	Mycobacterial membrane protein large
RND	Resistance, nodulation and division
MprA	Mycobacterial persistence regulator A
Cyp132	Cytochrome P450 132
AlkB	Alkane 1-monoxygenase
Cyp125	Cytochrome P450 125
LldD1	Possible L-lactate dehydrogenase 1
PPE	Proline-proline-glutamic acid
IniB	Isoniazid inducible protein B
AcpM	Acyl carrier protein M
Mas	Multi-functional mycocerosic acid synthase
MB	mycobactin
CMB	Carboxy mycobactin
FabD	Malonyl CoA:AcpM acyltransferase
SigA	Sigma factor A
ADT	6-azido-6-deoxy--trehalose
PS-ODN	Phosphorothioate-modified oligodeoxyribonucleotide
SOCS-1	Suppressor of cytokine signalling-1
MspA	<i>M. smegmatis</i> porin A
IdeR	Iron dependent repressor
GltA1	Probable citrate synthase 1
RubB	Rubredoxin B
RNA	Ribonucleic acid
DNA	Deoxyribonucleic acid
RT-PCR	Real time polymerase chain reaction



PBS	Phosphate buffer saline
PFA	Paraformaldehyde
OD	Optical density

### Publications

- 1)M. Rajavel, Thulasi Warriar, B. Gopal (2006) Old fold in a new X-ray diffraction data-set? Low-resolution molecular replacement using representative structural templates can provide phase information. *Proteins: Structure, Function, and Bioinformatics*, 64;4;923-930.
- 2)Podust LM, von Kries JP, Eddine AN, Kim Y, Yermalitskaya LV, Kuehne R, Ouellet H, Warriar T, Alteköster M, Lee JS, Rademann J, Oschkinat H, Kaufmann SH, Waterman MR (2007) Small-molecule scaffolds for CYP51 inhibitors identified by high-throughput screening and defined by X-ray crystallography. *Antimicrob Agents Chemother*. 51(11):3915-23.
- 3)Eddine AN, von Kries JP, Podust MV, Warriar T, Kaufmann SH, Podust LM (2008) X-ray structure of 4,4'-dihydroxybenzophenone mimicking sterol substrate in the active site of sterol 14 $\alpha$ -demethylase (CYP51). *J Biol Chem*. 30;283(22):15152-9.

Berlin, den

### Acknowledgements

I take this chance to express my sincere and deep-felt gratitude to Prof. Dr. Stefan H.E. Kaufmann for providing me an opportunity to pursue my PhD studies in his department and thus introducing me to the exciting field of TB research. His unwavering support and encouragement have enabled me to successfully complete my studies here. I am also grateful to Prof. Dr. Richard Lucius for being my Humboldt University supervisor.

Dr. Ali Nasser Eddine who directly supervised my work, has been a pillar of strength and support throughout my stay here. I am indebted to him for his tremendous faith in my abilities, constant support, encouragement and undying optimism particularly during the most

challenging times. I am also thankful to Dr. Markus Schade, our main collaborator for bringing the Ag85C inhibitors to us and making this project possible.

I would like to thank Prof. Dr. Mamadou Daffe and Dr. Marielle Tropis at the IPBS in Toulouse, France for their help with lipid analysis experiments, fruitful discussions and warm hospitality. The gene expression studies would not have been possible without the help and support of Dr. Hans J Mollenkopf and Mrs. Karin Hahnke. I am also grateful to Mr. Markus Alteköster, Dr. Anca Dorhoi, Mrs. Peggy Kaiser, Mr. Matthias Bild and Ms. Ellen Heinemann for walking me through the intricacies of working in an S3 facility with *Mtb* and also numerous other techniques.

I cannot thank Dr. Arunava Dasgupta enough for his willingness to discuss any and every aspect of this work. He has been a constant source of help and support. I am grateful to Dr. Anca Dorhoi for energetic and fruitful scientific discussions and most importantly for her friendship. This work would not have been successful without the stimulating and supportive environment created by all members in my department. I would like to thank all PhD students of this lab, past and present, for the lively ambience in the 'PhD offices' and their friendship and support during these years.

Thanks to all fellow Indians in our Institute, Shreemanta, Hakkim, Rajendra, Arunava, Fayaz, Ravi, Vibha, Shakti and Cindy, for help with everything. I am also grateful to all my friends in Berlin, especially Raghu, Smita, Aditi, Katya, Shyam, Kavitha, Santosh, Bhavesh and Ruby for their concern and encouragement. I owe all my achievements to my parents and my brother, Arun for their love, support and guidance over all these years. Thank you.

## **Erklärung**

Hiermit erkläre ich, Thulasi Warriar, geb. am 24.10.1983 in Trichur, Kerala, Indien, die vorliegende Dissertation selbstständig und ohne unerlaubte Hilfe angefertigt zu haben und alle verwendeten Hilfsmittel und Inhalte aus anderen Quellen als solche kenntlich gemacht zu haben. Desweiteren versichere ich, dass die vorliegende Arbeit nie in dieser oder anderer Form Gegenstand eines früheren Promotionsverfahrens war. Die dem angestrebten Promotionsverfahren an der Mathematischen-Naturwissenschaftlichen Fakultät I der Humboldt-Universität zu Berlin zugrunde liegende Promotionsordnung ist mir bekannt.

Berlin, im January 2010

---

Unterschrift